An examination of planetary fractionation: examples from meteorites

By:

Elizabeth Lymer
Department of Earth Science, Dalhousie University, Halifax NS

Supervisor:

Dr. Richard Cox
Dalhousie University

Distribution License

DalSpace requires agreement to this non-exclusive distribution license before your item can appear on DalSpace.

NON-EXCLUSIVE DISTRIBUTION LICENSE

You (the author(s) or copyright owner) grant to Dalhousie University the non-exclusive right to reproduce and distribute your submission worldwide in any medium.

You agree that Dalhousie University may, without changing the content, reformat the submission for the purpose of preservation.

You also agree that Dalhousie University may keep more than one copy of this submission for purposes of security, back-up and preservation.

You agree that the submission is your original work, and that you have the right to grant the rights contained in this license. You also agree that your submission does not, to the best of your knowledge, infringe upon anyone's copyright.

If the submission contains material for which you do not hold copyright, you agree that you have obtained the unrestricted permission of the copyright owner to grant Dalhousie University the rights required by this license, and that such third-party owned material is clearly identified and acknowledged within the text or content of the submission.

If the submission is based upon work that has been sponsored or supported by an agency or organization other than Dalhousie University, you assert that you have fulfilled any right of review or other obligations required by such contract or agreement.

Dalhousie University will clearly identify your name(s) as the author(s) or owner(s) of the submission, and will not make any alteration to the content of the files that you have submitted.

If you have questions regarding this license please contact the repository manager at dalspace@dal.ca.

Grant the distribution license by signing and dating below.

_____ _____

Name of signatory Date

Abstract

This study compares the geochemistry of chondrules in the carbonaceous chondrite Allende to that of terrestrial komatiite and basaltic komatiite samples from the Archean eon. This comparison provides a better understanding of the early evolution of Earth from its formation through the Hadean eon, which has no preserved geologic record.

Carbonaceous chondrites are a type of meteorite that are thought to be the most primitive and undifferentiated material in our solar system, and therefore can provide a better understanding of the early history and evolution of our solar system. Chondrites are defined by small spherical aggregates of minerals called chondrules. Chondrules are thought to be formed through impact jetting off of undifferentiated protoplanet crust during the first couple million years of our solar system formation. Planets such as the moon are achondrites, formed by partial melting and are considered to be differentiated material. Geologists have extensively studied the carbonaceous chondrite Allende CV3, which will be used in this study, since its observed fall in 1969 providing a foundation of geochemical and petrologic data. Allende contains many chondrules, which were studied as individual mafic rocks and were compared to the oldest mafic rocks on Earth. Due to rapid plate tectonics and bombardment during Earth's early history, there is no geologic rock record for the Hadean period. The oldest and most primitive mafic rocks on Earth are Archean in age (~3.8 Ga). Hadean rock composition was deduced using meteorite samples containing chondrules. Using chondrules as an analogue for Hadean rock composition, we can deduce the early evolution of Earth by geochemically comparing chondrules to Archean mafic rocks.

To study the evolution of our planet through geochemistry, phase distribution maps were created using the EDS detector on an electron microprobe to determine bulk composition of 5 different chondrules in Allende. The spectra of major elements in chondrules are overlapped to give a visual representation of phase distribution and petrography. The chondrules and the Archean samples were compared using TAS (Total alkali versus silica) classification, magnesium numbers and crystallization temperatures to discern whether the samples behaved similarly and therefore fractionation could be compared using distribution coefficients. The TAS classification, magnesium numbers and crystallization temperatures were relatively similar in the chondrules and the Archean samples. Therefore distribution coefficients, or more simply the ratio of element concentration in a single mineral to the concentration of the element in the whole rock, were calculated using the concentration of specific elements in olivine, pyroxene and plagioclase in different chondrules of Allende and Archean-aged mafic rock samples. Distribution coefficients for trace elements in these minerals of the chondrules showed incompatibility with Ni, and high concentrations of Ti, whereas the Archean samples contained minerals with compatible Ni and incompatible Ti. This indicates that the Archean samples clearly went through redistribution processes such as plate tectonics, mantle cooling and crustal growth that the chondrules did not experience.

Key words: Chondrite, Chondrule, Archean, Mantle, Fractionation, distribution coefficients, evolution, primitive Earth

Acknowledgments

I would like to thank my fellow classmates in the earth science department, as well as all the professors and instructors who have given me endless support, encouragement and knowledge throughout my undergraduate degree. I would like to thank Gordon Brown and Dan MacDonald for their help in sample preparation and data collection, as well as Dr. Martin Gibling for his generous contributions to this thesis through tireless editing and his attention to detail. I would also like to thank my supervisor Dr. Richard Cox his encouragement, knowledge and endless support throughout this project.

Table of Contents

Table of Figures

1.0 Introduction

1.1 Meteorites and our Solar System

Meteorites and other planetary bodies may hold the blueprints of our solar system's evolution and may provide information on the earliest formation of all the different planetary bodies in space, because of their primitive composition (Hutchison, 2004). The most primitive material in our solar system is thought to be that of chondritic meteorites because their chemical composition is similar to that of the suns photosphere (Sears, 2004). Chondritic meteorites are thought to be the by-products of planetary accretion during the earliest stages of our solar system's formation (Johnson *et al*., 2015). Understanding the most compositionally primitive material in our solar system formed as a result of planetary accretion, and relating primitive material to more differentiated bodies will help further our understanding of the evolution of our own planet and our solar system. There are many types of meteorites that have been found on earth, mostly ejected from the main asteroid belt located between Jupiter and Mars. Others have come from material ejected from near earth asteroids, comets and planets. The discovery of seemingly different meteorites on earth led to the classification and naming of meteorite material beginning in the mid to late 1800's (Weisberg *et al*., 2006). The classification of meteorites was important for communication between scientists, and also inspired curiosity about genetic relationships between meteorites (Weisberg *et al*., 2006). There are three main categories of meteorites: Chondrites, Achondrites and Primitive

Figure 1: Thin section of Allende CV3 meteorite. Rounded features are chondrules, and irregularly shaped features are CAI's (Calcium-aluminum-rich inclusions)

Achondrites. Chondrites are undifferentiated material, meaning they come from asteroids or comets that have not undergone planetary fractionation; whereas Achondrites are thought to have fractionated from chondritic material through partial melting or other processes, and are therefore differentiated. Achondrites include planetary material like the Moon and Mars, as well as larger asteroids that have undergone differentiation such as 4 Vesta. Primitive Achondrites are close to Chondrites geochemically by having a primitive composition, but contain textures that indicate igneous and/or secondary recrystallization processes similar to that of Achondrites (Weisberg *et al*, 2006).

1.2 Relationship Between Meteorites and Earth

Chondritic material is best known for their tiny (mm-sized) spherical features known as chondrules. Chondrules are thought to have formed as a result of impact during planetary accretion, and may be composed of the same material that formed the crust of differentiating planets in the very early stages of our solar evolution (Johnson *et al*., 2015). The planetary bodies in our solar system started forming ~4.56 billion years ago, shortly after the general formation of our solar system by accretion. Bodies that meteorites come from, and protoplanets that evolve to become planetary bodies such as Earth, Jupiter, and Mars; were all built from the same material: gas and dust from the solar nebula (Jacobsen, 2003). Chondritic material after accretion became frozen in time, and was left undifferentiated, creating a window into the early evolution and formation of our planet and our solar system. This window into Earth's early history allows us to analyze how Earth has evolved geochemically since its formation. There is no physical rock record from the Hadean period, the first 500 myr of Earth's history (Zahnle *et al*., 2007). There have

been discoveries of some detrital zircon grains in the Jack Hills formation in Australia date to 4.4 Ga and have a granitic origin, hinting that there was continental crust during the first 150 myr of our planets formation (Wilde *et al*., 2001). The most primitive volcanic mafic rocks on earth are about 3.7 – 3.8 Ga, found in the Isua greenstone belt in Greenland (Polat *et al*., 2001). There is no older record of mafic material on Earth due to rapid plate tectonics during the Hadean period (Sleep, 2010). To gain a full understanding of how our planet evolved, we must find a way to fill in the missing rock record from the Hadean period. Zahnle *et al*. (2007) suggests that Earth's early history must be deduced using geochemistry and meteorite samples. Chondrules are mm-sized spherical aggregates of minerals within chondrites, essentially rocks. These chondrules were formed shortly (1-3 myr) after our solar system started to form, from impacting of undifferentiated crust of protoplanets (Zahnle *et al*., 2007; Johnson *et al*., 2015). This means that they contain the same chemical constituents of the mantle during the early formation of Earth, and therefore we can use chondrules as an analogue for mafic rocks during the beginning of Earth's formation.

1.3 Samples

A non-differentiated, chondritic meteorite sample: Allende CV3 will be the focus of this study (Fig.1). Chondrules within Allende will be analyzed as individual whole rocks, and compared to that of Archean aged Komatiites from multiple cratons on Earth. By comparing chondrules in Allende with early terrestrial samples from Earth, the stages that a planetary body would go through may be represented, to better understand the formation and early history of Earth.

The Allende CV3 Carbonaceous Chondrite was an observed meteorite fall in 1969 near Chihuahua Mexico. Allende represents among the most primitive and undifferentiated material created in the early stages of our solar system (Clarke, et. al., 1970; Weisberg *et al*., 2006). Allende contains many types of 1-2mm sized chondrules with different compositions and textures surrounded by a matrix of glass and mineral fragments. Allende also contains many very fine-grained amoeboid-shaped calcium-aluminum-rich inclusions (CAIs) within surrounding matrix, which are thought to be the oldest material in our solar system, dating to 4.5 Ga (Johnson at al., 2015). The chondrules in Allende contain minerals such as: olivine, orthopyroxene, calcium-aluminum-rich silicates, clinopyroxene and feldspars.

Complied geochemical data from several publications on Archean – aged komatiites, basaltic komatiites and Archean basalts in the Georoc database will be used to compare to the Allende chondrules. Komatiites are Archean aged ultra-mafic volcanic rocks that are thought to have erupted at temperatures around 1400 - 1700°C (Huppert *et al*., 1984). Data were used from the Kaapvaal craton in the Barberton greenstone belt (Smith *et al*., 1980; Robin-Popieul *et al*., 2012; Smith and Erlank, 1982), Western Australia craton (Lesher and Arndt, 1995; Arndt and Lesher, 1992), Superior Province in the Abitibi Greenstone belt (Cattell and Arndt, 1987; Arndt *et al*., 1977; Puchtel *et al*., 2004), and the Zimbabwe Craton (Bickle *et al*., 1993; Shimzu *et al*., 2005; Nisbet *et al*., 1977). The ages of the Komatiites and basalts ranged from 3.4 – 2.7 Ga. Archean ultramafic rocks such as komatiites will be compared geochemically to chondrules found in Allende, because they are the oldest mafic rocks on Earth and will therefore help obtain information on the early evolution of Earth.

1.4 Systematic Approach

Major and minor element contents, phase distributions and distribution coefficients will be determined using microprobe analysis of Allende chondrules and will be compared to early terrestrial samples. Petrographic analysis of thin sections will be carried out using SEM images, mineral identification using wavelength dispersive spectroscopy (WDS) point analysis, and when possible petrographic microscopy. Polished sections of the Allende CV3 meteorite will be analyzed using energy dispersive x-ray spectroscopy (EDS) on the Dalhousie microprobe. EDS will provide small phase analysis and whole rock analysis through summing and averaging the integrated X-ray signals for major and minor elements. EDS mapping will be assisted by the use of ImgaeJ software to create stitched RGB compositional maps. Wavelength Dispersive X-ray Spectroscopy (WDS) will be used to analyze major and higher level trace elements within common minerals such as olivine clinopyroxene, and orthopyroxene. These minerals are used because they are some of the most abundant high-temperature and thus, early crystallizing silicate minerals in the mantle of planetary bodies and have an affinity for capturing trace elements within their structure (Dygert *et al*., 2013). These data will help calculate distribution coefficients for a select number of trace elements such as Ni, Ti, Cr, Mn, Ca and Al in olivine, orthopyroxene, and clinopyroxene. These data will then be compared to that of Archean-aged Komatiite and basalt from several cratons around the world to show similarities and differences, which will then be discussed in the context of early solar system evolution.

2.0 Scientific Background

2.1 Early History the of Solar System and Formation of Chondrites

Chondrites contain preserved protosolar material and material from the formation of the solar system within their matrix, which allows scientists to study the early history and formation of the solar system (Hutchison, 2004). There are many working theories on how the solar system formed described by Hutchison (2004). The main theory on solar system formation is Nebular condensation, which has been around for decades. The solar system is thought to have formed from a large interstellar rotating cloud of dust and gas that was well mixed which condensed, or gravitationally collapsed to form the sun. It is speculated that planet formation occurred during the formation of the sun or shortly after, and there are two main theories to how the planets and asteroids in the solar system formed. The first theory is formation of the sun could have emitted a burst of energy that was strong enough to heat the cold corotating accretionary disk, which formed into large bodies or planetisimals through melting. These planetisimals could have cooled down when travelling away from the heat, but trapped in our region of the solar system because of the large gravitational force caused by the sun or protojupiter. The second and more popular theory is the sun formed in a hot pre-solar nebula that had enough energy to vaporize silica as far away from it as the inner planets and asteroid belt (3 Au or about 450 million Km away from the sun) as described in Hutchison (2004).

Chondrites, specifically carbonaceous chondrites, are believed to be the most primitive material from the formation of the solar system. Their chemical composition and ratio of major non-volatile elements are similar to that of a pre-volatile sun. This indicates that the proto sun, planets, and chondrites were all formed from the same interstellar

material (Hutchison, 2004). Chondrites are aggregates of silicate, sulfides, metal; small spherical features (mm-sized) called chondrules, and calcium – aluminum – rich inclusions. Chondrites are defined by the small spherical inclusions called chondrules, which will be discussed further in chapter 2.3 (Weisberg *et al*., 2006). CI chondrites or carbonaceous Ivuna-like meteorites (fig. 2) are considered the most primitive carbonaceous chondrite group because their composition is closest to that of the volatile free sun. The other chondrite groups show depletion or enrichment in refractory elements, and depletion in slightly volatile lithophile and siderophile elements relative to CI's, which are controlled by volatile abundance within the chondrite. Each chondrite group is thought to represent a different parent body because they do not include polymictic grains of other types of meteorites (Weisberg *et al*., 2006). Differences in cooling temperatures and stages of cooling due to disequilibrium with surrounding gas is considered to be the reason why chondrites have different chemical compositions (Hutchison, 2004).

2.2 Classification Methods

Classification of meteorites is important for understanding relationships between meteorites and creating a common language for scientists to communicate. Meteorite classification schemes have grown and been regularly updated during the continuing study of meteorite samples. Weisberg *et al*. (2006) outlines the classification of meteorites in great detail, which is summarized in the following section. A meteorite is classified as a 'fall' if it was observed upon descent into the atmosphere and then collected. A meteorite is defined as a 'find' if it was not associated with an observed event before collection. Meteorites were first classified into irons, stony irons and stones. Irons are very heavy, iron

–rich metallic meteorites, whereas stones contain more silica. Stones were eventually divided into chondrites and Achondritic meteorites, which has now become a more conventional classification method. Meteorites are now divided into three main categories based primarily on texture and differentiation: chondrites, achondrites and primitive achondrites.

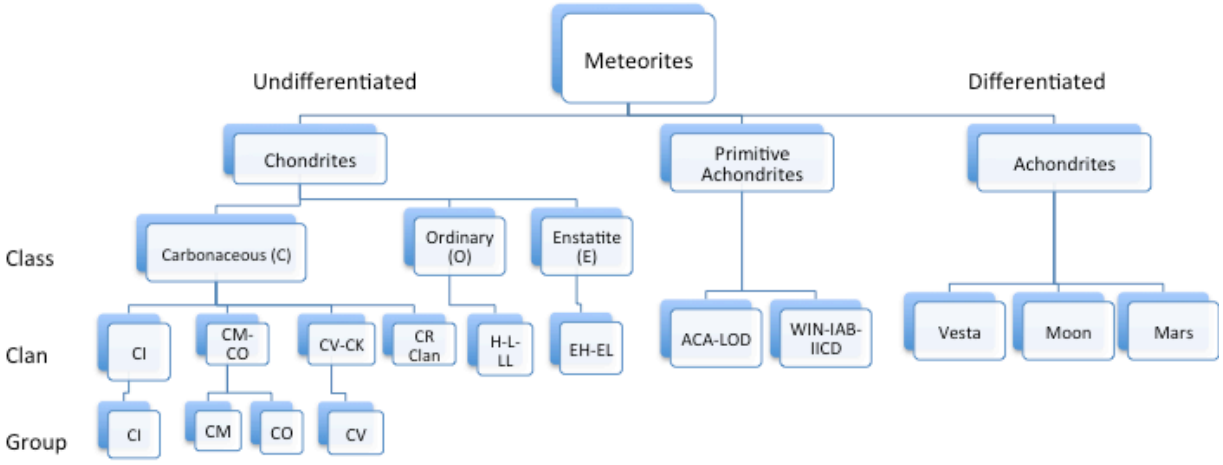

Figure 2: Classification tree for meteorites modified from Weisberg *et al.* (2006). The Carbonaceous chondrite clan has been expanded into groups for an example of further classification.

Chondrites are considered to be undifferentiated material; achondrites are differentiated material and primitive achondrites are chemically similar to chondrites, but show partial melt textures similar to achondrites. Typically, meteorites are classified based on whole-rock mineralogy, petrology, geochemistry and O-isotopes. Using these parameters chondrites, achondrites and primitive achondrites are divided into classes, clans, groups and subgroups as (Fig.2) (Weisberg *et al.*, 2006).

2.2.1 Chondrites

Chondrites are divided into three classes: Carbonaceous, Ordinary and Enstatite as outlined by Weisberg *et al.* (2006). A class is comprised of a group of meteorites with

similar geochemical and O-isotopic characteristics. These three classes are then divided into clans. A clan consists of chondrites thought to have formed in the same area within a nebula, and share chemical, mineralogical and isotopic characteristics. Meteorites typically are written with the clan abbreviation to identify them. CI chondrites mentioned in section 2.1 is an example of a clan name. C represents carbonaceous class and the second letter comes from the type meteorite of that clan (I = Ivuna - like, V = Vigarano - like) (Weisberg *et al*., 2006). The Ordinary chondrite class belongs to the clan H-L-LL, which each become their own individual groups: H, L, and LL. Groups are thought to show relationships to similar parent bodies by having similar petrologic, geochemical and isotopic data. The Ordinary chondrite groups are distinguished based on the ratio of metallic Fe to oxidized Fe within the sample and their total abundance of iron. The group's letters come from their relative ratios and abundances of Fe; H group has the highest value and LL has the lowest value. Some carbonaceous chondrites are further divided into subgroups from groups based on petrological differences and some chondrites do not fit into any of these groups and become part of an ungrouped set (Weisberg *et al*., 2006). Chondrites were also assigned a type number that corresponds to the degree of aqueous and metamorphic alteration, where type 3 is the least altered as seen in figure 3

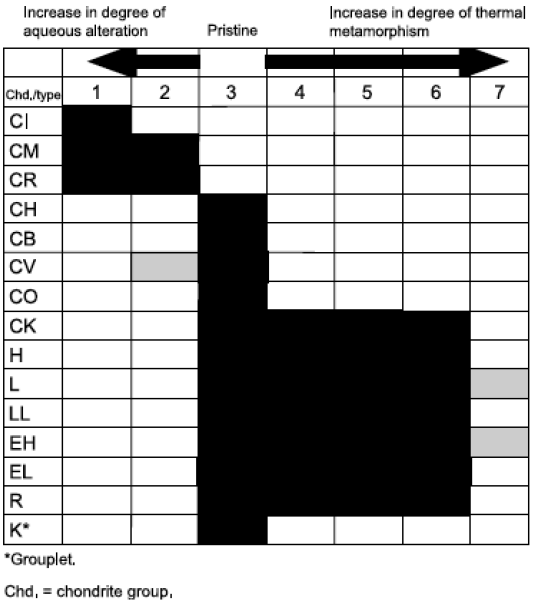

Figure 3: Chondrite alteration chart from Weisberg *et al.* (2006). A value of 3 represents the least altered material, increasing from 3 indicates increasing metamorphism and decreasing from 3 represents aqueous alteration.

(Weisberg *et al*., 2006). An example of the final result of meteorite classification is the name of Allende, the focus of this study. Allende is a CV3 meteorite, meaning carbonaceous class, Vigarano-like, and does not show much secondary alteration (3) (Stracke *et al*., 2012). Classification and abbreviation allows a lot of information to be told about a certain meteorite type immediately.

2.2.2 Achondrites

Primitive achondrites are generally interpreted as bodies that have gone through partial melting or are from planetary bodies where differentiation was not in isotopic equilibrium (Weisberg *et al*., 2006). Primitive achondrites have complicated histories and are not explained in detail because no samples of this type were used in this paper.

Achondrites are thought to be differentiated material with a chondritic origin, formed by melting of parent material. Achondritic meteorites come from asteroids such as Vesta, Mars, the Moon and other differentiated bodies. Achondrites are not divided as deeply as chondrites; most are put into groups, but few groups have a related clan (Fig. 2). Meteorite types that are considered achondrites are generally called irons, stony irons, and stones (Weisberg *et al*., 2006). Each type of meteorite is considered to represent a different part of a small planetary body, or a fragment of a larger planetary body today (eg. Mars). Irons are considered to come from cores of differentiated asteroids, whereas stony irons may be mixtures of core and mantle, or core and crustal material. Stony irons are also considered to form by impact on differentiated asteroids (Weisberg *et al*., 2006). In chondrite classification, when two meteorites are thought to have come from the same parent body they are in the same group. Achondrites are not grouped based on apparent

genetic relationships; in fact two achondrites from the same parent body could be in different groups (Weisberg *et al*., 2006). Achondrites that share similar chemical and petrologic characteristics and are considered to be from the same parent body are said to have petrogenic association (Weisberg *et al*., 2006).

2.3 Chondrule Controversy

Chondrules are small; typically mm sized spherical aggregates of minerals, and chondrules are one of the defining features of chondritic meteorites. Not all chondrites contain chondrules, such as CI chondrites, however most chondrites have a high concentration of chondrules (Weisberg *et al*., 2006). Chondrules are often the most abundant object within other types of chondrites and are comprised of silicates, sulfides and occasionally metal alloys. Chondrules can be feldspathic dominant or ferromagnesium dominant (more common) with olivine and/or pyroxene minerals present (Hutchison, 2004). There is controversy surrounding how chondrules were formed. There are many theories on the formation of chondrules, as well as the timing of formation and their role in chondrite formation. The main problem with most of the theories is the need for a flash-heating event or mechanism to create enough energy to melt the parent body (Sears, 2004). One of the main assumptions of chondrule formation is that all chondrules form by a common process. One assumption of chondrule formation is based on the premise that chondrules were partially or completely melted before or during accretion of material into chondrites (Hutchison, 2004).

There were many theories on chondrule formation in the Solar system outlined by Hutchison (2004), some involving the melting of dust balls or dispersed solids forming

small molten sphericals, others relying on condensation during chondrite accretion. The origin and formation of chondrules remains controversial despite the extensive research completed on chondrules from many meteorites over several decades, however recent models such as Johnson *et al*. (2015) have provided new evidence for a realistic formation of chondrules within the early stages of our solar system formation, and provide an explanation for the abundance of chondrules within this very primitive material. Johnson *et al*. (2015) proposes that impact jetting can create enough heat and velocity to eject undifferentiated material from the crusts of accreting planets into surrounding space. Chondrules are melted undifferentiated material from the crust of these planets that were then ejected off of the surface along with material that would form the matrix surrounding the chondrules (Johnson *et al*., 2015).

2.4 Geologic Background and Geochemical Data Consolidation

The Plank institute consolidated the geochemical data from Archean-aged cratons used in this study into the Georoc database. Geochemical data were used from Kaapvaal, Western Australian, Superior and Zimbabwe cratons.

The Kaapvaal craton is comprised of the Barberton greenstone belt and the Komati formation, and is located in northeastern South Africa and Swaziland. The Komati formation contains some of the oldest mafic rocks on earth, with an age of 3.5 - 3.3 Ga (Robin-Popieul *et al*., 2012). Three separate geochemical datasets were used for the Kaapvaal craton: 5400, 16702, and 5590. These datasets came from the publications Smith *et al*. (1980), Robin – Popieul *et al*. (2012), and Smith and Erlank (1982) respectively.

The Western Australian craton contains komatiites that are ~2.7 Ga, from the Silver lake formation of the Kambalda domain. Parts of the Kambalda domain have been known to have contamination in the komatiite samples from wall rock, however the Silver lake formation is the least contaminated section (Lesher and Arndt, 1995). The geochemical data for the Western Australian craton, 5319/6810 was published by Lesher and Arndt (1995), and Arndt and Lesher (1992).

The Superior craton has a similar age to Western Australia, ~2.7 Ga komatiites. The Superior craton is located in Ontario, Canada and contains the Abitibi greenstone belt (Arndt *et al*., 1977). 3 datasets for the Superior craton (5611, 8628, and 6819), published by Cattell and Arndt (1987), Arndt *et al*. (1977), and Puchtel *et al*. (2004) respectively were used in this study.

The Zimbabwe craton contains komatiites, basaltic komatiites and Archean-age basalts. The Zimbabwe craton contains the Belingwe greenstone belt and the Reliance formation where komatiite flows are found. The Zimbabwe craton is adjacent to the Kaapvaal craton in southern Africa, and it is ~ 2.7- 2.8 Ga (Shimizu *et al*., 2005). There were 3 datasets used in this study from the Zimbabwe craton (5996, 8498, and 5415) that were originally published by Bickle *et al*. (1993), Shimizu *et al*. (2005), and Nisbet *et al*. (1977) respectively.

3.0 Methods

3.1 Sample preparation and petrography

A small sample (golf-ball sized) of the Allende meteorite was cut into slabs to make 2 thin and 3 polished sections. The polished sections were analyzed under a petrographic microscope in transmitted and cross-polarized light depending on thickness. Petrographic descriptions of chondrule mineralogy and textures were made. Petrographic descriptions were also used to locate chondrules that appeared to be fresh (not much alteration or fracturing), and contained different mineral compositions and aggregates of minerals to obtain a full suite of chondrule types. Chondrules were then selected for analysis, and their position in the sample was recorded for positioning the electron microprobe.

3.2 Spectral analysis

3.2.1 Electron Dispersive X-ray Spectroscopy (EDS)

The EDS detector on the electron microprobe at Dalhousie University was used for spectral imaging and x-ray mapping of specified chondrules in the Allende samples. EDS analyzes major element weight percent for each pixel in each spectral image taken. Spectral images were taken at high resolution using 10 frames/second, 100 seconds/frame, dwell-time of 127 seconds, total acquisition time of 1000 seconds and each frame was 1024 x 768 pixels. The weight percent compositions of the major elements were tabulated using the spectra obtained. Spectral images are x-ray maps that show the abundance of individual major elements such as Mg, Fe, Si, Al, and Ca etc. These images are then overlain showing different mineral assemblages and phases using ImageJ software as described by Lydon (2005). The spectral image maps were then stitched together using PT GUI software to

form compositional maps of chondrules in the Allende samples. Using K_2O, Na_2O, and SiO_2 weight percentages, each chondrule can be classified as a rock type using a Total Alkalis versus Silica plot (TAS) as shown in Rollinson (1993) (Fig. 9).

3.2.2 Wavelength Dispersive X-ray Spectroscopy (WDS)

WDS was used to analyze major, minor and trace element abundances within different minerals that form chondrules in Allende. WDS point analysis was used to quantitatively identify minerals and end-member compositions present within each chondrule and to obtain the major element data for each mineral identified. A probe diameter of 1 um, acceleration voltage of 15kv, probe current of 20 nA, and background count of 10 seconds were used on major and minor elements. Clinopyroxene, orthopyroxene and olivine crystals were then analyzed again in order to determine the trace and minor element contents using WDS with longer count times. Long count times allowed for the determination of transition metal contents such as chromium and nickel in olivine, orthopyroxene and clinopyroxene crystals. This data was then used to calculate distribution coefficients. Distribution coefficients are calculated using the Nernst distribution coefficient equation where K_d = (Concentration of trace elements/ Concentration of melt) as shown in Rollinson (1993).

3.3 Database Consolidation

Major, minor and trace element data for Archean-aged komatiite, basaltic-komatiites and Archean basalts were consolidated from the GEOROC database entered by the Max Planck Institute for Chemistry. Major and minor element data were analyzed, and

distribution coefficients were calculated for the Archean mafic rocks. K_2O and Na_2O weight percent were plotted against SiO_2 content to form a TAS diagram (fig. 9) as seen in Le Maitre *et al*. for the Archean mafic rocks (1989).

4.0 Petrography

4.1 Allende Petrography

Small samples of Allende were sliced into thin and polished sections, allowing for a cross-sectional view of the meteorite and chondrules within (figure 1). Our samples of Allende contain many chondrules, making up over 60% of a thin sections surface area. Most chondrules are very round, with a visible reaction rim and an aggregate of minerals inside. These Allende samples also contain calcium-aluminum-rich inclusions (CAIs) that appear as light coloured amoeboid-like structures. The matrix of Allende is very dark material located between the chondrules and other features, composed primarily of glass. Some extremely fine-grained mineral fragments are also found within the glassy matrix.

4.2 Chondrule X-ray Petrography

EDS maps were created using the electron microprobe for 5 chondrules from 2 different Allende CV3 polished sections named Al2 and Al3. In Sample Al3 3, fine-grained, mm-sized chondrules were mapped and named, chondrule Al3-03, Al3-06 and Al3-07. Sample Al2 had 2 different chondrules mapped and named, Al2-01, and Al2-02. EDS spectral images show compositional (mineral phase) differences in each chondrule, and also highlight textural differences. All of the chondrules, except for Al3-03 and Al3-06 had olivine and pyroxene minerals aggregated in a similar to cumulates.

Chondrule Al3-03 has a round shape with a diameter close to 1 mm (Fig. 4a). This chondrule contains porphyritic olivine and pyroxene in a very fine calcium-aluminum-rich

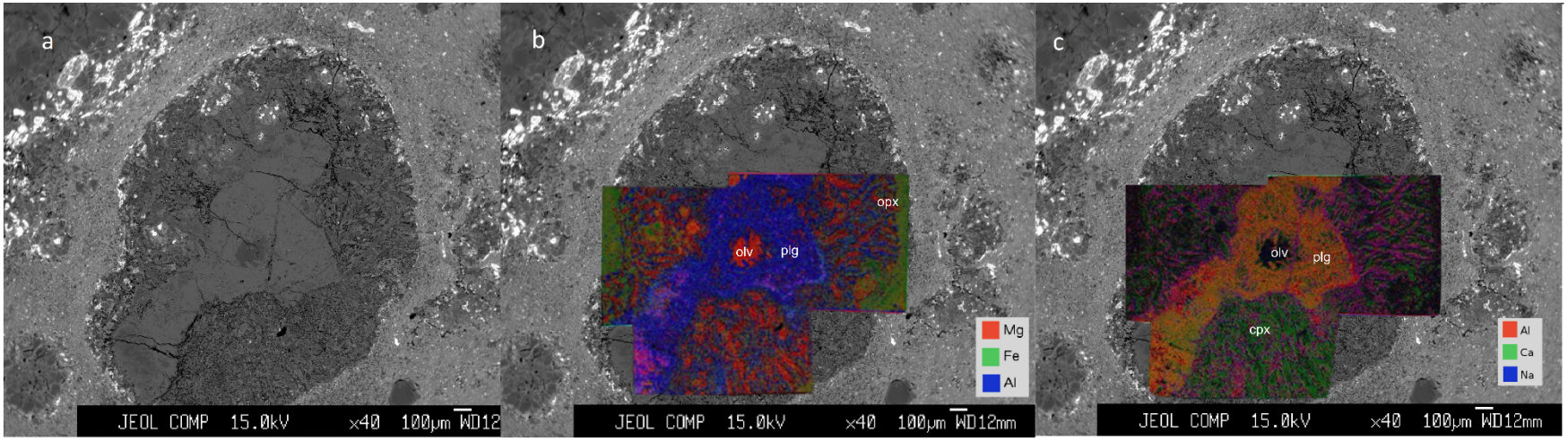

Figure 4: SEM image (a) of Al3-06. EDS map overlay displaying Mg (red), Fe (green) and Al (blue) concentrations (b). EDS map overlay of Al (red), Ca (green) and Na (blue) (c).

Figure 5: SEM image (a) of Al3-03. EDS map with overlain Mg (red), Fe (green) and Al (blue) (b). EDS map overlay of Al (red), Ca (green) and Na (blue) (c).

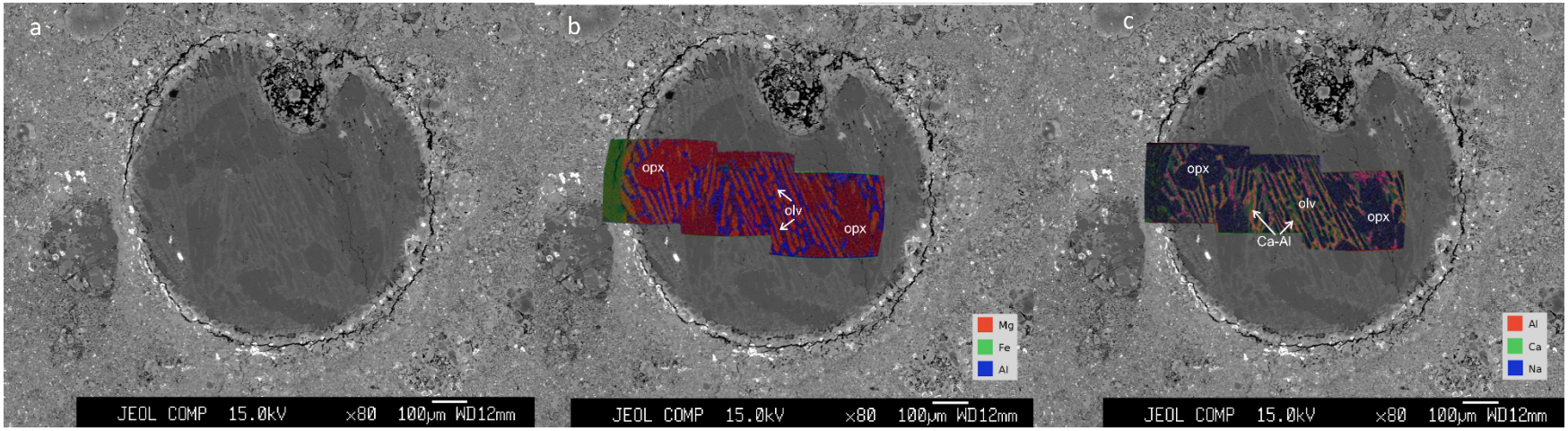

Silicate groundmass. Al3-03 contains a porphyritic texture with elongated, sub-parallel, skeletal olivine grains. Al3-03 also contains anhedral rounded and elongated orthopyroxene, with some small calcium-aluminum-rich silicates in the matrix. These minerals are visible under a petrographic microscope, and were further identified using WDS point analysis. The distribution of major elements such as Mg, Al, Na, Ca, and Fe are shown in figure 5b and 5c. Mg is displayed as red, and the intensity of the colour is proportional to the concentration of Mg in each mineral. The distribution of minerals such as olivine and pyroxene are therefore visible within figure 5b, where olivine is depicted as a bright red colour and orthopyroxene as a darker red. Al is displayed as blue (Fig. 5b), and is concentrated within the groundmass surrounding the olivine and orthopyroxene phenocrysts. Fine-grained clinopyroxene crystals and very fine-grained calcium-aluminum-rich silicates can be seen within the crystalline groundmass. Fe is displayed as green (Fig. 5b), and is mainly concentrated around the rim of the chondrule, and not in the ferromagnesium minerals. Na is displayed as blue and Ca is displayed as green, and are both seen between the skeletal olivine and orthopyroxene grains (Fig. 5c). The distribution is similar to that Al (Fig. 5b). In Figure 5c, Al is displayed as red and is often mixed with Ca to create an orange colour. This orange colour is representative of the calcium-aluminum rich silicates present in the groundmass. Na is also present in small amounts within the orthopyroxene phenocrysts.

Allende sample Al3-06 seen in Figure 4a has a slightly irregular, rounded shape and has a diameter of ~1mm. Al3-06 contains a large central aggregate of fibrous calcium-aluminum- rich silicate minerals surrounding a cluster of olivine crystals. Surrounding the

large calcium- aluminum- rich aggregate are fine-grained prismatic orthopyroxene crystals. These minerals were identified primarily using WDS point analysis due to their very fine grain size. Mg in figure 4b is displayed as red, Al as blue and Fe as green. Magnesium is concentrated in the center of the large aggregate feature, as well as in the orthopyroxene grains surrounding the aggregate. In Figure 4c, Al is represented as red, Ca as green and Na as blue. Ca and Al concentrations highlight the fine-grained, fibrous nature of the calcium – aluminum rich silicate aggregate displayed as yellow; a combination of Ca (green) and Al (red). Some of the calcium-aluminum-rich silicates within Al3-06 had compositions very close to that of anorthite (see appendix for compositions). Ca, represented as green in figure 4c, is observed as part of the calcium-aluminum rich silicate aggregate in the center of the chondrule (yellow), as well as in a separate phase (green) without Al in surrounding minerals. The green phase within Figure 4c is most likely a Ca-rich clinopyroxene. A purple phase is also present in the minerals surrounding the aggregate, represented as a combination of Al (red) and Na (blue). This Na and Al phase may be Na-rich clinopyroxene, however this was not analyzed using WDS point analysis.

Allende chondrule Al3-07 (Fig. 6a) is a rounded aggregate of olivine and orthopyroxene crystals with a very fine-grained calcium-aluminum-rich silicate groundmass filling between the grains. Al3-07 appears to be slightly more altered than the other chondrules, due to its texture and slight visible changes in the rims of the olivine crystals within the SEM image. The rim of Al3-07 appears to show a reaction or melt rim, and has many very fine-grained pieces of orthopyroxene protruding into it. Figure 6b shows Mg as red, Fe as green and Al as blue. Mg is observed in two phases, olivine and

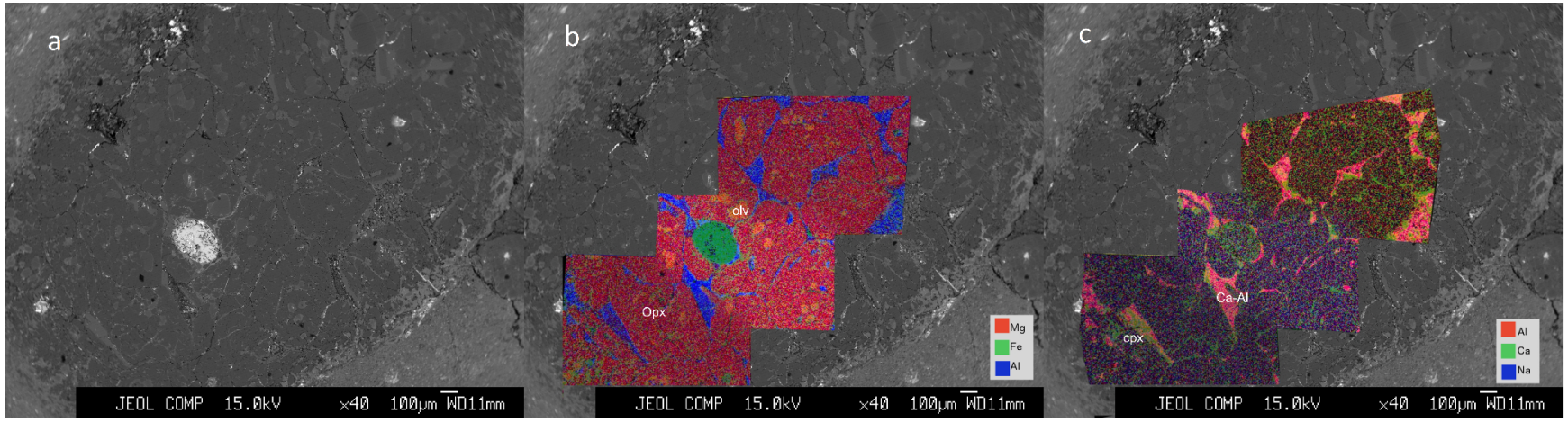

Figure 7: SEM image (a) of Al3-02. EDS map with overlain Mg (red), Fe (green) and Al (blue) (b). EDS map overlay of Al (red), Ca (green) and Na (blue) (c).

Figure 6: SEM image (a) of Al3-07. EDS map with overlain Mg (red), Fe (green) and Al (blue) (b). EDS map overlay of Al (red), Ca (green) and Na (blue) (c).

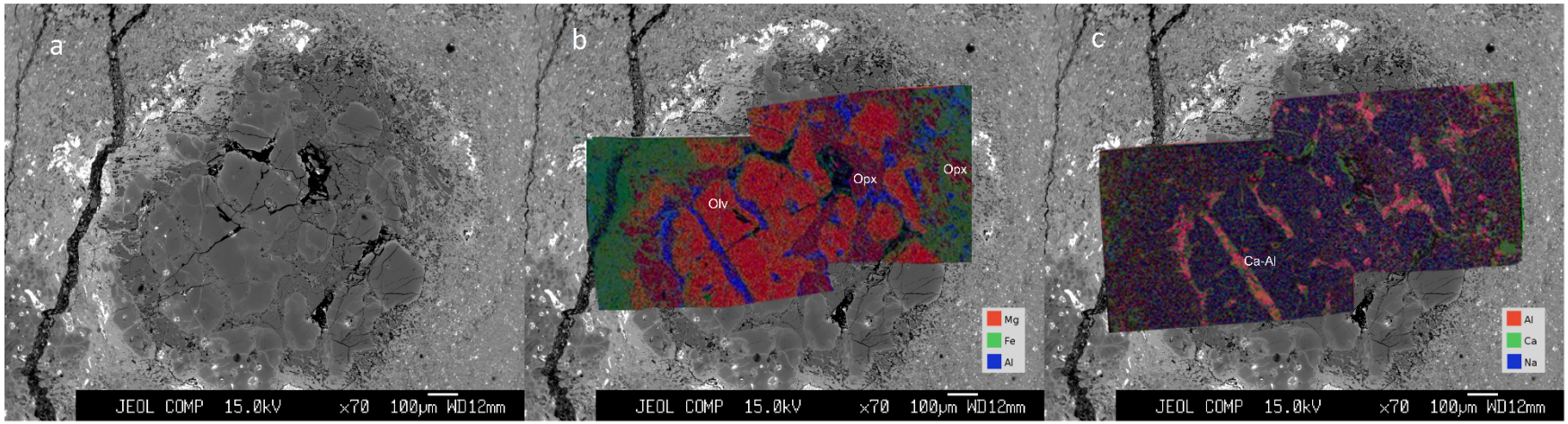

orthopyroxene. Olivine and orthopyroxene minerals are both identifiable under a petrographic microscope, and were identified using WDS point analysis. The brighter (pinkish) red phase seems to correlate to the olivine crystals, and the darker red phase correlates to the orthopyroxene phase. The rims of the olivine crystals appear to have a slightly increased concentration of Fe, shown in green on Figure 6c. Al (blue) is concentrated between the olivine and orthopyroxene grains (Fig. 6c). In figure 6c, Al is represented as red, Ca as green and Na as blue. Most of the Ca, Al and Na are concentrated within the very fine-grained groundmass between some of the olivine and pyroxene crystals. These minerals were primarily using WDS analysis as calcium-aluminum-rich silicates.

Chondrule Al2-01 is rounded with a diameter of ~2mm, seen in Figure 7a. Al2-01 contains fine-grained, angular, olivine and clinopyroxene crystals, in a very fine-grained calcium-aluminum-rich silicate, crystalline groundmass. These minerals were identified using major element data collected using WDS point analysis. EDS maps show the distribution of major elements such as Mg, Fe, Al, Ca and Na (Fig. 7b and 7c). The distribution of Mg (red), Fe (green) and Al (blue) are displayed in figure 7b. Olivine appears as a light pink/red colour and clinopyroxene is displayed as a dark red colour (Fig. 7b). Al (blue) is mainly concentrated between the olivine and clinopyroxene phenocrysts, and appears as a second phase with Mg (red), concentrating in what is most likely a pyroxene end member (purple). Iron (green) is concentrated in the rim of the chondrule, and also in small inclusions within the very-fine calcium-aluminum-rich ground mass. Figure 7c displays the distribution of Al (red), Ca (green) and Na (blue) within Al2-01. Ca and Al occur in one phase (yellow) showing the distribution of the calcium-aluminum-rich

silicates. In Al2-01 the calcium-aluminum-rich silicates are also very similar in composition to anorthite. Ca (green) is also visible in a separate phase within the orthopyroxene crystals. Al (red) and Na (blue) are both present in pyroxene (purple).

Chondrule Al2-02 is a larger, round chondrule, with a diameter of ~2mm (Figure 8a). Al2-02 contains fine-grained, orthopyroxene crystals and some smaller rounded olivine crystals, with a very fine-grained calcium-aluminum-rich silicate and clinopyroxene cryptocrystalline groundmass. The distribution of major elements can be seen in Figure 8b and 8c. Mg is represented as red in figure 8b, Fe as green and Al as blue. Mg is concentrated within the olivine and orthopyroxene crystals, which were identified using WDS point analysis. Olivine is displayed as a bright red/orange colour and orthopyroxene is the dominant red mineral within the chondrule (Fig. 8b). Al (blue) in figure 8b is concentrated between the olivine and orthopyroxene grains, filling the surrounding space. Fe (green) is concentrated in a large, round; metal alloy in the center of the EDS maps (Fig. 8b), and appears to concentrate around some olivine rims, not just around the rim of the chondrule. Figure 8b shows the distribution of Al, Ca and Na within Al2-02. Al is represented as red, Ca as green and Na as blue. From Figure 8c, we can observe the concentration of Al and Ca between the grain boundaries of orthopyroxene and olivine, concentrating in calcium-aluminum-rich silicates (pink) and Ca in a separate phase (green) most likely concentrating in a calcium end member of clinopyroxene.

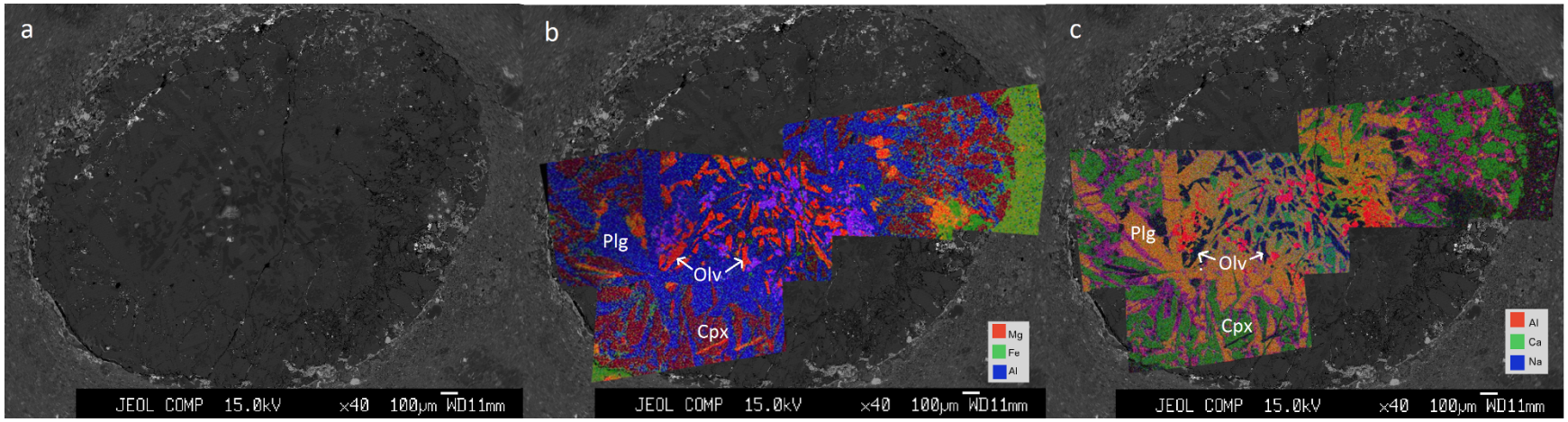

Figure 8: SEM image (a) of Al3-03. EDS map with overlain Mg (red), Fe (green) and Al (blue) (b). EDS map overlay of Al (red), Ca (green) and Na (blue) (c).

5.0 Results

5.1 TAS Classification of Chondrules

Each of the 5 chondrules analyzed from Allende were treated as individual rocks, where the surrounding matrix and other features of the chondrite were not taken into account. Chondrule bulk-rock data was collected using major element EDS analysis over several areas of each chondrule (whole rock compositions in appendix). Reed and Ware (1974), state that the accuracy of EDS is within ~2%. The total alkalis ($Na_2O + K_2O$) were plotted against silica (SiO_2) content to obtain a volcanic rock TAS classification for each

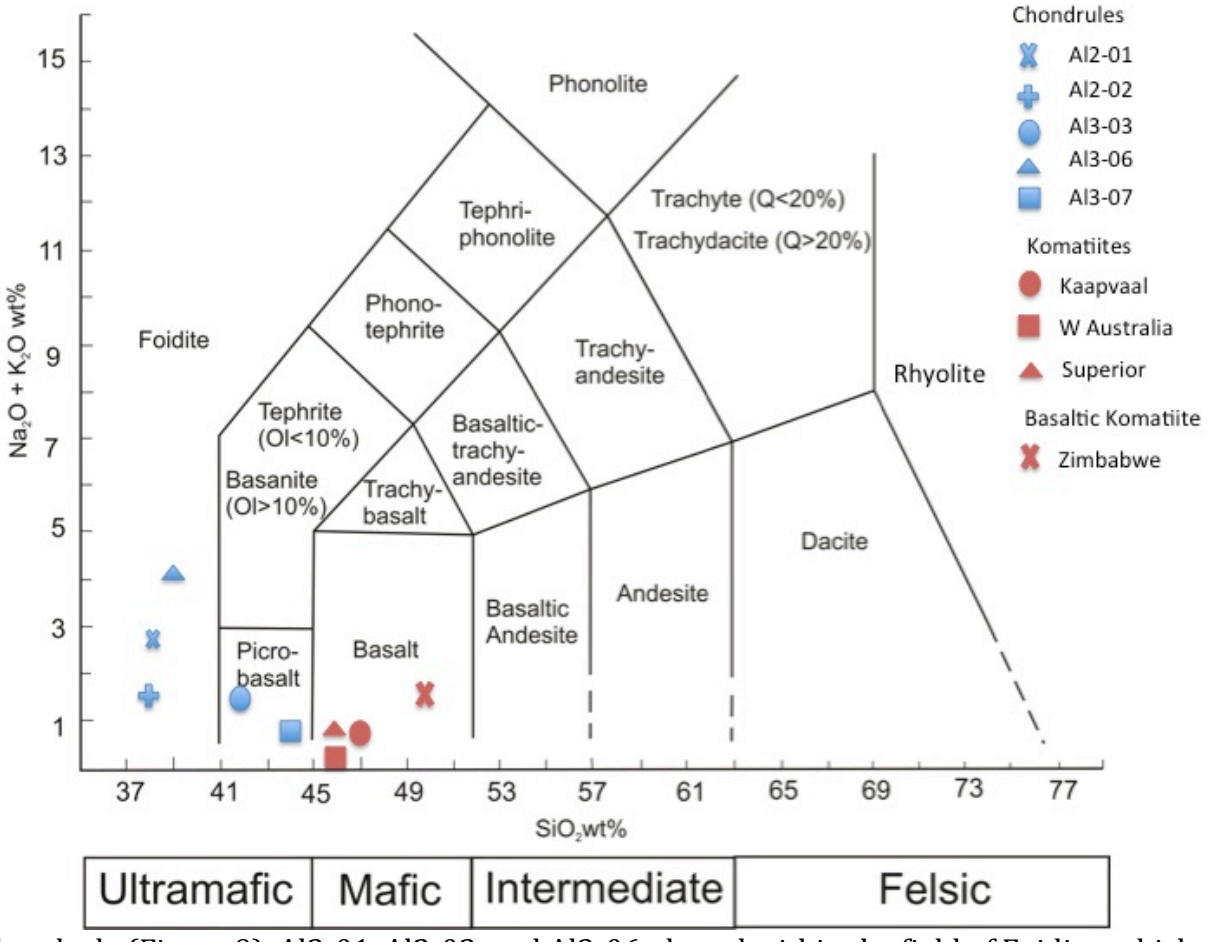

Figure 9: TAS classification diagram modified from Le Bas (1985). Chondrules are represented as blue markers, and Archean mafic rock samples as red markers.

are ultramafic rocks and have silica content less than 41%. Al3-03 and Al3-07 both plotted in the field of picrobasalts, which are also ultramafic rocks with slightly higher silica content than Foidites (41-45% SiO_2). As seen in Figure 9, most of the chondrules have similar silica and alkali concentrations, however Al3-06 has significantly more alkalis than the other chondrules. Komatiite data from Kaapvaal, Western Australia, Superior Greenstone belt and Zimbabwe craton were also plotted on the TAS diagram for comparison. The samples from Kaapvaal, Superior and Western Australia Archean cratons plot within the basalt field, very close to the picrobasalt – basalt field line. These Komatiite samples plot closely to that of Al3-07 and Al3-03 chondrules (Figure 9), meaning they have comparable bulk silica and total alkali content to that of the chondrules. The data from the Zimbabwe craton contained Archean aged basalt, basaltic komatiite and komatiite rock types. The samples from the Zimbabwe craton plot in the TAS diagram as basalt, close to the basalt-andesite line, away from Kaapvaal, Superior and Western Australia. Kaapvaal, the oldest Archean Komatiite sample at (3.4 Ga) plots with higher silica content than any of the chondrule samples. Generally, the chondrules are not very different in composition than the komatiites when plotted on the TAS diagram. The chondrules and Archean rocks plot with similar total alkali contents, all plotting lower than a total alkali weight% of 4. The total Silica content in the chondrules and Archean rocks had a spread of about 10%, with the majority of values plotting between 41% and 47% SiO_2 Wt%.

5.2 Magnesium number

The magnesium numbers for olivine, orthopyroxene and 'whole-rock' for each chondrule was calculated using the formula (MgO/ MgO+ FeO) (in Wt%O) from Rollinson

(1993), as well as the magnesium numbers for olivine and whole rock were calculated for each

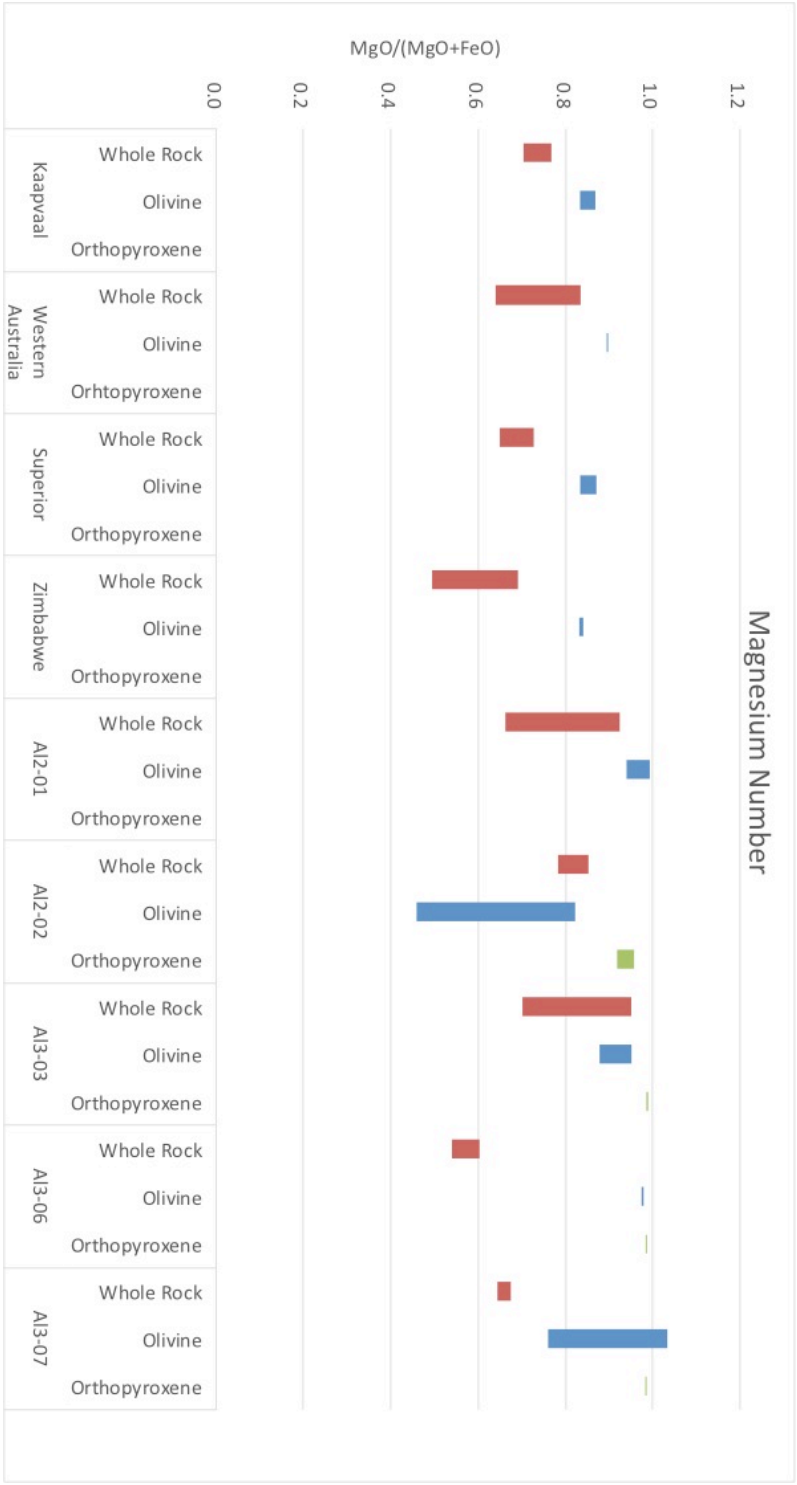

Figure 10: Magnesium numbers calculated for whole rock and olivine for Archean samples. Magnesium numbers calculated for whole rock, olivine and orthopyroxene for chondrules.

komatiite sample (Fig. 10). Magnesium numbers are a ratio with values between 0 – 1. A high magnesium number indicates that there is a high ratio of Mg in a sample compared to Fe (Rollinson, 1993). Komatiite whole-rock magnesium numbers plot between 0.6 and 0.73, with the highest magnesium number corresponding to the oldest komatiite sample, Kaapvaal. Zimbabwe whole-rock magnesium numbers plotted much lower than the other komatiite data, at around 0.58. Chondrule whole-rock magnesium numbers plot between 0.57 and 0.82. Al2-01, Al2-02, Al3-03 have higher whole- rock magnesium numbers than Al3-06 and Al3-07, plotting between 0.79 and 0.82. Al3-06 and Al3-07 plot between 0.57 and 0.65, which is similar to, and slightly lower than Zimbabwe komatiite whole-rock magnesium numbers. In general, the magnesium numbers for olivine in chondrules were higher than that of olivine in the komatiite samples. Komatiite olivine magnesium numbers plotted between 0.83 and 0.89 with the majority of values plotting around 0.85. Chondrule olivine magnesium numbers plot between 0.64 and 0.97 with the majority of values plotting between 0.90 and 0.97. Chondrule Al2-02 olivine magnesium number plots much lower than any of the other chondrule or komatiite olivine magnesium numbers at 0.64. Orthopyroxene olivine numbers were also calculated for each chondrule, but not for komatiite samples due to the lack of orthopyroxene data present in those samples. The chondrule orthopyroxene magnesium numbers generally higher than that of the chondrule olivine magnesium numbers, with values from 0.93 – 0.98. Al3-03, Al3-06 and Al3-07 all plotted around 0.98, and Al2-02 plotted lower at 0.93. These are especially high values, very close to 1, meaning there is almost 100% Mg when Mg and Fe concentrations are compared in the samples. Overall, the magnesium numbers are comparable between the

chondrules and Archean mafic rocks. The chondrules show greater spread in values, but on average are very similar to that of the Archean mafic rocks.

5.3.1 Olivine and Orthopyroxene Zoning within chondrules

Within the chondrules, the minerals appear to be in equilibrium, and do not show any textural zoning features. If the minerals were zoned, the concentrations of major and trace elements would be different in the core and the rims, rendering calculations of distribution coefficients difficult. Line scans were taken from the core to the rim of olivine and orthopyroxene crystals using WDS analysis to ensure that there was no zoning present. Figure 11 displays examples of line scans completed on olivine and orthopyroxene minerals within the chondrules. Figure 11 shows the concentration of major elements in olivine and pyroxene are constant within the chondrules, meaning they are not zoned.

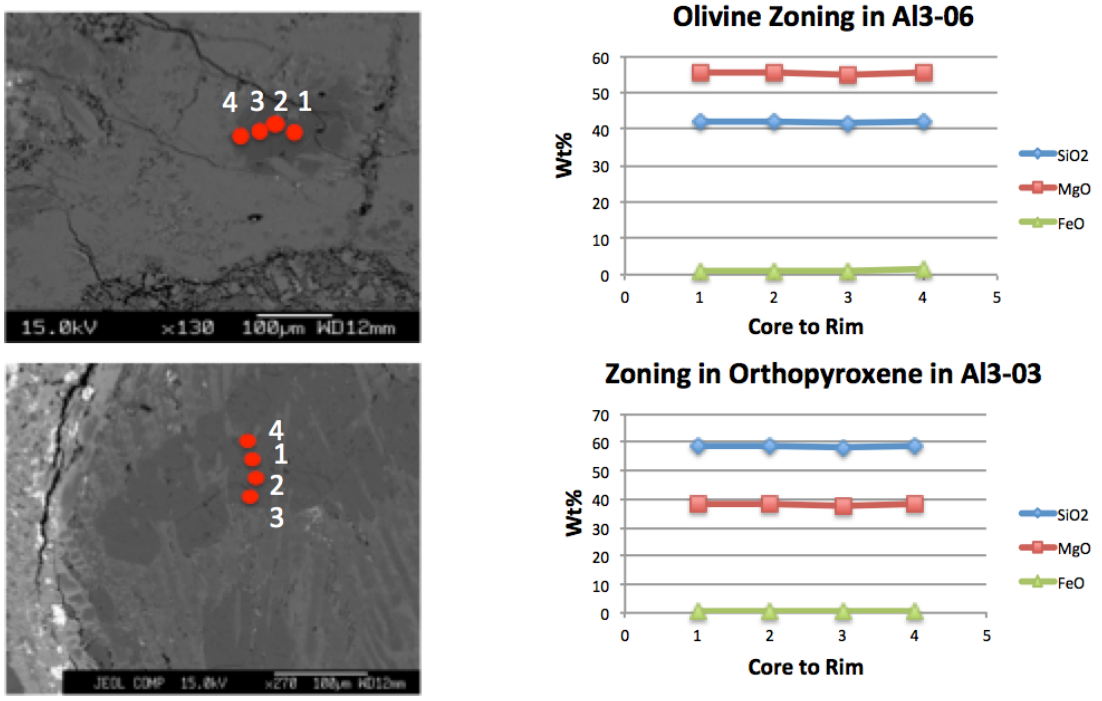

Figure 11: Concentrations of SiO2, MgO, and FeO are constant from core to rim of olivine in Al3-06 and orthopyroxene in Al3-03.

5.3.2 Two-pyroxene Thermometer Results

The crystallization temperature was calculated for chondrules Al2-02, Al3-03, Al3-06 and Al3-07 using Wells' (1977) two-pyroxene thermometer (calculation in appendix). Wells (1977) reports that the two-pyroxene thermometer can calculate crystallization temperatures within 70°C. This thermometer can be used to obtain a crystallization temperature for the chondrules because the minerals appear to be in equilibrium. Within the chondrules there doesn't appear to be any zoning within the olivine and orthopyroxene minerals, and textures indicate rapid cooling rather than quenching. There is no glass found within the chondrules, they are micro lithic features, and therefore are not displaying quenching textures. Major element data were used from orthopyroxene and clinopyroxene minerals in the chondrules for the temperature calculations. The crystallization temperature for Al2-01 could not be calculated using this method because there were no orthopyroxene crystals identified within the chondrule. The calculated crystallization temperature for Al2-02, Al3-03, Al3-06 and Al3-07 were 1132.89°C±70°C, 784.53°C±70°C, 1271.00°C±70°C, and 1054.46°C±70°C respectively. The temperatures between chondrules are very similar, with an average value of 1060.72°C±313.72°C. Al3-03 has an anomalously low temperature of 784.53°C±70°C. This is most likely because it contains ferroan augite crystals, which have very low magnesium concentrations. This causes the magnesium number to be lower in Al3-03 for clinopyroxene, and drops the temperature using this thermometer. With the anomalous value removed, the average temperature is 1152.78°C±179.63°C. This value is comparable to that of Alkali basalts with glass, orthopyroxene, clinopyroxene and olivine have a crystallization temperature ~1130°C (French and Cameron, 1981). Hawaiite with glass, orthopyroxene, clinopyroxene and

olivine has a crystallization temperature of 1075°C, which is lower than the crystallization temperatures on average found in the chondrules (French and Cameron, 1981).

5.4 Concentration of trace elements when normalized to CI chondrite

5.4.1 Chondrules

The average concentrations of trace elements (Ni, Mn, Ti, Cr) in olivine, orthopyroxene and pyroxene within each chondrule were normalized to CI chondrite. CI type was chosen for normalization based on the primitive nature of CI composition, and the lack of chondrules present within CI chondrites (Weisberg *et al*., 2006). Each chondrule is treated as an individual rock, and the surrounding matrix and other material are not taken into account. The trace elements in minerals within the chondrules are normalized to CI chondrite bulk composition shown in Rollinson (1993), originally from Wood *et al*. (1979) (Appendix). By using normalization factors, comparison between chondrules and komatiites is possible. When chondrite-normalized element concentrations found in a certain mineral are lower than 1 (bulk- rock of CI), then the mineral is considered to be depleted in that element compared to CI. The standard deviation of each concentration was calculated and reported in table 17 (appendix).

In figure 12a, we can see that olivine is depleted in Ni relative to CI in the chondrules with values ranging from 0.005-0.02. Olivine is also depleted in Mn within the chondrules compared to CI, however these values are higher than that of Ni and range from 0.03- 0.65. Ti concentrations normalized to CI show that olivine in generally around equilibrium and enriched in Ti within the chondrules, with values ranging from 0.88- 2.12.

The concentrations of Cr in olivine for chondrules normalized to CI are spread around 1, with values ranging from 0.32- 4.48. Al2-02 and Al3-03 have olivine enriched in Cr

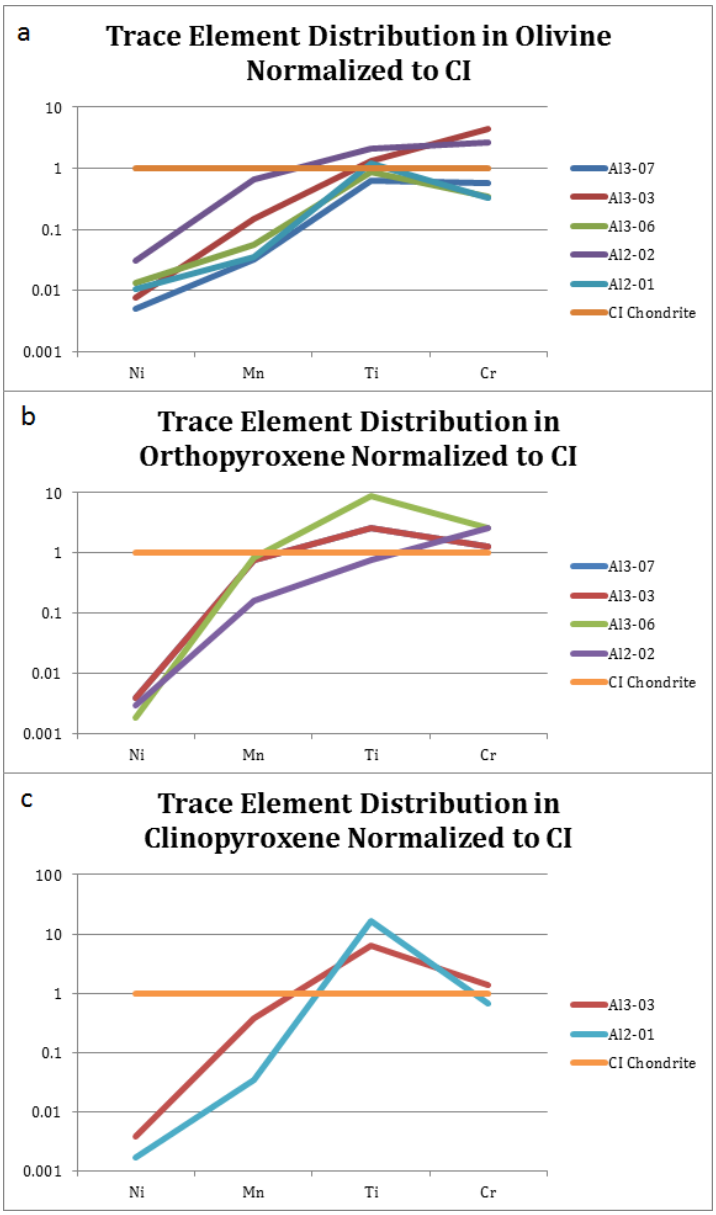

Figure 12: Averaged concentrations of trace elements normalized to CI within olivine, orthopyroxene and clinopyroxene within each chondrule. Standard deviations for each point recorded in appendix Table 16.

compared to CI, whereas Al2-01, Al3-06, and Al3-07 have olivine depleted in Cr when normalized to CI.

Trace element concentrations in clinopyroxene for chondrules were also normalized to CI (Fig. 12b). Orthopyroxene is also depleted in Ni compared to CI, with values ranging from 0.001-0.03. Mn concentrations in orthopyroxene within the chondrules range from 0.16 – 1.0 when normalized to CI. Al2-02, and Al3-07 contain orthopyroxene that is depleted in Mn, whereas AL3-06 and Al3-03 contain orthopyroxene with Mn values of 1.0, which mean they are at equilibrium with the composition of whole-rock CI. The chondrules contain orthopyroxene with Ti concentrations ranging from 0.78 – 8.93 when they are normalized to CI. The majority of chondrules contain orthopyroxene that is enriched with Ti when compared to CI. Cr concentrations within orthopyroxene found in the chondrules are between 1.0 and

2.65 when normalized to CI. All of the chondrules show orthopyroxene enriched in Cr compared to the bulk-rock composition of CI.

Trace element concentrations in clinopyroxene for chondrules Al3-03, and Al2-02 were normalized to CI (Fig. 12c). The concentration of Ni in clinopyroxene for both chondrules ranges from 0.001-0.003 when normalized to CI, indicating that clinopyroxene in the chondrules are depleted of Ni compared to CI bulk-composition. The concentration of Mn in clinopyroxene for the chondrules when normalized to CI ranged from 0.03 – 0.37, which is higher than the concentration of Ni. These values indicate that Mn in clinopyroxene for the chondrules Al3-03 and Al2-01 is depleted compared to that of CI composition. The concentrations of Ti in clinopyroxene for Al3-03 and Al2-01 were both extremely high when normalized to CI, ranging from 6.49 – 16.6. High values such as these indicate that clinopyroxene in the chondrules are very enriched in Ti when compared to the bulk composition of CI. Cr concentrations were also normalized to CI for Al2-01 and Al3-03 in clinopyroxene, and ranged from 0.65 – 1.34. Al3-03 contained clinopyroxene with higher concentrations of Ti (>1), and indicates that the clinopyroxene minerals were enriched in Cr compared to the CI bulk-rock composition. Al2-01 contains clinopyroxene with lower concentrations of Ti (<1), indicating that the clinopyroxene in Al2-01 is depleted in Cr compared to that of CI composition.

5.4.2 Archean-aged komatiites and basaltic komatiites normalized to CI

The concentrations of trace elements within olivine and clinopyroxene for Archean-aged komatiites, and basaltic komatiites were normalized to the bulk-rock composition of CI due to its primitive composition. Trace element (Ni, Mn, Ti, Cr) concentrations in olivine

were normalized to the bulk composition of CI (Fig. 13a). Olivines in the Archean-aged cratons show Ni concentrations clustered around 0.3, indicating that olivine in komatiites are depleted in Ni relative to CI. Olivine in the Archean-aged rocks also show depletion of Mn compared to CI, with values ranging from 0.25 – 0.65. Archean-aged rocks contain olivine with Ti concentrations that when normalized to CI, show a large spread. The concentrations of Ti in olivine range from 0.03 – 2.06, with the majority of cratons containing olivine with a Ti concentration <1.

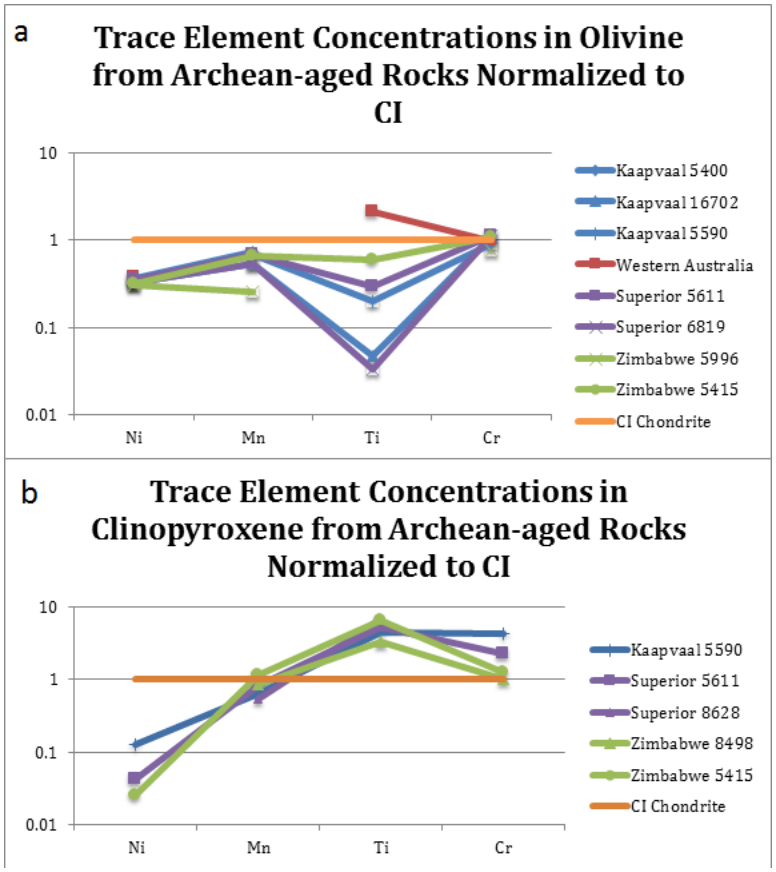

Figure 13: Trace element concentrations normalized to CI for olivine and clinopyroxene in Archean aged mafic rocks.

The Western Australian craton contains olivine with a Ti concentration of 2.06 when normalized to CI, demonstrating that this craton contains olivine that are more enriched in Ti than the bulk composition of CI. Olivines within the Archean-aged cratons have Cr concentrations clustered around 1, with values ranging from 0.76 – 1.11 when normalized to CI. Most olivines show Cr concentrations that are around 1, indicating that the olivines in the cratons are generally slightly enriched in Cr compared to CI or are close to equilibrium.

Trace element concentrations in clinopyroxene for the Archean cratons were normalized to CI and plotted in figure 13b. Ni concentrations when normalized to CI range from 0.02 – 0.12 in clinopyroxene for the Archean cratons, indicating that clinopyroxene is depleted in Ni compared to the bulk composition of CI. The Archean cratons contain clinopyroxene with Mn chondrite-normalized concentrations ranging from 0.52 – 1.12. Zimbabwe (5415) is the only craton containing clinopyroxene that has concentrations of Mn >1 when normalized to CI. Kaapvaal, Superior and Zimbabwe (8498) all have Mn concentrations <1, indicating that the majority of the Archean cratons have clinopyroxene depleted in Mn compared to the bulk composition of CI. TI concentrations normalized to CI ranged from 3.33 – 6.35 in the Archean cratons. These values demonstrate that clinopyroxene in the Archean cratons are enriched in Ti compared to CI. The chondrite-normalized concentrations of Cr range from 1.0- 4.29 in clinopyroxene within the Archean cratons. These values indicate that Cr in clinopyroxene within the Archean cratons range from being at equilibrium with the bulk composition of CI to more enriched in Cr than CI.

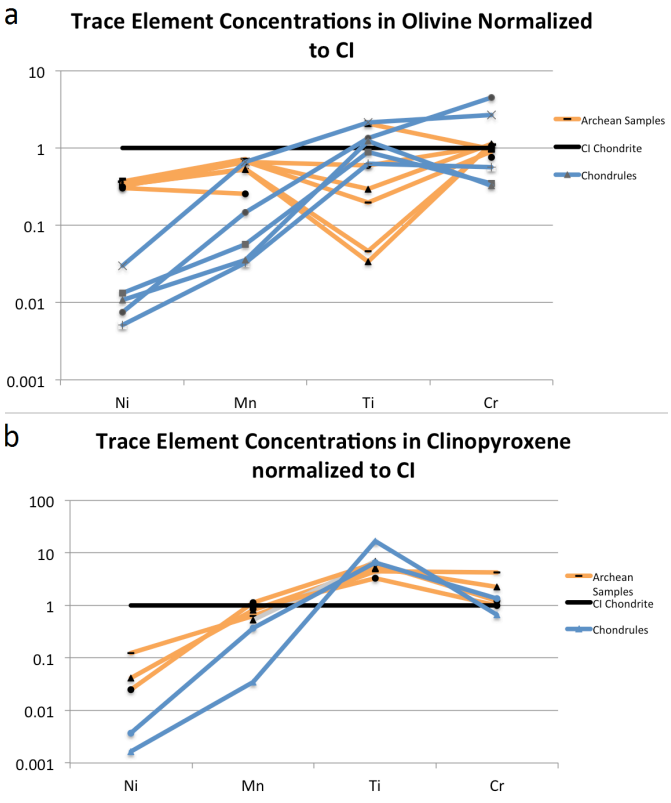

Figure 14: Concentrations of trace elements in olivine (a) and clinopyroxene (b) for chondrules and Archean samples. This image shows that the Archean samples (orange) are depleted in Ni within olivine, however not nearly as much as in the chondrules (blue). Ti concentrations in olivine for chondrules are enriched when normalized to CI, unlike the Archean samples, which contain olivine with depleted Ti when normalized to CI.

5.5 Distribution Coefficients in Chondrules

5.5.1 Distribution coefficients for minerals in chondrules

Distribution coefficients (Kd's) were calculated using the Nernst equation (Rollinson, 1993): $K_d = C_{Mineral}^{Element} / C_{Whole\ rock}^{Element}$. The Nernst equation was used because the olivines in the chondrules did show significant zoning. The average distribution coefficient of trace elements such as Ni, Mn, Ti and Cr were found for each chondrule of Allende in olivine, orthopyroxene and clinopyroxene. The standard deviations for each distribution coefficient calculated for the chondrules is reported in Table 16 (appendix). If the distribution coefficient of an element is less than 1, then it is incompatible and has an affinity to be in the melt, whereas a distribution coefficient of 1 or greater implies that the element is compatible and has an affinity to be in the mineral phase (Rollinson, 1993).

The distribution coefficients for trace elements in olivine, orthopyroxene and clinopyroxene for chondrules were calculated and plotted in Figure 15. It can be observed in Fig. 15a that Ni in olivine has very low Kd's in all chondrules, with Kd's mostly around 0.1. Al3-07 has especially low Kd value for Ni in olivine than the other chondrules, with a Kd of ~0.01. All of the chondrules contain olivine with low Ni distribution coefficients, which implies that Ni is incompatible with the mineral phase. Al2-02, Al2-01, and Al3-03 all contain olivine crystals with high Mn Kd's, ranging from 1 – 3.36; Whereas Al3-06 and Al3-07 have olivine crystals with low Mn Kd's ranging from 0.17 – 0.45. Al2-01, Al2-02 and Al3-03 contain olivine with Mn Kd's >1, indicating that Mn is compatible with the mineral phase, whereas Al3-06 and Al3-07 contain olivines with Mn <1, indicating that Mn is incompatible with olivine. The Kd values for Ti in olivine for the chondrules have a large spread, ranging from 0.008 – 2.99. Al2-01 has the lowest Ti Kd value (0.008) in olivine,

indicating that Ti is incompatible with olivine in Al2-01. Al3-06, Al3-07, Al3-03 also contain olivine crystals with low Ti Kd values of 0.08, 0.37, 0.46 respectively. Al2-02 contains olivine crystals with a high Kd for Ti, 2.994. The distribution of Cr in olivine within each chondrule can also been observed in Fig. 15a. There is a spread of Kd values for Cr in olivine, ranging from 0.22 – 3.05. Al3-07, Al2-01 and Al3-06 contain olivine crystals with low Cr Kd's (<1), whereas Al3-03 and Al2-02 have olivine crystals with high Cr Kd's (>1). The general trends seen in the trace element distributions in olivine within the chondrules are negative anomalies in Ni, increasing Kd values approaching Mn; Decreasing Kd values towards Ti for Al3-03, Al3-06, and Al2-01, and increasing Kd values for Al2-

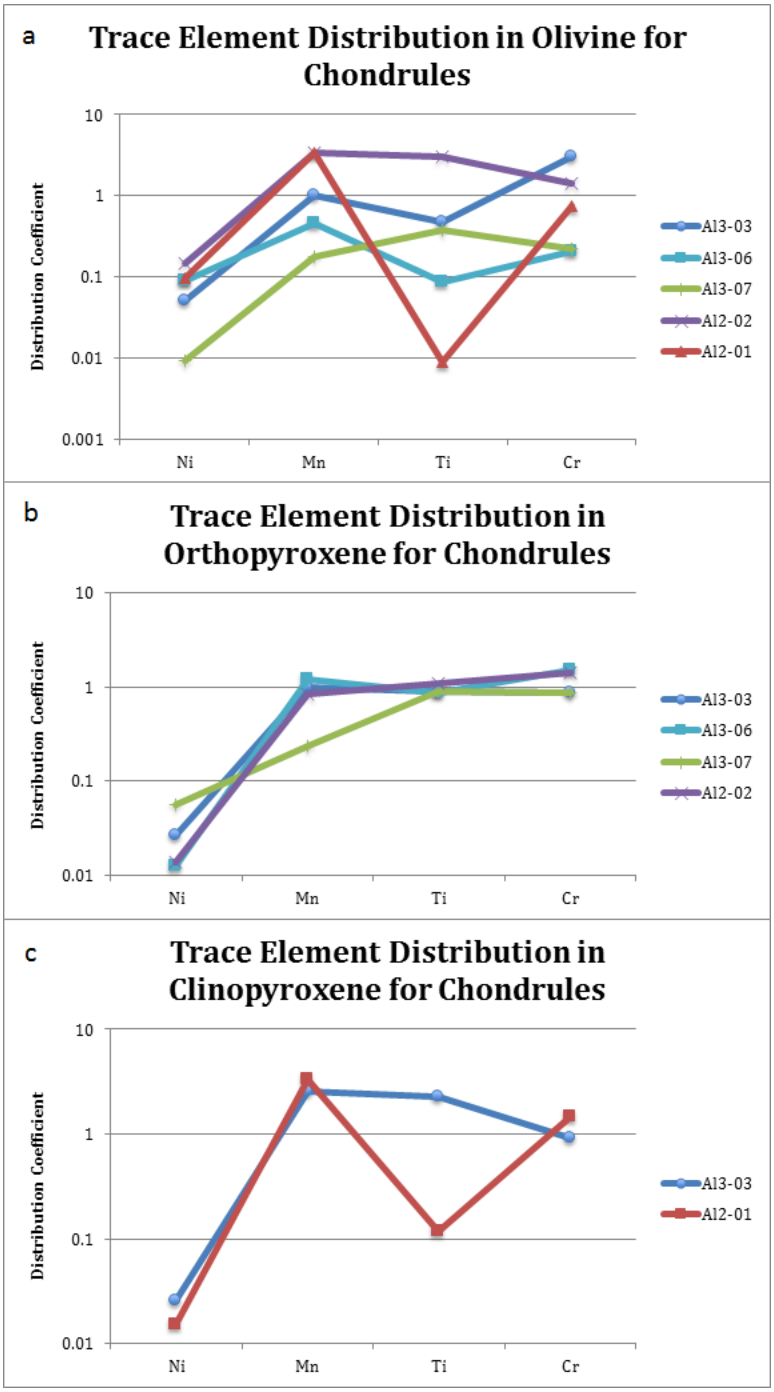

Figure 15: Averaged distribution Coefficients (Kd's) of trace element in olivine, orthopyroxene and clinopyroxene in chondrules. Standard deviations recorded in appendix.

02 and Al3-07 towards Ti; and Increasing values for Al2-01, Al3-06, and Al3-03 towards Cr, decreasing Kd values for Al3-07, Al2-02 towards Cr.

Distribution coefficients for Ni, Mn, Ti, and Cr were also calculated in orthopyroxene for each chondrule (Fig. 15b) except for Al2-01, because it did not contain orthopyroxene. The distribution coefficients in orthopyroxene show less spread than that of olivine for each trace element. The Kd values for Ni in orthopyroxene range from 0.01 – 0.05, showing that Ni is incompatible with orthopyroxene in all 4 of the chondrules. The Kd values for Mn in orthopyroxene are mostly concentrated around 1, except for Al3-07, which has a lower Kd around 0.23. Al3-03 and Al2-02 have Kd values around 0.84, and Al3-06 has a Kd slightly over 1, at 1.22. All of the chondrule Kd's for Ti in orthopyroxene are clustered around 1, with values ranging from 0.86 – 1.09. Al3-03, Al3-06, and Al3-07 contain orthopyroxene with Kd's for Ti that are all slightly below 1, with values of 0.86, 0.90, and 0.91 respectively. Al2-02 contained orthopyroxene with Ti that had a Kd value of 1.09, meaning Ti is compatible with orthopyroxene in the chondrule. The distribution of Cr in orthopyroxene for Al2-02 is similar to that of Cr in orthopyroxene for Al3-06, with values of 1.41 and 1.53 respectively. Al3-03 and Al3-07 have similar Kd values for Cr in orthopyroxene of 0.88 and 0.87 respectively. Al2-02 and Al3-06 both contain orthopyroxene minerals with Cr Kd's >1, indicating that Cr is compatible with orthopyroxene, compared to Al3-07 and Al3-03, which contain orthopyroxene with Cr Kd's <1, indicating that Cr is incompatible with orthopyroxene. The general trends of the distribution of Ni, Mn, Ti and Cr in orthopyroxene are very low Kd's for Ni; increasing Kd toward Mn, with some chondrules having Mn compatible with orthopyroxene; generally

decreasing Kd values toward Ti with most values around 1.0; slight increase in Kd values toward Cr.

Trace element data was also collected for clinopyroxene minerals in Al2-01 and Al3-03 (Fig. 15c), and distribution coefficients were calculated. The distribution of Ni in clinopyroxene for Al2-01 and Al3-03 were 0.015 and 0.02 respectively. The Kd values of Ni in clinopyroxene show that Ni is incompatible with clinopyroxene in Al2-01 and Al3-03. The Kd values for Mn in clinopyroxene for Al2-01 and Al3-03 are much higher than that of Ni, at 3.33 and 2.59 respectively. Kd values for Mn in clinopyroxene within Al2-01 and Al3-03 show that Mn is compatible with clinopyroxene. The Kd values for Ti have a large spread in clinopyroxene between Al2-01 and Al3-03, with values of 0.11 and 2.27 respectively. Al3-03 Kd values show that clinopyroxene is compatible with Ti, whereas clinopyroxene in Al2-01 is incompatible with Ti. Kd values for Cr in clinopyroxene within Al2-01 and Al3-03 are similar, with Al2-01 having a Kd of 1.48, and 0.92 for Al3-03. These Kd values show that Al2-01 has Cr that is compatible with clinopyroxene, and Al3-03 has Cr slightly incompatible with clinopyroxene. The general trend for Kd values in clinopyroxene for Al2-01 and Al3-03 clinopyroxene show low Kd's for Ni; increasing Kd values towards Mn, with increasing compatibility; spread in Ti with Al3-03 having Ti compatible with clinopyroxene, and Al2-01 containing Ti incompatible with clinopyroxene; Kd values approaching 1 towards Cr, with Al2-01 containing clinopyroxene with compatible Cr, and Al3-03 containing clinopyroxene slightly incompatible with Cr.

The Kd's of Ni, Mn, Ti and Cr in olivine, clinopyroxene and orthopyroxene for the Allende chondrules can be compared in figures 15a, 15b, and 15c. Olivine, orthopyroxene and clinopyroxene all show low Kd's for Ni, indicating that Ni may be incompatible in these

mineral phases. Mn in olivine has a large spread, with some olivine in chondrules enriched, and some depleted in Mn. Orthopyroxene in each chondrule generally has Kd's for Mn around 1, or slightly depleted, and clinopyroxene has Kd's >1 for Mn in Al2-01 and Al3-03. Olivine is generally has Kd's <1 for Ti within the chondrules, except for in Al2-02. Each chondrule contains orthopyroxene with Ti Kd's mostly around 1, and between chondrules, clinopyroxene contains Ti Kd's with a large spread. Al3-03 contains clinopyroxene with Ti Kd's >1, and Al2-01 contains clinopyroxene with Kd's <1. Olivine, orthopyroxene and clinopyroxene all have Cr Kd's distributed on either side of 1. Olivine shows large spread, with Al3-03 and Al2-02 olivine containing Cr Kd's >1, and Al2-01, Al3-06 and Al3-07 olivine containing Cr Kd's <1. Orthopyroxene in each chondrule has a smaller spread between Cr Kd's, with values close to 1, and shows Al2-02 and AL3-06 orthopyroxene with high Kd values (>1) for Cr, and Al3-07 and Al3-03 orthopyroxene with low Cr values (<1).

5.5.2 Distribution coefficients in Archean rocks

The distribution coefficient (Kd) was calculated for 4 trace elements (Ni, Mn, Ti, Cr) in olivine and clinopyroxene within Archean-aged komatiites, and basaltic komatiites using the Nernst equation as shown in the previous section (Rollinson, 1993). The Kd values were calculated using bulk-rock and trace element data for different minerals from komatiites, basaltic komatiites, and Archean-aged basalt from Kaapvaal, Western Australia, Superior, and Zimbabwe cratons (Fig. 16a). Kd values were obtained for Ni in olivine and clinopyroxene for several areas in each craton. Kaapvaal had Kd's for Ni in olivine of 1.59, 1.71 and 2.27, all showing that Ni is compatible with olivine within the Kaapvaal craton. Western Australian craton had a Kd value for Ni in olivine of 1.97, also showing that Ni is

compatible in olivine. Kd values for Ni in olivine for Superior were 1.97 and 2.71, meaning Ni was compatible with olivine in the Superior craton. Zimbabwe craton had Kd's for Ni in olivine of 1.51, 2.48, and 7.34, demonstrating that Ni is compatible with olivine within the Zimbabwe craton. Kd values were calculated for Mn in each craton, and were concentrated slightly below 1. Kaapvaal had Kd values for Mn in olivine of 0.77, 0.84 and 0.85, all falling below 1. This could mean that Mn is incompatible with olivine in the Kaapvaal craton. The Western Australian craton did not have Mn concentrations in the corresponding olivine data, resulting in no Kd calculated for Mn in olivine for this craton. Superior craton had olivine with an Mn Kd of 0.74, which shows that Mn is slightly incompatible in olivine within Superior. Zimbabwe craton contained olivine with Mn Kd's of 0.31 and 0.83, both of which are <1, and may indicate that Mn is incompatible with olivine in the Zimbabwe craton. All of the Archean-aged cratons contain olivine that had Kd's <1 for Mn, however they are higher

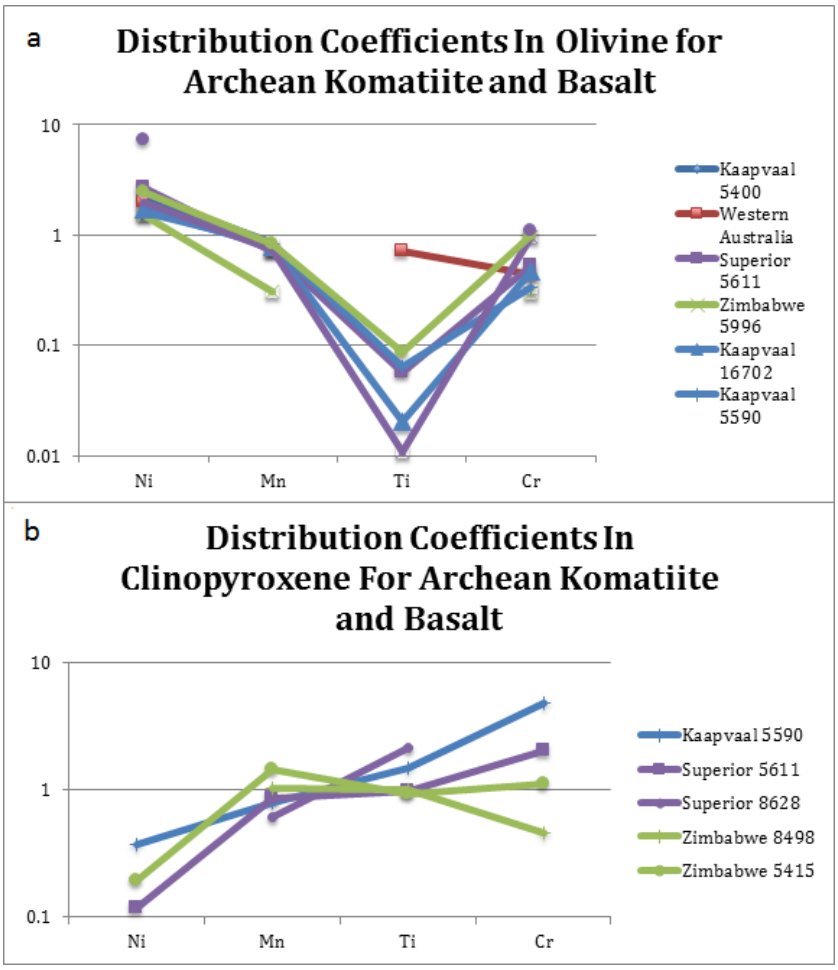

Figure 16: Distribution Coefficients for trace elements in olivine (a) and clinopyroxene (b) for the Archean craton samples

than Ni Kd's for olivine for the Archean cratons. Kaapvaal contain olivine with Kd's for Ti of 0.02 and 0.06, which demonstrate that Ti is incompatible with olivine in Kaapvaal. The Western Australian craton had a Kd of 0.71 for Ti in olivine, which was anomalously higher than any other Ti Kd for olivine in the Archean-aged cratons. This Kd however, is in trend with the other Archean olivine Kd values for Ti because it continues to show Ti incompatibility with olivine. Superior craton has olivines with Ti Kd's of 0.05 and 0.01, indicating that Superior also contains Ti that is incompatible with olivine. Zimbabwe craton had one sample site with Ti data in olivine minerals, and a Kd was calculated to be 0.08, demonstrating that the Zimbabwe craton also contains Ti that is incompatible with olivine. Kd values were also calculated for Cr in olivine for the Archean-aged cratons. Kaapvaal contains olivine with Cr Kd's of 0.53, 0.46 and 0.33, demonstrating a small spread in values, and Cr incompatibility with olivine in the craton. The Western Australian craton had olivine with a Cr Kd of 0.44, similar to Kaapvaal; also demonstrating that Cr is incompatible with olivine for the Western Australian craton. Superior contained olivine with calculated Cr Kd's of 0.52, 0.97 and 1.07, demonstrating a larger spread Cr of Kd's within a single craton. A Cr Kd of 0.52 is very similar to that of Kaapvaal and Western Australian cratons, however 0.97 and 1.07 are much higher values, and indicate that some olivine minerals have Cr that are close to equilibrium, or compatible with olivine compared to the bulk-rock. Zimbabwe craton contained olivine with Kd's of 0.29 and 0.98 for Cr, also demonstrating a large spread of Kd's between different sample sites similarly to Superior. A Cr Kd of 0.29 in olivine demonstrates that in parts of the Zimbabwe craton, Cr is incompatible with olivine, whereas a Cr Kd of 0.98 shows that Cr is still slightly incompatible with olivine, but is approaching equilibrium. In figure 16a, we can observe the general trends of the Kd's for

Ni, Mn, Ti, and Cr in olivine for the Archean-aged cratons. The Kd's for Ni in olivine for the Archean-aged cratons are clustered together between 1.5 and 2.5, showing compatibility of Ni in olivine. The Kd's then decrease towards Mn, and generally show slight incompatibility of Mn in olivine, with most Kd values clustered between 0.83 and 0.73. Towards Ti, the Kd's generally decrease and create a large spread in values ranging from 0.01 – 0.08, and Western Australia much higher at 0.7. The Kd's then generally increase towards Cr and are clustered between 0.33 and 1. The Cr Kd for olivine in Western Australia decreases slightly instead of following the general trend of increasing Cr Kd.

The distribution coefficients (Kd's) were also calculated for clinopyroxene in the Archean-aged cratons, where data was available (Fig. 16b). Kaapvaal contained clinopyroxene with Ni that had a Kd of 0.37, indicating that the Ni is incompatible with the clinopyroxene in Kaapvaal craton. Western Australia did not have Kd's calculated for clinopyroxene due to a lack of data available. Superior craton contained clinopyroxene that had a Ni Kd of 0.11, demonstrating that Ni was incompatible with olivine in Superior. Zimbabwe craton contained clinopyroxene that had a Ni Kd of 0.19, which is on par with Ni Kd's for clinopyroxene in Kaapvaal and Superior, in showing that Ni is incompatible with clinopyroxene within the cratons. The Kd's for Ni in clinopyroxene in the cratons were very similar, and all showed incompatibility of Ni in clinopyroxene minerals. Kaapvaal had a Kd of 0.79 for Mn clinopyroxene, indicating that clinopyroxene is slightly depleted in Mn within the craton. Superior had calculated Kd's of 0.86 and 0.62 for Mn in clinopyroxene, which are similar values to that calculated for Kaapvaal, indicating that clinopyroxene is slightly depleted in Mn. Zimbabwe craton had calculated Kd's of 1.03 and 1.43, indicating that clinopyroxene in Zimbabwe craton is at equilibrium with, and enriched in Mn in

certain areas. These Kd values are higher than that of Kaapvaal and Superior, which show depleted Mn in clinopyroxene. Kd values were also calculated for Ti in clinopyroxene for Kaapvaal, Superior and Zimbabwe. Kaapvaal had a Kd of 1.46 for Ti in clinopyroxene, indicating that clinopyroxene was enriched in Ti relative to the bulk-rock. Superior craton had Kd's of 0.98 and 2.15, which demonstrate a large spread in Kd's for the craton. A Kd of 0.98 indicates that the clinopyroxene minerals are close to equilibrium with the whole-rock composition, whereas a Kd of 2.15 indicated that clinopyroxene is enriched in Ti compared to the bulk-rock composition. Zimbabwe craton has calculated Kd values for Ti in clinopyroxene of 0.99 and 0.93. These values are similar to that of the lower end of the Superior spread, and indicate that the clinopyroxene minerals within Zimbabwe are close to equilibrium with the bulk-rock composition. The Kd values were also calculated for Cr in Kaapvaal, Superior and Zimbabwe. Kaapvaal contained clinopyroxene with Cr that has a Kd of 4.73, which indicated compatibility of Cr in clinopyroxene within the craton. Superior craton has clinopyroxene with a calculated Cr Kd of 2.0, which also indicates that Cr is compatible with clinopyroxene in the craton. Zimbabwe craton contains clinopyroxene with calculated Cr Kd's of 0.46 and 1.12, which is a large spread in values for a single craton. A Cr Kd of 0.46 indicates that Cr is incompatible with clinopyroxene compared to the bulk-rock composition, whereas a Kd of 1.12 indicates that Cr is compatible with clinopyroxene compared to the bulk-rock composition. Overall, there is a large spread between the Kd's for Cr in clinopyroxene within the cratons, ranging from 0.46 to 4.73. General trends for the trace element Kd's in clinopyroxene for each craton can be seen in Figure 16b. Generally, the Kd's for Ni show depletion in clinopyroxene, with increasing Kd's at Mn. The Kd's for Mn in clinopyroxene show some spread, with Mn compatible with

clinopyroxene in the Zimbabwe craton. Kaapvaal and Superior clinopyroxene minerals have Mn Kd's slightly <1. The clinopyroxene minerals with low Mn Kd's in Kaapvaal and Superior have increasing Kd values at Ti that are >1. The clinopyroxene minerals with high Kd's for Mn in Zimbabwe have lower Kd's at Ti in clinopyroxene, towards 1. The Kd values then fan out at Cr, with Kaapvaal clinopyroxene Cr Kd's at 4.73 and Zimbabwe clinopyroxene Cr Kd's at 0.46 with Superior and other sites of Zimbabwe clinopyroxene Kd's for Cr in between.

The olivine and clinopyroxene distribution coefficients can be compared in Figures 15a and 15b. Olivine has positive trends >1 for Ni in the Archean-aged cratons, whereas clinopyroxene has negative trends <1 for Ni. The Kd's for Mn are similar between olivine and clinopyroxene, concentrated around 1 in the cratons. All of the cratons contain olivine that have Mn Kd's slightly below 1. Mn in clinopyroxene has a larger spread, with some Kd values >1, and others slightly <1. Ti Kd's in olivine are generally very low, and show negative trends. Ti Kd's in clinopyroxene are 0.93 and above, much higher than that of olivine. The majority of Cr Kd's in olivine are <1, whereas the majority of Kd's for Cr in clinopyroxene are >1, indicating that Cr is more compatible in clinopyroxene than in olivine within the Archean cratons.

6.0 Discussion

Using different methods of comparison such as TAS classification, magnesium numbers, and thermometry, we can see that the chondrules are relatively similar in general composition and geochemical behavior to that of Archean-aged mafic rocks. The TAS classification diagram shows that the chondrules and Archean-aged mafic rocks are similar in silica and alkali content, and are therefore similar and comparable, although the chondrules are more mafic. The magnesium numbers for the whole rock analyses in each chondrule have a larger spread than in the Archean-aged mafic rocks, however the average magnesium numbers are very similar. The temperature range recorded by the two-pyroxene method (Wells, 1977) of ~1060°C±313°C - 1150°C±172°C is comparable to that of alkali basalts, which are thought to represent partial melting from a have a primitive mantle source. These temperatures are also slightly higher than that of Hawaiites, which represent different stages and volumes of melting of a modern mafic mantle source, with a relatively primitive mantle signature. Both the chondrules and Archean-aged mafic rocks contain olivine that has trace element concentrations when normalized to CI that show, depleted trends in Ni content (Fig. 13a), however the chondrules contain olivines that are much more depleted in Ni when normalized to CI than the Archean craton olivines. The chondrules contain olivine with Ni distribution coefficients much lower than that of Archean-aged olivine distribution coefficients for Ni (Fig 14a & 15a). The chondrules contain olivine with Ni distribution coefficients around 0.001 – 0.14, indicating that Ni is incompatible with olivine in the chondrules, or that Ni has been strongly fractionated into another mineral phase. The Archean cratons contain olivine with Ni distribution coefficients of ~1.5 – 7.0, indicating that Ni is compatible with olivine in these samples. We

know that the whole rock Ni content is similar in chondrules and the Archean cratons because the magnesium numbers are similar. In addition, the temperatures of crystallization appear to be similar in the chondrules as for samples from basaltic rocks on earth. This means that the chondrules contain olivine with low Ni content and Ni distribution coefficients, not because there in a lack of Ni in the system, not due to temperature differences, but most likely because Ni has been partitioned into other phases. Ni is present in the chondrules, but appears to have been concentrated in sulfides or alloys. We can see some of these Ni alloys in the trace element maps (Fig. 18-22 appendix) within the chondrules, forming round features that are also rich in Fe. We have shown that chondrules and the samples from the Archean cratons are similar in composition and mineral contents are also similar. Thus there must be a process, or processes that have occurred in the Archean craton mantle source within the almost 1 billion year time difference between chondrule formation and the crystallization of these early Earth samples. This process is most likely reworking and redistribution of material through tectonics and crustal growth. After the formation of the moon, the Earth has been slowly cooling (Zahnle *et al*., 2007); therefore elements must be redistributed from high temperature phases, such as Fe-Ni alloys in the Earth's core/mantle boundary into more stable, cooler phases such as olivine in the upper mantle. Chondrules do not show this reworking because they were fragmented from larger bodies and therefore have been separated from these Ni-rich sources. Clearly, the mantle sources that the Archean mantle derived rocks have evolved from must have had significant Ni-enrichment during the first billion years of Earth's history, as they now contain olivine that has compatible Ni. We also see differences in the chondrules containing olivine with high concentrations of Ti

compared to olivine in the Archean cratons. Ti is a semi compatible element within olivine in the chondrules. In the Archean craton samples the olivine is incompatible with respect to Ti. This is most likely because there are other minerals being formed on earth within the mantle such as perovskite (Hernlund, 2013) that, although lower in Ti than lower pressure forms, still take up significant volumes of Ti at depth. Thus perovskite acts as a buffer for Ti transfer into the upper mantle. This deep mantle mineral formation process did not happen in chondritic meteorites, due to the early break-up of the parent bodies. Thus, because Ti has nowhere else to go in the chondrules, it is taken up in part by olivine. These findings as well as a large spread in magnesium number indicate that chondrules did not undergo any large-scale chemical fractionation or redistribution processes like the sources for the rocks in the Archean cratons. The large spread in magnesium numbers indicates that a process such as tectonics were clearly not a factor during chondrule formation, because the chondrules would then contain more uniform magnesium numbers similar to the Archean cratons. We can use chondrules as an analogue for Hadean rocks because their compositions are so similar to that of terrestrial ultramafic rocks. Hadean rocks would have had similar compositions as chondrules, but would have soon undergone evolution through large-scale element fractionation and redistribution processes on Earth. For example, olivines in these rocks would gain higher concentrations of Ni as the mantle cooled and Ni was redistributed from alloys into the upper levels of the Earth and thus, into minerals such as olivine. Ti concentrations in olivine would lower as evolution progressed and other deep-mantle minerals were able to form such as perovskite. Over 500 – 1 billion years, chondrule-type rocks could easily evolve into Archean mafic rocks through redistribution and recycling of material through tectonics and mantle cooling. However, this was

prevented due to the widespread break-up of the planets that were forming in what is now the asteroid belt.

7.0 Conclusion

There is no geologic record preserved from the early formation and first 500 myr of our planet. The oldest volcanic mafic rocks on Earth are ~3.8 Ga (Archean) (Polat, 2001). To understand the evolution of our planet and solar system, we must understand the early history and formation of planetary bodies (Zahnle *et al*., 2007). Primitive, undifferentiated chondritic meteorites contain chondrules, which are essentially mm sized, individual rocks formed from impact jetting off, and condensation of undifferentiated protoplanets. These chondrules provide a window into the early history of our planet because they are formed from the first stages of our solar system and planet's formation. Chondrules in the Allende CV3 meteorite were analyzed using EDS and WDS analysis on an electron microprobe to obtain major and trace element contents in each chondrule (whole rock) and within olivine, clinopyroxene and orthopyroxene within the chondrules. To determine whether chondrules would be a suitable analogue for early terrestrial rocks, they were compared to Archean-aged mafic rock samples. The geochemical data for these samples was consolidated in the Georoc database. In order to determine if the chondrules and the samples from Archean cratons are chemically similar, their compositions were compared using TAS classification, magnesium numbers, and two-pyroxene thermometry. The TAS classification showed that chondrules are similar in composition to the Archean craton samples, by plotting in similar positions. The magnesium numbers on average for the samples of Archean-aged mafic rocks were similar to that of the chondrules. The chondrules had a large spread in magnesium numbers, but showed relatively similar average values as the samples from the Archean mafic rocks. Using the two-pyroxene thermometer described in Wells (1977), crystallization temperature was calculated to be

1060°C - 1150°C for minerals in the chondrules. These temperatures are on par with alkali basalt crystallization temperatures, and slightly higher than Hawaiite crystallization temperatures (French and Cameron, 1981). Because the chondrules have similar composition, geochemical behavior and similar temperatures as the samples of Archean mafic rocks, trace element distribution coefficients for minerals within the chondrules and the samples of Archean mafic rocks can be compared. The comparison of distribution coefficients shows how Earth has evolved in the first billion years of formation, since the time of chondrule formation to the formation of Archean mafic rocks. The distribution coefficient of Ni in olivine within the chondrules are very low and <<1, whereas the distribution of Ni in olivine in the samples for the Archean mafic rocks are >1. The distribution coefficients for Ti in olivines within the chondrules are around 1, whereas the distribution coefficients for Ti in olivine for the samples of Archean mafic rocks are <<1. The distribution of Ni in olivine for the chondrules is most likely low because Ni is concentrated within Ni alloys or is fractionated in another phase. The olivine in chondrules have high Ti distribution coefficients due to the fact that there are no mantle minerals being formed such as perovskite to buffer out the Ti, and there is no crust being formed. Clearly the samples of Archean mafic rocks have gone through redistribution through tectonics and crustal formation during the first billion years of Earth's formation. This evolution is not seen in chondrules because chondrites were fragmented from their parent bodies before processes like this could begin. Therefore, we can infer that hadean rocks most likely had a composition similar to chondrules, but would however rapidly evolve towards the composition of what we see in samples of Archean mafic rocks.

8.0 Future work

This type of study can be used as preliminary science for future missions to asteroid similar to carbonaceous chondrites such as the OSIRIS-Rex mission. Comparing chondrules to other meteorite types would be useful to understand how trace elements such as Ni are distributed in other systems. Lunar data could be compared to this data set, to represent a slightly more evolved Earth than chondrules are in this study. This data could also be compared to Hawaiites to gain a clearer understanding of fractionation over time in our planet.

References

Arndt, N., Naldrett, A., & Pyke, D. (1977). Komatiitic and Iron-rich Tholeiitic Lavas of Munro Township, Northeast Ontario. *Journal of Petrology,* 319-369.

Bas, M., Maitre, R., Streckeisen, A., & Zanettin, B. (1985). A Chemical Classification of Volcanic Rocks Based on the Total Alkali-Silica Diagram. Journal of Petrology, 745-750.

Bickel, Arndt, & Nibet. (1993). Geochemistry of the igneous rocks of the Belingwe greenstone belt: Alteration, contamination and petrogenesis. *The Geology of the Belingwe Greenstone Belt, Zimbabwe,*175-213.

Cattell, & Arndt. (1987). Low- And High- Alumina Komatiites from Late Archean Sequence, Newton township, Ontario.*Contributions to Mineralogy and Petrology,*218-227.

Clarke, R. S., Jarosewich, E., Mason, B., Nelen, J., Gomez, M., & Hyde, J. R. (1971). Allende, Mexico, Meteorite Shower. *Smithsonian Contributions to the Earth Sciences*, *5*, 1-53.

Dygert, N., Liang, Y., & Hess, P. (2013). An Experimental Study of REE and Other Trace Element Partitioning Between Augite and Fe-Rich Basalts: A Parameterized Model for Planetary Applications. *44th Lunar and Planetary Science Conference*.

French, W., & Cameron, E. (1981). Calculation of the Temperature of Crystallization of Silicates from Basaltic Melts. Mineralogical Magazine, 44, 19-26.

Hernlund, J. (2013). Deep Earth: Mantle fabric unravelled? Nature Geoscience, 516-518.

Huppert, H., Sparks, R., Turner, J., & Arndt, N. (1984). Emplacement and cooling of komatiite lavas. *Nature,* 19-22.

Hutchison, R. (2004). *Meteorites: A Petrologic, Chemical and Isotopic Synthesis*. New York: Cambridge University Press.

http://georoc.mpch-mainz.gwdg.de/georoc/Start.asp

Jacobsen, S. (2003). GEOCHEMISTRY: How Old Is Planet Earth? Science, 300, 1513-1514.

Johnson, B., Minton, D., Zuber, M., & Zuber, M. (2015). Impact jetting as the origin of chondrules. Nature, 517, 339-341.

Le Maitre, R., Bateman, P., & Dudek, A. (1989). A classification of igneous rocks and a glossary of terms.

Lesher, C., & Arndt, N. (1995). REE and Nd isotope geochemistry, petrogenesis and volcanic evolution of contaminated komatiites at Kambalda, Western Australia.*Lithos,* 127-157

Nisbet, E., Bickle, & Martin. (1977). The mafic and ultramafic lavas of the Bilingwe Greenstone belt, Rhodesia. Petrology, 18, 521-566.

Polat, A., Hofmann, A., & Rosing, M. (2001). Boninite-like volcanic rocks in the 3.7–3.8 Ga Isua greenstone belt, West Greenland: Geochemical evidence for intra-oceanic subduction zone processes in the early Earth. Chemical Geology, 231-254.

Puchtel, I., Humayun, M., Campbell, A., Sproule, R., & Lesher, C. (2004). Platinum group element geochemistry of komatiites from the Alexo and Pyke Hill areas, Ontario, Canada. Geochimica Et Cosmochimica Acta, 1361-1383.

Reed, S., & Ware, N. (1974). Quantitative Electron Microprobe Analysis of Silicates Using Energy-Dispersive X-Ray Spectrometry. Journal of Petrology, 499-519.

Robin-Popieul, C., Arndt, N., Chauvel, C., Byerly, G., Sobolev, A., & Wilson, A. (2012). A New Model for Barberton Komatiites: Deep Critical Melting with High Melt Retention. *Journal of Petrology,* 2191-2229.

Rollinson, H. (1993). *Using geochemical data: Evaluation, presentation, interpretation*. Harlow, Essex, England: Longman Scientific & Technical

Shimizu, K. (2005). The Geochemistry of Ultramafic to Mafic Volcanics from the Belingwe Greenstone Belt, Zimbabwe: Magmatism in an Archean Continental Large Igneous Province. *Journal of Petrology,* 2367-2394

Sleep, N. (2010). The Hadean-Archaean Environment. Cold Spring Harbor Perspectives in Biology.

Smith, & Erlank. (1982). Geochemistry and petrogenesis of Komatiites from the Barberton greenstone belt, South Africa.*Komatiites*.

Smith, H., Erlank, A., & Duncan, A. (1980). Geochemistry of some ultramafic komatiite lava flows from the Barberton Mountain Land, South Africa. *Precambrian Research,*399-415.

Stracke, A., Palme, H., Gellissen, M., Münker, C., Kleine, T., Birbaum, K., *et al*. (2012). Refractory element fractionation in the Allende meteorite: Implications for solar nebula condensation and the chondritic composition of planetary bodies.*Geochimica et Cosmochimica Acta*, *85*, 114-141.

Weisberg, M., McCoy, T., Krot, A. (2006). Systematics and Evaluation of Meteorite Classification. D.S. Lauretta (Ed.), H. Y. Mcsween JR. (Ed.), *Meteorites and the Early Solar System II.* (19-52). Tucson Arizona: The University of Arizona Press.

Wells, P. (1977). Pyroxene thermometry in simple and complex systems. Contributions to Mineralogy and Petrology, 129-139.

Wilde, S., Valley, J., Peck, W., & Graham, C. (2001). Evidence from detrital zircons for the existence of continental crust and oceans on the Earth 4.4 Gyr ago. Letters to Nature, 409.

Zahnle, K., Arndt, N., Cockell, C., Halliday, A., Nisbet, E., Selsis, F., & Sleep, N. (2007). Emergence of a Habitable Planet. Space Science Reviews, 129, 35-78.

Appendix Table of Contents

Table of Tables

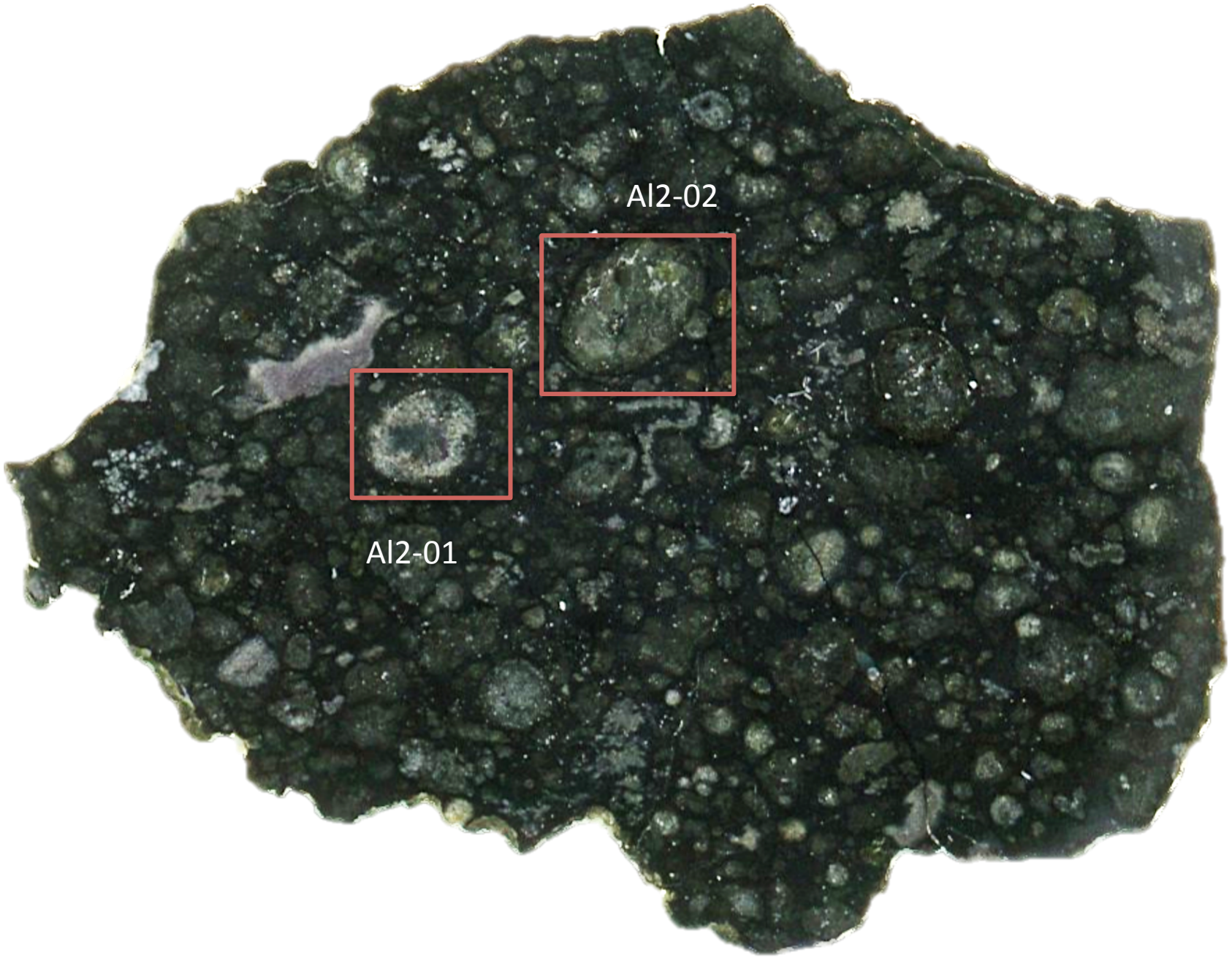

Fig.16 Allende thin section Al2

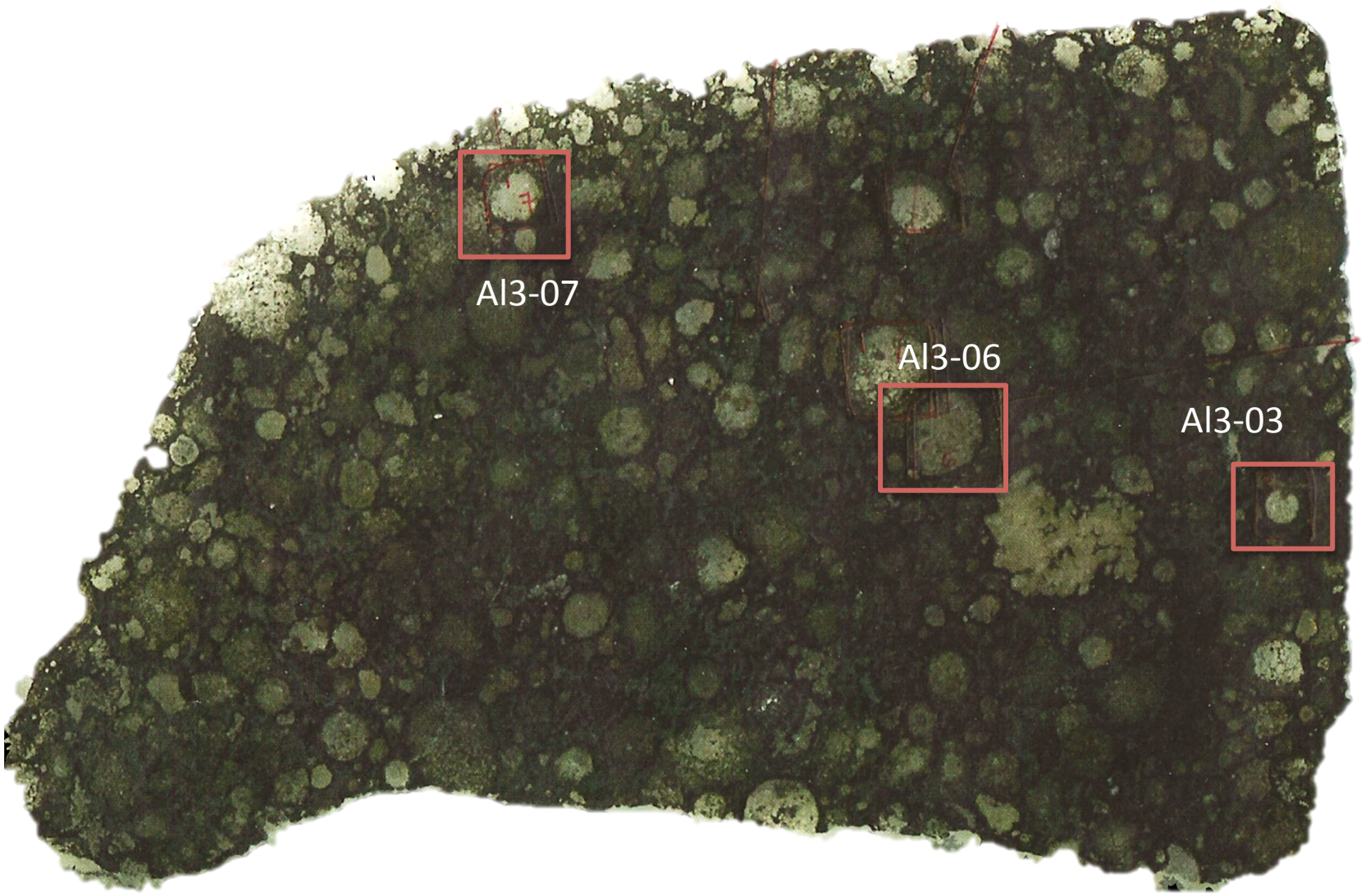

Fig.17 Allende thin section Al3

Fig.18 Trace Element Map of Al2-01

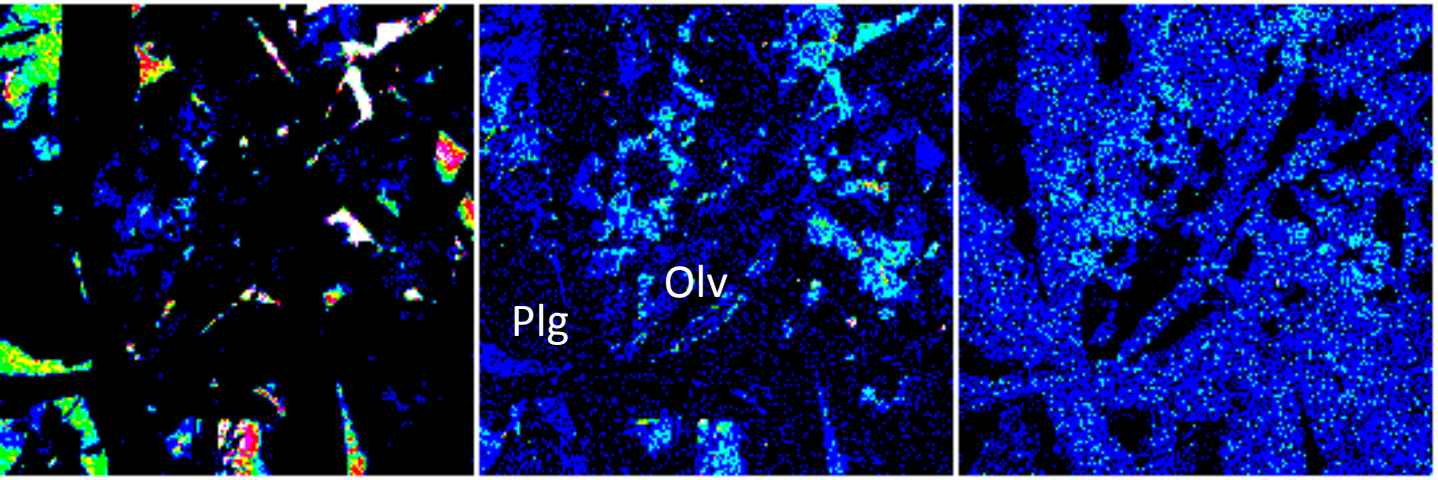

Ti —— 100 um Cr —— 100 um Co —— 100 um

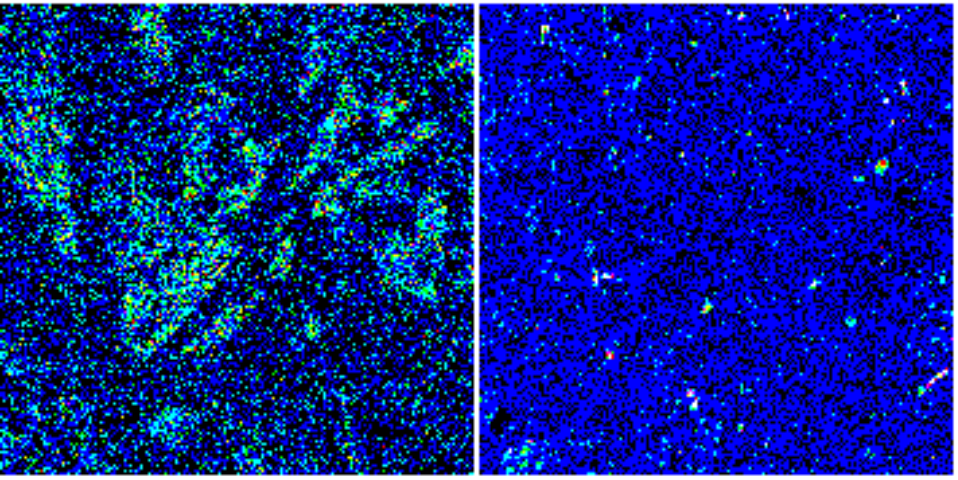

Mn —— 100 um Ni —— 100 um

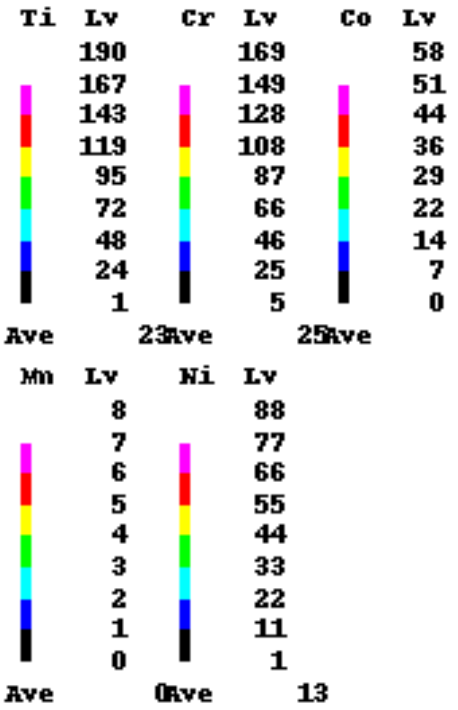

Group : Dalhousie
Sample : Beth01Map
Allende2_Chondrule1_wds_m

Jan 23 04:54 2015
Stage Scan
Acc. V 15.0 kv
Prob C 1.001e-07A
Scan ON Mag 55
Prob Diam.(um) 3
Dwell(ms) 100.00
Stage No.9
X : 73.2460 mm
Y : 19.1764 mm
Z : 10.2015 mm
Direction: Single
Points 200*200
Interval(um) X:3.00
Y:3.00

Ti WDS 1ch PETJ
Ka Order 1
Peak Pos.(mm) 88.6640
Accum. 1
Max 1212

Fig. 19 Trace Element Map of Al2-02

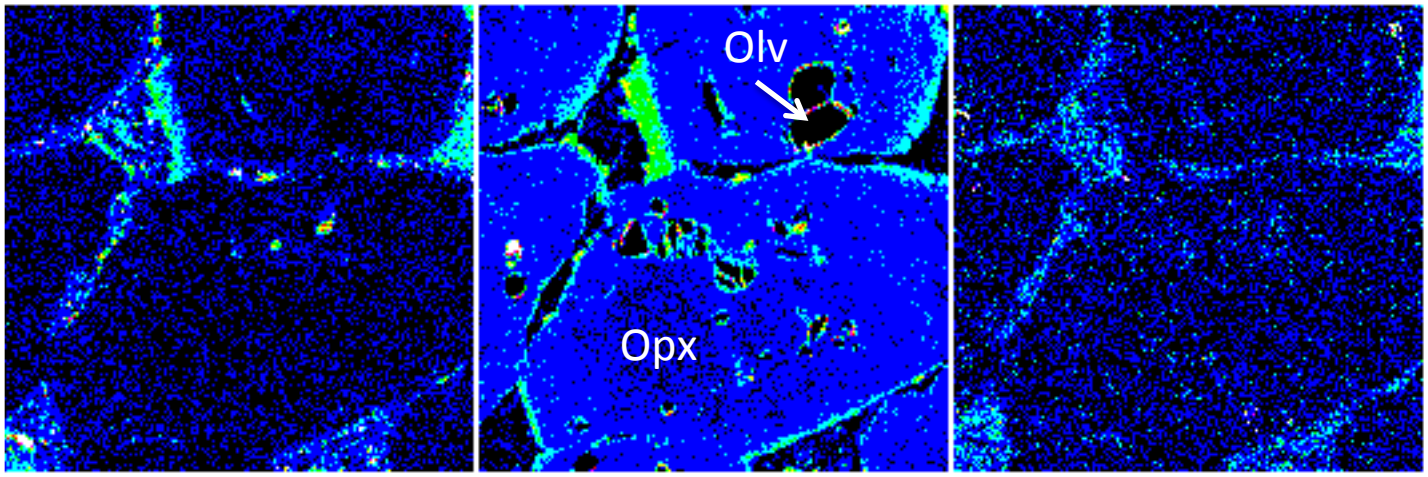

Ti —— 100 um Cr —— 100 um Co —— 100 um

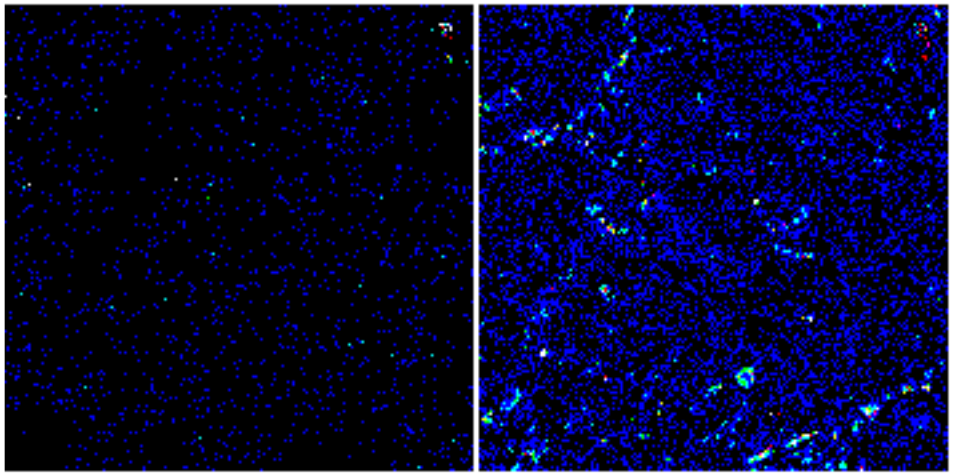

Mn —— 100 um Ni —— 100 um

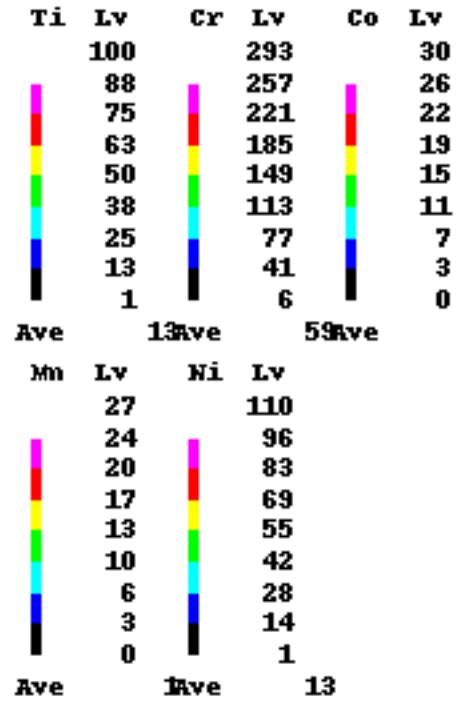

Group : Dalhousie
Sample : Beth01Map
Allende2_Chondrule2_wds_m

Jan 23 08:26 2015
Stage Scan
Acc. V 15.0 kV
Prob C 9.980e-08A
Scan ON Mag 55
Prob Diam.(um) 3
Dwell(ms) 100.00
Stage No.12
X : 67.7392 mm
Y : 15.6878 mm
Z : 10.1833 mm
Direction: Single
Points 200*200
Interval(um) X:3.00
Y:3.00

Ti WDS 1ch PETJ
Ka Order 1
Peak Pos.(mm) 88.6640
Accum. 1
Max 765

Fig. 20 Trace Element Map of Al3-03

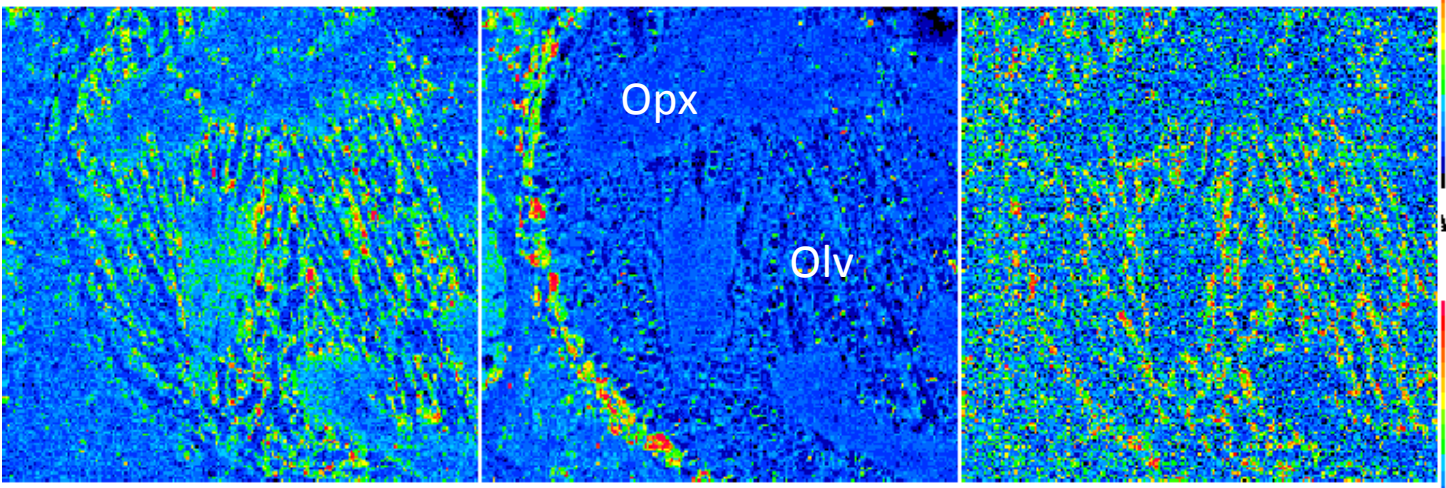

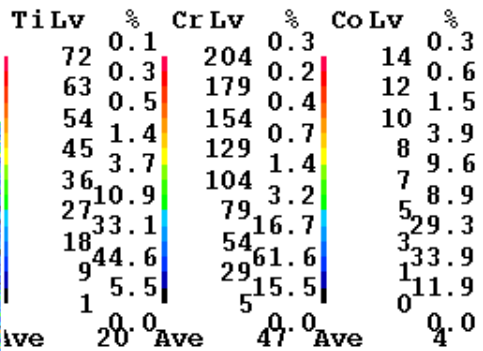

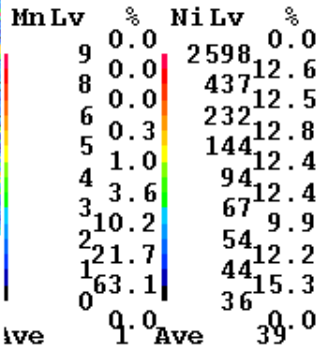

Ti —— 100 um

Cr —— 100 um

Co —— 100 um

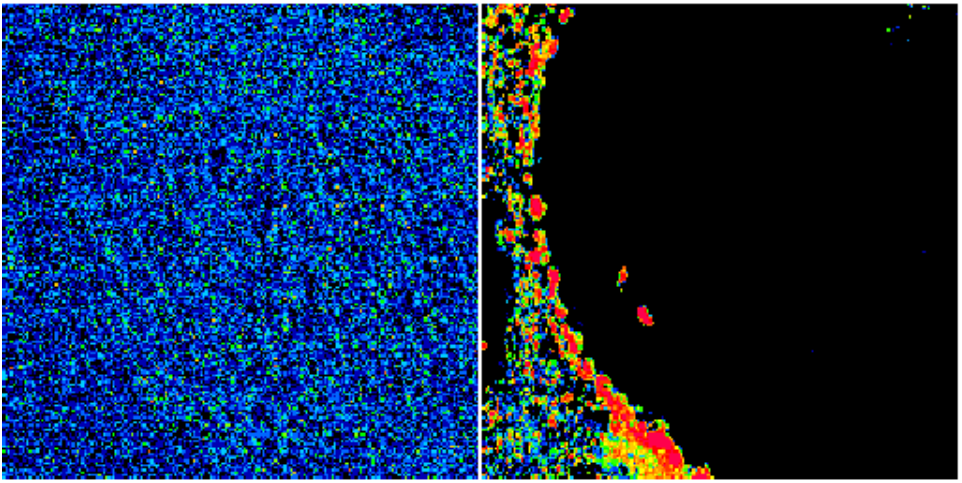

Mn —— 100 um

Ni —— 100 um

```
Group  : Dalhousie
Sample : Beth01Map
Allende3_Chondrule3_wds_m

Jan 22 22:59 2015
Stage Scan
Acc. V    15.0 kV
Prob C  1.002e-07A
Scan ON  Mag 55
Prob Diam.(um) 3
Dwell(ms) 100.00
Stage No.4
  X :  8.4013 mm
  Y : 51.0491 mm
  Z :  9.8255 mm
Direction: Single
Points  200*200
Interval(um) X:3.00
             Y:3.00

  Ti WDS  1ch  PETJ
  Ka       Order 1
  Peak Pos.(mm) 88.6640
  Accum. 1
  Max      141
  Min        1
  Ave       20
  A, B value  0.0000, 0.0000

  Cr WDS  2ch  PETJ
  Ka       Order 1
  Peak Pos.(mm) 72.6680
  Accum. 1
  Max      572
  Min        5
  Ave       47
```

Fig. 21 Trace Element Map of Al3-06

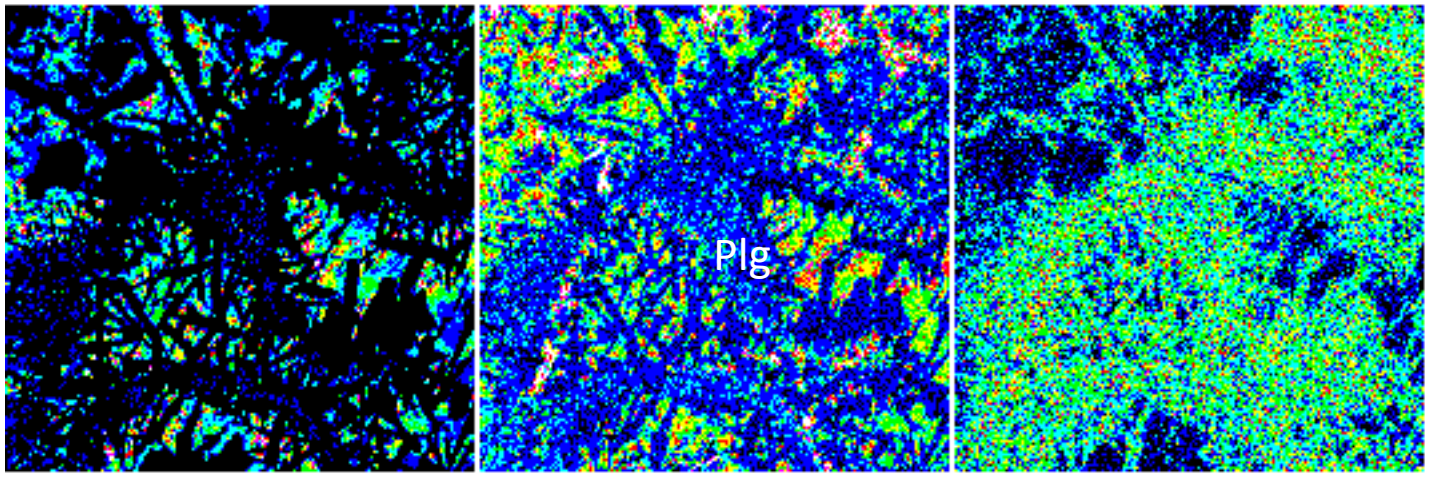

Ti —— 100 um Cr —— 100 um Co —— 100 um

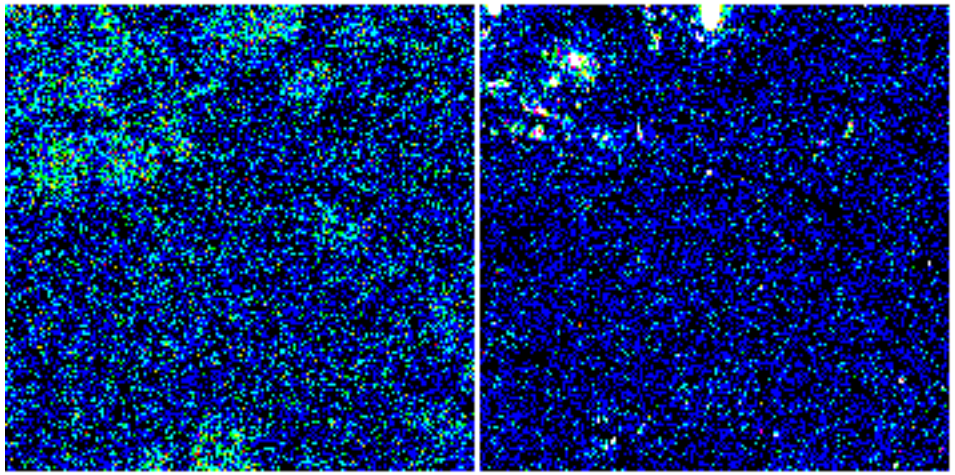

Mn —— 100 um Ni —— 100 um

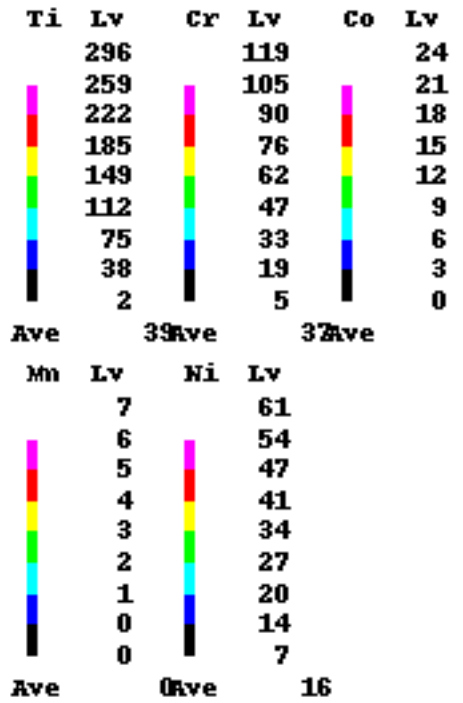

Group : Dalhousie
Sample : Beth01Map
Allende3_Chondrule6_wds_m

Jan 23 01:21 2015
Stage Scan
Acc. V 15.0 kV
Prob C 1.006e-07A
Scan ON Mag 55
Prob Diam.(um) 3
Dwell(ms) 100.00
Stage No.6
X : 16.2328 mm
Y : 48.8512 mm
Z : 9.8419 mm
Direction: Single
Points 200*200
Interval(um) X:3.00
Y:3.00

Ti WDS 1ch PETJ
Ka Order 1
Peak Pos.(mm) 88.6640
Accum. 1
Max 805

Fig. 22 Trace Element Map of Al3-07

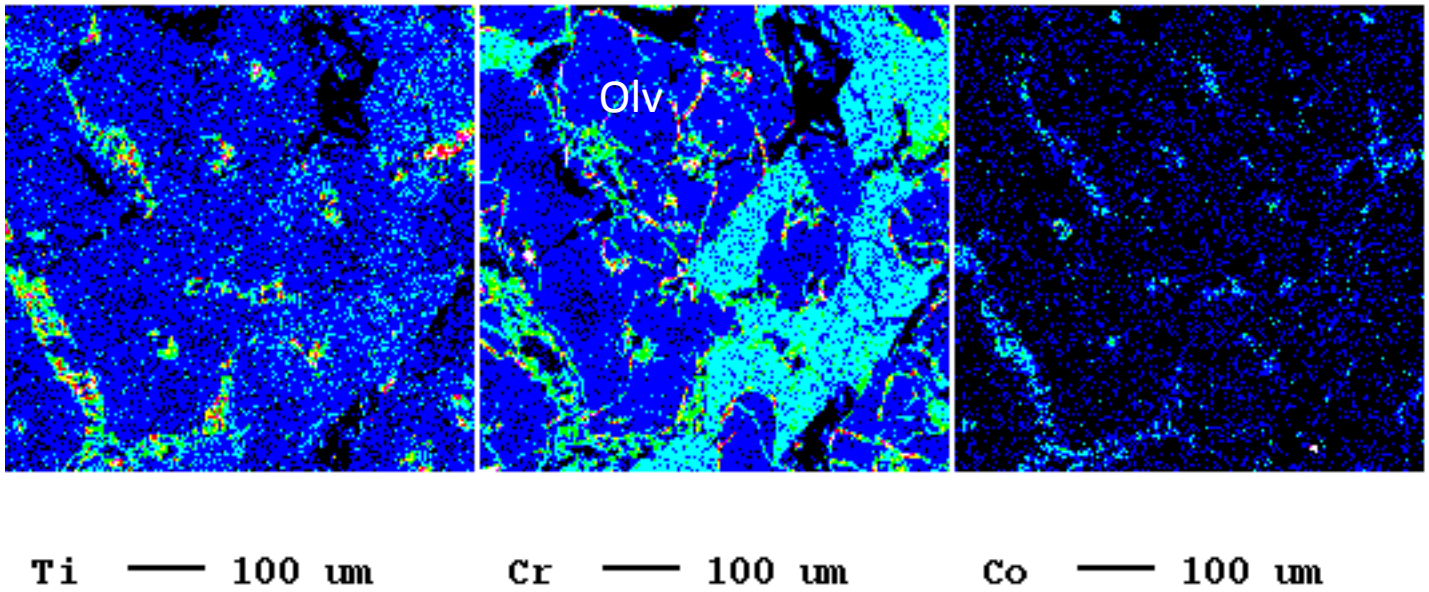

Ti —— 100 um Cr —— 100 um Co —— 100 um

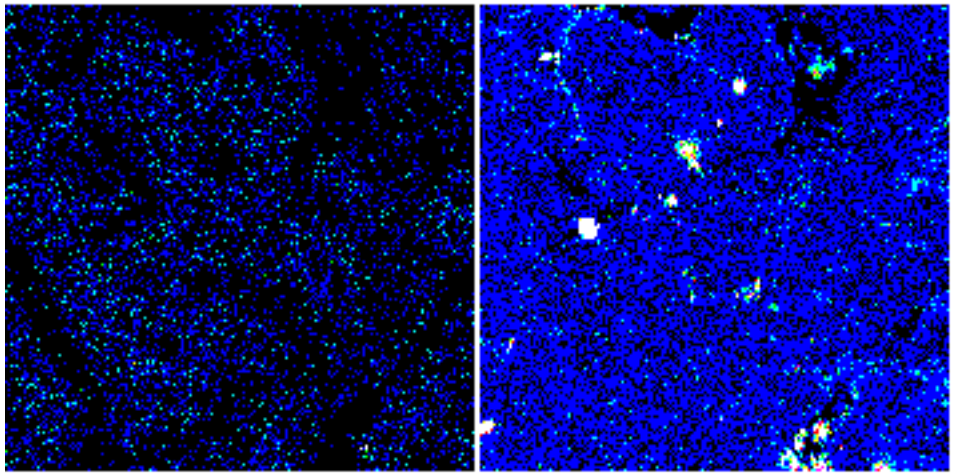

Mn —— 100 um Ni —— 100 um

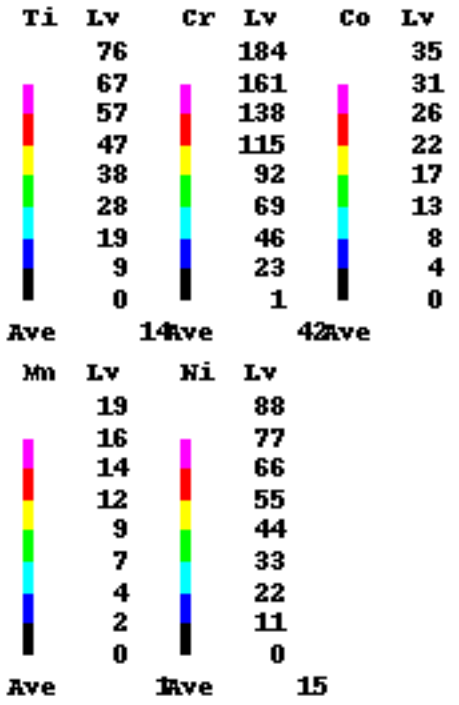

Group : Dalhousie
Sample : Beth01Map
Allende3_Chondrule7_wds_m

Jan 23 02:32 2015
Stage Scan
Acc. V 15.0 kV
Prob C 1.004e-07A
Scan ON Mag 55
Prob Diam.(um) 3
Dwell(ms) 100.00
Stage No.7
X : 26.6459 mm
Y : 43.3121 mm
Z : 9.8198 mm
Direction: Single
Points 200*200
Interval(um) X:3.00
Y:3.00

Ti WDS 1ch PETJ
Ka Order 1
Peak Pos.(mm) 88.6640
Accum. 1
Max 162

Table 1: Whole- Rock Chondrule Data

Al2-01	
Element	PPM Avg
O K	420600
Na K	27020
Mg K	74480
Al K	118020
Si K	181720
S K	2120
Cl K	5000
K K	400
Ca K	85800
Ti K	2920
Cr K	1020
Mn K	100
Fe K	22460
Ni K	1040
Mo L	300
In L	620
Th M	100

Al2-02	
Element	PPM Avg
O K	342733.33
F K	253400
Na K	11033.33
Mg K	146033.33
Al K	12433.33
Si K	178633.33
S K	4933.33
Cl K	833.33
K K	200.00
Ca K	8233.33
Ti K	433.33
Cr K	4300.00
Mn K	1833.33
Fe K	32466.67
Ni K	1966.67
Th M	433.33

Al3-03	
Element	PPM Avg
O K	464239.95
N K	74952.20
Na K	9621.64
Mg K	153073.22
Al K	13128.73
Si K	198027.76
S K	2962.27
Cl K	534.39
K K	1247.15
Ca K	25646.25
Ti K	1746.04
Cr K	3372.54
Mn K	1359.15
Fe K	38714.17
Ni K	1394.30
Ag L	2008.34

Al3-06	
Element	PPM Avg
O K	469162.15
Na K	29769.13
Mg K	63961.40
Al K	105873.34
Si K	185298.99
S K	2940.73
Cl K	8680.08
K K	1879.29
Ca K	70550.60
Ti K	6307.16
Cr K	3804.98
Mn K	1203.13
Fe K	48505.65
Ni K	1415.43

Al3-07	
Element	PPM Avg
O K	432834.96
Na K	6721.09
Mg K	204878.11
Al K	2641.95
Si K	208478.27
P K	493.04
S K	6855.95
Cl K	768.88
K K	736.96
Ca K	14401.40
Ti K	1033.67
Cr K	5885.23
Mn K	1779.55
Fe K	105963.10
Ni K	5343.19
Ag L	1184.68

Table 2: WDS Point Analysis - Olivine composition

No.	CaO	TiO2	Na2O	SiO2	MnO	K2O	Cr2O3	MgO	Al2O3	FeO	NiO	Total	Comment	
113	0.233	0	0.014	41.335	0.262	0.029	0.012	51.77	0	6.188		99.843	Al3-03-J8-M10-01	olivine
114	0.215	0.029	0.01	40.175	0.149	0.037	0.322	48.29	0.461	11.16		100.848	Al3-03-J8-M10-02	olivine
115	0.227	0.066	0.021	41.507	0.222	0.026	0.241	52.638	0	4.742		99.69	Al3-03-J8-M10-03	olivine
116	0.265	0.031	0.015	41.504	0.198	0.028	0.008	53.705	0	3.108		98.862	Al3-03-J8-M11-01	olivine
135	0.19	0	0.034	42.098	0.195	0.032	0	54.954	0	1.678	0	99.181	Al3-03-J15-M1-01	olivine
136	0.205	0	0.036	41.911	0.153	0.013	0	55.009	0	1.687	0	99.014	Al3-03-J15-M1-02	olivine
137	0.204	0	0.037	41.698	0.172	0.019	0	54.207	0	2.583	0	98.92	Al3-03-J15-M1-02	olivine
138	0.321	0	0.099	42.299	0.202	0.016	0	53.987	0.266	2.234	0	99.424	Al3-03-J15-M1-04	olivine
139	0.213	0.02	0.053	41.788	0.152	0.016	0.31	54.528	0.078	2.009	0	99.167	Al3-03-J15-M2-01	olivine
140	0.212	0.102	0.054	41.02	0.186	0.022	1.099	53.457	0.474	2.64	0	99.266	Al3-03-J15-M2-02	olivine
141	0.339	0.021	0.055	40.812	0.196	0.022	0.54	51.632	1.44	4.846	0	99.903	Al3-03-J15-M2-03	olivine
146	0.173	0.003	0.057	41.912	0.115	0.023	0.254	50.709	0.536	5.531	0	99.313	Al3-03-J15-M3-05_I	olivine
147	0.19	0.06	0.022	41.144	0.12	0.077	0.068	51.847	0.015	5.23	0	98.773	Al3-03-J15-M3-05_I2	olivine
148	0.673	0.103	0.087	43.491	0.142	0.049	0.248	48.537	0.955	5.672	0	99.957	Al3-03-J15-M3-05_I3	olivine
149	0.531	0.091	0.157	48.023	0.093	0.071	0.894	44.256	1.658	3.976	0	99.75	Al3-03-J15-M3-05_I4	olivine
150	0.203	0.042	0.096	41.056	0.147	0.065	0.173	50.605	0.841	6.73	0	99.958	Al3-03-J15-M3-05_I5	olivine
178	0.241	0.059	0.022	41.972	0.14	0.022	0.143	48.633	0.096	8.459	0.039	99.826	Al3-03-J15-M8-07_I1	olivine
179	0.217	0.069	0.018	40.784	0.157	0.023	0.089	49.211	0.042	9.251	0.032	99.893	Al3-03-J15-M8-07_i2	olivine
180	0.52	0.222	0.125	57.304	0.061	0.023	0.482	37.907	1.315	1.249	0	99.208	Al3-03-J15-M8-07_I3	olivine
181	0.226	0.035	0.027	40.764	0.186	0.037	0.095	47.932	0.043	10.954	0.016	100.315	Al3-03-J15-M8-07_I4	olivine
182	0.607	0.143	0.234	44.609	0.164	0.254	0.364	42.419	1.921	7.612	0.037	98.364	Al3-03-J15-M8-07_I5	olivine
196	0.233	0.012	0.039	40.954	0.159	0.007	0.684	52.098	0.433	5.336	0	99.955	Al3-03-J15-M10-01	olivine
197	0.179	0.028	0.025	41.653	0.211	0.01	0.113	53.305	0	3.743	0	99.267	Al3-03-J15-M10-02	olivine
198	0.169	0.072	0.053	40.823	0.179	0.006	0.862	51.993	0.455	4.988	0	99.6	Al3-03-J15-M10-03	olivine
54	0.24	0	0.019	41.792	0.05	0.007	0.002	54.469	0	1.5		98.079	Al3-06-J8-M1-01	olivine
55	0.22	0.001	0.02	42.35	0.076	0.007	0.067	55.805	0.002	1		99.548	Al3-06-J8-M1-02	olivine
56	0.205	0.005	0.018	42.338	0.086	0.016	0	55.181	0	1.869		99.718	Al3-06-J8-M1-03	olivine
235	0.237	0.076	0.006	42.216	0.043	0.018	0.1	55.616	0	1.029	0	99.341	Al3-06-J15-M8-01	olivine
236	0.249	0.076	0.015	42.086	0.044	0.024	0	55.596	0	1.125	0	99.215	Al3-06-J15-M8-02	olivine
237	0.23	0.059	0.016	41.699	0.088	0.016	0.085	54.787	0	1.153	0	98.133	Al3-06-J15-M8-03	olivine
238	0.237	0.071	0.015	42.011	0.074	0.009	0.1	55.273	0	1.442	0.003	99.235	Al3-06-J15-M8-04	olivine
34	0.522	0.01	0.019	42.148	0.041	0.016	0.16	55.529	0.213	0.842		99.5	Al3-07-J8-M2-01	olivine
35	0.495	0.016	0.012	42.122	0.018	0.014	0.179	55.67	0.175	0.657		99.358	Al3-07-J8-M2-02	olivine
36	0.409	0.002	0.023	41.662	0.079	0.015	0.174	53.38	0.114	3.929		99.787	Al3-07-J8-M2-03	olivine
37	0.393	0.109	0.019	58.928	0.045	0.012	0.592	38.263	0.828	0.46		99.649	Al3-07-J8-M3-01	olivine
38	0.405	0.119	0.015	58.759	0.041	0	0.608	38.23	0.787	0.491		99.455	Al3-07-J8-M3-02	olivine
45	0.286	0	0.272	42.19	0.062	0.023	0.183	54.106	0.446	2.161		99.729	Al3-07-J8-M4-01	olivine
46	0.142	0	0.034	41.404	0.097	0.015	0.113	53.939	0.002	2.547		98.293	Al3-07-J8-M4-02	olivine
51	0.389	0	0.022	42.147	0.018	0.016	0.062	55.383	0.129	1.484		99.65	Al3-07-J8-M6-01	olivine
52	0.369	0	0.206	41.076	0.085	0.04	0.098	50.367	0.563	7.186		99.99	Al3-07-J8-M6-02	olivine
53	0.151	0	0.032	41.262	0.111	0.012	0.083	51.681	0.054	6.448		99.834	Al3-07-J8-M6-03	olivine
266	0.275	0.037	0	41.77	0.089	0.004	0.073	53.925	0.018	3.3	0	99.491	Al3-07-J15-M2-01	olivine
267	0.311	0.029	0	41.792	0.06	0.015	0.064	53.78	0.057	3.862	0	99.97	Al3-07-J15-M2-02	olivine
268	0.112	0.018	0.015	41.543	0.107	0.016	0.112	51.225	0.041	7.561	0	100.75	Al3-07-J15-M2-03	olivine

No.	CaO	TiO2	Na2O	SiO2	MnO	K2O	Cr2O3	MgO	Al2O3	FeO	NiO	Total	Comment	
269	0.332	0.012	0.003	41.719	0.055	0.02	0.037	53.279	0.035	4.44	0	99.932	Al3-07-J15-M2-04	olivine
270	0.341	0.015	0.01	41.548	0.072	0.023	0.146	52.63	0.127	4.898	0	99.81	Al3-07-J15-M2-05	olivine
287	0.371	0.126	0.066	38.152	0.203	0.068	0.771	32.796	0.658	27.403	0.105	100.719	Al3-07-J15-M7-01	olivine
288	0.351	0.099	0.232	37.29	0.19	0.139	0.718	32.77	0.907	27.958	0.09	100.744	Al3-07-J15-M7-02	olivine
297	0.515	0.027	0	42.011	0	0.027	0.172	55.599	0.186	0.994	0.001	99.532	Al3-07-J15-M8-01	olivine
298	0.428	0	0	42.075	0.027	0.016	0.133	54.729	0.166	2.117	0	99.691	Al3-07-J15-M8-02	olivine
299	0.309	0.044	0	41.608	0.063	0.03	0.211	53.638	0.171	3.829	0.011	99.914	Al3-07-J15-M8-03	olivine
300	0.295	0.057	0	40.202	0.133	0.032	0.182	47.905	0.156	11.125	0.027	100.114	Al3-07-J15-M8-04	olivine
309	0.358	0.054	0.001	41.791	0.089	0.015	0.268	54.562	0.237	2.224	0	99.599	Al3-07-J15-M11-03	olivine
310	0.454	0.014	0	42.026	0.01	0.013	0.159	55.497	0.197	1.072	0	99.442	Al3-07-J15-M11-04	olivine
311	0.486	0.018	0.002	41.877	0.039	0.021	0.22	54.694	0.183	1.681	0	99.221	Al3-07-J15-M11-05	olivine
328	0.549	0.194	0.005	41.537	0.026	0.014	0.176	54.827	0.104	0.769	0	98.201	Al2-01-J15-M2-01	olivine
329	0.517	0.114	0.003	41.757	0.049	0.009	0.177	54.358	0.065	1.233	0.002	98.284	Al2-01-J15-M2-02	olivine
330	0.507	0.134	0	41.661	0.011	0.011	0.16	55.079	0.117	0.703	0	98.383	Al2-01-J15-M2-03	olivine
332	0.532	0.075	0.012	41.882	0.012	0.019	0.025	54.876	0.008	1.063	0	98.504	Al2-01-J15-M3-02	olivine
333	0.522	0.232	0	41.517	0.026	0.004	0.096	54.83	0.039	0.913	0	98.179	Al2-01-J15-M3-03	olivine
341	0.385	0.027	0.003	41.297	0.043	0.018	0.025	52.237	0	5.284	0.029	99.348	Al2-01-J15-M5-01	olivine
342	0.329	0.018	0.007	41.458	0.082	0.014	0	53.196	0	3.848	0.01	98.962	Al2-01-J15-M5-02	olivine
343	0.29	0.04	0.015	41.399	0.052	0.018	0	53.699	0	3.045	0	98.558	Al2-01-J15-M5-03	olivine
370	0.245	0.142	0.081	36.34	0.722	0.046	0.694	27.273	1.172	32.732	0.079	99.526	Al2-02-J15-M2-01	olivine
371	0.324	0.352	0.116	28.394	0.895	0.058	0.464	19.793	11.941	39.248	0.098	101.683	Al2-02-J15-M2-02	olivine
372	0.334	0.186	0.065	35.643	0.813	0.057	1.033	25.941	0.735	36.035	0.112	100.954	Al2-02-J15-M2-03	olivine
379	0.987	0.399	0.182	39.634	0.651	0.048	1.985	34.378	3.321	16.592	0.06	98.237	Al2-02-J15-M4-04	olivine
380	0.189	0.008	0.007	40.74	0.335	0.033	0.116	49.696	0.03	8.371	0.013	99.538	Al2-02-J15-M5-01	olivine
382	0.171	0.023	0.002	40.48	0.365	0.038	0.06	48.627	0	9.781	0	99.547	Al2-02-J15-M5-03	olivine
383	0.173	0.009	0.018	40.542	0.317	0.033	0.106	49.624	0.033	8.893	0.003	99.751	Al2-02-J15-M5-04	olivine

Table 3: WDS Point Analysis - Orthopyroxene composition

No.	SiO2	TiO2	Al2O3	FeO	MnO	MgO	CaO	Na2O	K2O	Cr2O3	NiO	Total	Comment	
80	58.734	0.108	0.627	0.423	0.071	38.526	0.366	0.009	0.024	0.349		99.237	Al3-03-J8-M1-02	enstatite
81	58.752	0.168	0.972	0.436	0.081	38.192	0.39	0.004	0.029	0.386		99.41	Al3-03-J8-M1-03	enstatite
82	58.746	0.127	1.196	0.704	0.076	37.648	0.416	0.078	0.092	0.348		99.431	Al3-03-J8-M1-04	enstatite
83	58.859	0.142	0.918	0.415	0.108	37.905	0.573	0.033	0.057	0.421		99.431	Al3-03-J8-M1-05	enstatite
84	58.593	0.229	1.317	0.37	0.139	37.862	0.586	0.003	0.026	0.569		99.694	Al3-03-J8-M2-01	enstatite
85	58.37	0.357	1.679	0.403	0.105	37.505	0.584	0	0.027	0.483		99.513	Al3-03-J8-M2-02	enstatite
86	58.12	0.354	1.771	0.467	0.099	37.574	0.647	0.001	0.024	0.562		99.619	Al3-03-J8-M2-03	enstatite
87	58.536	0.274	1.169	0.387	0.107	38.135	0.472	0.007	0.014	0.451		99.552	Al3-03-J8-M2-04	enstatite
92	58.541	0.15	1.014	0.393	0.08	37.802	0.462	0.044	0.061	0.412		98.959	Al3-03-J8-M5-01	enstatite
93	58.717	0.188	1.097	0.333	0.111	37.913	0.499	0.033	0.049	0.498		99.438	Al3-03-J8-M5-02	enstatite
94	57.434	0.235	1.907	0.534	0.105	36.674	0.803	0.139	0.237	0.474		98.542	Al3-03-J8-M5-03	enstatite
95	59.069	0.128	0.835	0.492	0.087	38.168	0.406	0.057	0.025	0.372		99.639	Al3-03-J8-M6-01	enstatite
96	58.751	0.074	0.647	0.792	0.098	37.871	0.602	0.033	0.03	0.293		99.191	Al3-03-J8-M6-02	enstatite
100	58.566	0.209	1.105	0.393	0.049	37.888	0.472	0	0.017	0.354		99.053	Al3-03-J8-M8-01	enstatite
101	59.149	0.155	0.672	0.372	0.11	38.346	0.388	0	0.006	0.412		99.61	Al3-03-J8-M8-02	enstatite
102	58.549	0.104	0.926	0.491	0.068	38.014	0.495	0.073	0.068	0.324		99.112	Al3-03-J8-M8-03	enstatite
110	58.466	0.113	0.798	0.826	0.123	37.637	0.466	0.097	0.087	0.387		99	Al3-03-J8-M8-05	enstatite
164	58.894	0.114	0.676	0.356	0.063	38.423	0.396	0.004	0.021	0.354	0.001	99.302	Al3-03-J15-M6-01	enstatite
165	58.708	0.291	1.166	0.395	0.066	38.052	0.512	0	0.013	0.467	0.005	99.675	Al3-03-J15-M6-02	enstatite
166	58.916	0.163	0.846	0.605	0.059	38.26	0.426	0.057	0.046	0.378	0	99.756	Al3-03-J15-M6-03	enstatite
167	58.264	0.212	1.063	0.416	0.147	37.646	0.604	0.047	0.123	0.481	0.029	99.032	Al3-03-J15-M6-04	enstatite
172	58.44	0.293	1.347	0.367	0.062	37.754	0.505	0.008	0.021	0.425	0	99.222	Al3-03-J15-M8-01	enstatite
173	58.607	0.224	1.107	0.386	0.038	38.365	0.434	0.01	0.026	0.42	0.008	99.625	Al3-03-J15-M8-02	enstatite
174	58.862	0.177	0.916	0.418	0.043	38.228	0.484	0.013	0.022	0.45	0.017	99.63	Al3-03-J15-M8-03	enstatite
175	58.743	0.178	0.888	0.401	0.083	38.123	0.52	0.015	0.024	0.435	0	99.41	Al3-03-J15-M8-04	enstatite
176	59.146	0.187	0.952	0.504	0.062	38.295	0.515	0.011	0.028	0.435	0	100.135	Al3-03-J15-M8-05	enstatite
177	58.789	0.193	0.866	0.471	0.065	38.113	0.456	0.018	0.019	0.399	0	99.389	Al3-03-J15-M8-06	enstatite
73	57.511	0.481	1.424	0.438	0.141	36.398	2.111	0	0.033	0.627		99.164	Al3-06-J15-M4-02	enstatite
244	56.232	1.037	2.369	0.524	0.193	32.963	4.898	0.013	0.015	0.911	0	99.155	Al3-06-J15-M10-03	enstatite
245	55.761	1.143	2.393	0.566	0.187	32.081	6.594	0.034	0.02	0.88	0	99.659	Al3-06-J15-M10-04	enstatite
246	55.422	1.357	2.455	0.502	0.217	30.532	8.315	0.003	0.015	0.843	0	99.661	Al3-06-J15-M10-05	enstatite
48	59.133	0.072	0.771	0.617	0.032	38.28	0.334	0.024	0.016	0.585		99.864	Al3-07-J8-M5-01	enstatite
49	58.853	0.071	0.752	0.669	0.038	38.301	0.353	0.009	0.015	0.62		99.681	Al3-07-J8-M5-02	enstatite
50	58.849	0.07	0.715	0.756	0.05	38.321	0.34	0.024	0.021	0.637		99.783	Al3-07-J8-M5-03	enstatite
280	58.529	0.158	0.855	0.53	0.05	38.114	0.398	0	0.039	0.649	0	99.322	Al2-07-J15-M6-01	enstatite
281	58.911	0.165	0.811	0.553	0.059	38.28	0.355	0	0.031	0.642	0	99.807	Al2-07-J15-M6-02	enstatite
282	58.759	0.172	0.904	0.509	0.064	38.142	0.42	0	0.026	0.69	0.01	99.696	Al2-07-J15-M6-03	enstatite
283	58.85	0.154	0.897	0.656	0.069	38.512	0.374	0	0.019	0.67	0.015	100.216	Al2-07-J15-M6-04	enstatite
284	58.899	0.146	0.832	0.635	0.127	38.287	0.397	0	0.019	0.685	0	100.027	Al2-07-J15-M6-05	enstatite
286	58.757	0.18	0.957	0.768	0.08	38.135	0.386	0	0.019	0.655	0	99.937	Al2-07-J15-M6-07	enstatite
312	59.025	0.029	0.693	0.486	0.015	37.793	0.457	0	0.024	0.687	0	99.209	Al2-07-J15-M12-01	enstatite
313	58.95	0.053	0.606	0.696	0.075	38.115	0.482	0	0.015	0.684	0.012	99.688	Al2-07-J15-M12-02	enstatite
373	58.12	0.041	0.561	1.929	0.206	36.975	0.296	0	0.016	0.823	0	98.967	Al2-02-J15-M3-01	enstatite
374	58.202	0.052	0.615	1.496	0.23	36.967	0.333	0	0.015	0.848	0	98.758	Al2-02-J15-M3-02	enstatite
375	58.315	0.018	0.666	1.546	0.185	37.104	0.335	0	0.015	0.88		99.064	Al2-02-J15-M3-03	enstatite
377	58.061	0.074	0.65	1.576	0.396	36.736	0.366	0.013	0.033	0.991	0	98.896	Al2-02-J15-M4-02	enstatite
378	56.489	0.116	1.097	2.987	0.419	32.605	3.699	0.144	0.039	1.248	0.008	98.851	Al2-02-J15-M4-03	enstatite

WDS Point Analysis - Clinopyroxene composition

No.	SiO2	TiO2	Al2O3	FeO	MnO	MgO	CaO	Na2O	K2O	Cr2O3	NiO	Total	Comment	
111	49.396	0.067	0.441	25.01	0.614	2.225	23.123	0.034	0.058	0.132		101.1	Al3-03-J8-M9-01	Ferroan Augite
112	48.59	0.072	0.054	27.465	0.735	0.413	22.866	0.01	0.053	0.109		100.367	Al3-03-J8-M9-02	cpx
117	53.357	2.603	2.969	0.457	0.246	22.116	16.343	0.097	0.034	0.641		98.863	Al3-03-J8-M11-02	cpx
74	52.833	2.086	3.427	0.427	0.207	21.746	17.745	0.015	0.023	0.843		99.352	Al3-06-J8-M4-03	cpx
212	52.092	3.155	3.614	0.818	0.214	21.194	17.94	0.097	0.031	0.844	0	99.999	Al3-06-J15-M4-01	cpx
213	49.986	5.132	4.974	0.703	0.26	17.014	20.539	0.32	0.026	1.128	0.017	100.099	Al3-06-J15-M4-02	cpx
215	49.667	4.853	6.319	0.788	0.239	16.032	20.096	0.864	0.033	1.092	0.039	100.022	Al3-06-J15-M4-04	cpx
243	51.648	3.444	3.632	0.552	0.246	19.261	20.36	0.034	0.027	0.973	0.021	100.198	Al3-06-J15-M10-02	cpx
274	53.555	1.22	2.612	0.865	0.19	21.765	18.529	0.113	0.039	0.945	0.011	99.844	Al3-07-J15-M4-01	Diopside
307	48.667	0.034	0.385	27.532	0.488	0.254	23.248	0.009	0.041	0.097	0	100.849	Al3-07-J15-M11-01	cpx
303	43.347	0	35.224	0.235	0	0	1.406	18.69	1.969	0	0.094	100.871	Al3-07-J15-M10-01	Na-cpx
384	50.801	0.74	5.579	1.255	0.871	18.837	18.458	0.109	0.031	2.653	0.017	99.351	Al2-02-J15-M6-01	cpx
385	48.72	1.03	7.838	1.144	0.862	16.958	19.367	0.124	0.036	3.206	0	99.285	Al2-02-J15-M6-02	cpx
386	47.837	1.329	8.984	1.253	0.918	16.339	19.501	0.14	0.035	3.023	0.012	99.371	Al2-02-J15-M6-03	cpx
387	47.978	1.282	9.071	1.205	0.812	16.403	19.397	0.135	0.035	2.85	0.024	99.192	Al2-02-J15-M6-04	cpx
345	50.755	1.476	6.105	0.492	0.045	18.779	19.888	1.609	0.046	0.189	0.025	99.409	Al2-01-J15-M6-02	diopside
346	50.574	2.052	5.57	0.114	0.042	18.308	21.606	0.005	0.022	0.195	0.008	98.496	Al2-01-J15-M7-01	diopside
347	50.521	1.693	5.374	1.169	0.069	18.576	20.771	0.09	0.028	0.197	0.049	98.537	Al2-01-J15-M7-02	diopside
349	43.448	0.031	35.23	0.193	0.001	0.37	19.634	0.487	0.035	0	0.013	99.442	Al2-01-J15-M8-01	cpx
358	43.519	0.007	35.536	0.169	0	0.373	19.69	0.486	0.015	0	0	99.795	Al2-01-J15-M8-01	cpx
359	43.565	0	35.458	0.214	0	0.359	19.671	0.463	0.03	0.022	0.023	99.805	Al2-01-J15-M8-02	cpx
360	43.797	0.006	35.563	0.204	0	0.344	19.702	0.471	0.027	0.026	0	100.14	Al2-01-J15-M8-03	cpx
364	52.899	1.656	3.72	0.195	0.042	20.887	19.462	0.003	0.027	0.294	0.017	99.202	Al2-01-J15-M10-01	cpx
365	52.177	1.476	4.318	0.154	0.04	20.02	20.823	0.005	0.019	0.256	0	99.288	Al2-01-J15-M10-02	cpx
366	51.91	1.907	4.636	0.187	0.012	20.259	20.127	0	0.022	0.282	0	99.342	Al2-01-J15-M10-03	cpx

Table4: WDS Point Analysis - CAI and Feldspar compositions

No.	CaO	TiO2	Na2O	SiO2	MnO	K2O	Cr2O3	MgO	Al2O3	FeO	NiO	Total	Comment	
90	17.861	0.024	1.642	46.45	0.033	0.032	0.04	0.484	33.471	0.382		100.419	Al3-03-J8-M4-01	CAI
91	17.2	0.045	1.863	46.95	0.033	0.04	0.062	1.203	32.862	0.279		100.537	Al3-03-J8-M4-02	CAI
97	17.815	0.035	1.088	45.758	0.04	0.065	0.055	1.939	32.89	0.261		99.946	Al3-03-J8-M7-01	CAI
98	18.574	0.028	1.075	45.375	0.032	0.039	0.052	0.518	34.654	0.364		100.711	Al3-03-J8-M7-02	CAI
99	16.686	0.272	0.734	49.925	0.104	0.035	0.197	8.732	25.619	0.275		102.579	Al3-03-J8-M7-03	CAI
151	8.144	0.671	10.691	45.308	0.121	0.117	0.221	11.051	21.659	0.634	0.004	98.621	Al3-03-J15-M4-01	CAI
154	6.671	0.142	13.052	41.755	0.03	0.167	0.107	6.586	29.504	0.668	0.007	98.689	Al3-03-J15-M5-02	CAI
155	4.491	0.496	1.133	55.126	0.283	0.228	0.721	30.391	5.143	0.955	0	98.967	Al3-03-J15-M5-03	CAI
191	17.071	0.001	1.278	46.538	0.004	0.015	0	2.938	31.814	0.27	0	99.929	Al3-03-J15-M9-01	CAI
192	18.59	0.372	0.744	46.33	0.035	0.011	0.015	3.664	30.882	0.231	0	100.874	Al3-03-J15-M9-02	CAI
194	16.578	0.881	0.252	52.757	0.159	0.041	0.565	22.186	4.336	0.508	0	98.263	Al3-03-J15-M9-04	CAI
195	17.742	0	1.131	45.217	0.004	0.159	0	1.779	33.425	0.303	0	99.76	Al3-03-J15-M9-05	CAI
199	17.583	0.035	1.055	45.699	0.018	0.003	0	2.81	32.394	0.443	0	100.04	Al3-03-J15-M11-01	CAI
200	10.901	0.398	0.491	52.249	0.184	0.043	0.378	19.7	14.974	0.698	0	100.016	Al3-03-J15-M11-02	CAI
201	18.612	0.607	0.911	49.282	0.095	0.069	0.302	11.878	17.156	0.381	0	99.293	Al3-03-J15-M11-03	CAI
202	5.834	0.082	0.299	42.653	0.05	0	1.295	35.129	13.963	3.249	0	102.554	Al3-06-J15-M1-01	CAI
203	19.426	0	0.549	43.961	0	0.02	0	0.839	35.037	0.219	0	100.051	Al3-06-J15-M1-02	CAI
204	19.091	0	1.116	44.793	0	0.032	0	0.425	34.766	0.243	0	100.466	Al3-06-J15-M1-03	CAI
205	19.716	0	0.64	44.193	0	0.033	0	0.39	35.412	0.16	0	100.544	Al3-06-J15-M2-02	CAI
206	19.79	0	0.51	43.994	0	0.018	0	0.32	35.66	0.163	0	100.455	Al3-06-J15-M2-02	CAI
207	17.756	0.042	0.808	44.474	0.03	0.033	0.018	4.031	33.074	0.65	0	100.916	Al3-06-J15-M2-03	CAI
208	19.412	0.021	0.678	44.234	0.005	0.016	0	0.544	35.187	0.262	0	100.359	Al3-06-J15-M2-04	CAI
209	19.165	0.044	0.848	44.534	0.015	0.027	0.003	0.426	35.028	0.191	0	100.281	Al3-06-J15-M3-01	CAI
210	18.752	0.067	1.121	45.515	0.015	0.027	0	0.448	34.485	0.254	0	100.684	Al3-06-J15-M3-02	CAI
211	18.419	0.067	1.397	45.878	0.001	0.027	0.014	0.43	33.81	0.395	0	100.438	Al3-06-J15-M3-03	CAI
225	18.951	0.08	0.961	44.807	0.014	0.029	0	0.289	34.715	0.326	0.008	100.18	Al3-06-J15-M5-01	CAI
226	19.225	0.044	0.765	44.522	0.009	0.026	0.006	0.278	35.068	0.306	0.046	100.295	Al3-06-J15-M5-02	CAI
227	19.575	0.035	0.668	44.118	0.006	0.03	0	0.293	35.381	0.328	0.007	100.441	Al3-06-J15-M5-03	CAI
228	18.523	0.054	1.206	45.518	0.009	0.027	0	0.338	34.439	0.513	0.002	100.629	Al3-06-J15-M5-04	CAI
232	15.942	5.307	3.051	44.443	0.271	0.052	1.413	13.664	8.991	5.624	0.02	98.778	Al3-06-J15-M7-01	CAI
233	16.08	6.162	1.166	46.198	0.327	0.042	1.697	15.255	7.054	5.872	0.046	99.899	Al3-06-J15-M7-02	CAI
234	15.651	4.326	2.181	48.066	0.212	0.069	1.06	10.204	15.309	4.54	0.037	101.655	Al3-06-J15-M7-03	CAI
239	19.816	0	0.415	43.591	0	0.03	0.018	0.208	35.943	0.351	0.024	100.396	Al3-06-J15-M9-01	CAI
240	16.484	0.363	0.42	42.713	0.068	0.022	0.369	5.493	33.651	1.172	0.015	100.77	Al3-06-J15-M9-02	CAI
241	18.676	0.724	0.381	44.921	0.046	0.023	0.256	4.085	30.391	0.608	0.031	100.142	Al3-06-J15-M9-03	CAI
277	16.941	0.062	1.984	47.242	0.027	0.019	0.023	0.427	32.736	0.656	0.046	100.163	Al3-07-J15-M5-01	CAI
278	16.891	0.049	1.992	47.363	0	0.031	0.049	0.549	32.689	0.442	0.031	100.086	Al3-07-J15-M5-02	CAI
316	15.49	1.06	2.961	50.857	0.163	0.384	1.03	17.943	9.287	0.881	0.041	100.097	Al3-07-J15-M12-05	
326	19.826	0.047	0.398	43.499	0	0.034	0.035	0.394	35.59	0.038	0.002	99.863	Al2-01-J15-M1-02	CAI
335	19.731	0.08	0.458	43.66	0.014	0.021	0	0.386	35.642	0.107	0	100.099	Al2-01-J15-M3-05	Anorthite
336	19.808	0.004	0.343	43.399	0	0.027	0	0.29	35.915	0.142	0.035	99.963	Al2-01-J15-M4-01	Anorthite
337	19.826	0.007	0.324	42.95	0.014	0.019	0	0.268	35.912	0.136	0.036	99.492	Al2-01-J15-M4-02	Anorthite
338	19.848	0.031	0.312	42.993	0.021	0.039	0	0.243	35.807	0.083	0.026	99.403	Al2-01-J15-M4-03	Anorthite
339	19.692	0.015	0.356	43.291	0	0.021	0.004	0.303	35.437	0.155	0.024	99.298	Al2-01-J15-M4-04	Anorthite
340	19.328	0.01	0.596	43.935	0.016	0.042	0	0.583	35.162	0.067	0.018	99.757	Al2-01-J15-M4-05	Anorthite
57	18.082	1.122	0.309	48.028	0.078	0.024	0.302	8.974	23.869	0.316		101.104	Al3-06-J8-M2-01	Ca-Al-Si
58	18.754	0	1.185	43.494	0	0.04	0	0.313	35.819	0.233		99.838	Al3-06-J8-M2-02	Ca-Al-Si/Anorthite

No.	CaO	TiO2	Na2O	SiO2	MnO	K2O	Cr2O3	MgO	Al2O3	FeO	NiO	Total	Comment	
59	10.752	1.481	1.298	51.425	0.29	0.171	1.212	20.43	13.369	1.479		101.907	Al3-06-J8-M2-03	Ca-Al-Si
60	20.092	0.069	0.283	43.378	0.016	0.039	0.031	0.193	36.011	0.165		100.277	Al3-06-J8-M2-04	Ca-Al-Si/Anorthite
61	14.822	1.112	0.249	48.297	0.143	0.054	0.6	12.681	20.491	0.862		99.311	Al3-06-J8-M2-05	Ca-Al-Si
62	7.475	0.497	0.242	36.613	0.036	0.038	0.452	25.22	28.486	0.498		99.557	Al3-06-J8-M2-06	Ca-Al-Si
63	10.555	0.304	0.089	22.466	0.029	0.029	1.405	9.895	50.033	5.483		100.288	Al3-06-J8-M2-07	Ca-Al-Si

Table 5: Chondrule whole rock magnesium numbers

Al2-01	Mg	Fe	Mg + Fe	Mg #
Map 1	6.36	1.55	7.91	0.80404551
Map 2	6.77	0.92	7.69	0.88036411
Map 3	8.85	0.66	9.51	0.93059937
Map 4	7.68	1.9	9.58	0.80167015
Map 5	7.58	6.2	13.78	0.55007257
			Average	0.79335034
			STD	0.13097814

Al2-02	Mg	Fe	Mg + Fe	Mg #
Map 1	14.85	3.26	18.11	0.81998896
Map 2	13.61	3.97	17.58	0.7741752
Map 3	15.35	2.51	17.86	0.85946249
			Average	0.81787555
			STD	0.03485044

Al3-03	Mg	Fe	Mg + Fe	Mg #
Map 1	16.425839	8.84424105	25.2700801	0.65001136
Map 2	14.6102837	1.44580933	16.0560931	0.90995261
Map 3	14.8858447	1.32420091	16.2100457	0.91830986
			Average	0.82609127
			STD	0.12455404

Al3-06	Mg	Fe	Mg + Fe	Mg #
Map 1	6.22060207	5.20931326	11.4299153	0.54423868
Map 2	7	5.62	12.62	0.55467512
Map 3	5.9678194	3.72238232	9.69020173	0.61586121
			Average	0.57159167
			STD	0.03159192

Al3-07	Mg	Fe	Mg + Fe	Mg #
Map 1	20.5427303	11.3487414	31.8914717	0.64414494
Map 2	20.4328916	9.84387774	30.2767693	0.67487027
			Average	0.65950761
			STD	0.01536266

Table 6: Olivine Magnesium numbers - Chondrules

Al3-03 - olivine

Mineral	Average Mg	Average Fe	Mg + Fe	Mg#
Al3-03-J8-M10	50.8993333	7.36333333	58.2626667	0.87361833
Al3-03-J8-M11	53.705	3.108	56.813	0.94529421
Al3-03-J15-M1	54.53925	2.0455	56.58475	0.96385068
Al3-03-J15-M2	53.2056667	3.165	56.3706667	0.94385378
Al3-03-J15-M3_I	49.1908	5.4278	54.6186	0.9006236
Al3-03-J15-M8_I1	45.2204	7.505	52.7254	0.85765874
Al3-03-J15-M10	52.4653333	4.689	57.1543333	0.91795898
			Average	0.91469404
			STD	0.03655116

Al3-03 - orthopyroxene

Mineral	Average Mg	Average Fe	Mg + Fe	Mg#
Al3-03-J8-M1	37.8756	0.5376	38.4132	0.98600481
Al3-03-J8-M2	37.769	0.40675	38.17575	0.98934533
Al3-03-J8-M5	37.463	0.42	37.883	0.98891323
Al3-03-J8-M6	38.0195	0.642	38.6615	0.98339433
Al3-03-J8-M8	37.97125	0.5205	38.49175	0.98647762
Al3-03-J15-M6	38.09525	0.443	38.53825	0.98850493
Al3-03-J15-M8	38.1463333	0.4245	38.5708333	0.98899427
			Average	0.98737636
			STD	0.00202398

Al3-06 - olivine

Mineral	Average Mg	Average Fe	Mg + Fe	Mg#
Al3-06-J8-M1	55.1516667	1.45633333	56.608	0.97427337
Al3-06-J15-M8	55.318	1.18725	56.50525	0.97898868
			Average	0.97663102
			STD	0.00235766

Al3-06 - orthopyroxene

Mineral	Average Mg	Average Fe	Mg + Fe	Mg#
Al3-06-J8-M4	36.398	0.438	36.836	0.98810946
Al3-06-J15-M10	31.8586667	0.53066667	32.3893333	0.98361601
			Average	0.98586273
			STD	0.00224673

Al3-07 - olivine

Mineral	Average Mg	Average Fe	Mg + Fe	Mg#
Al3-07-J8-M2	54.8596667	1.80933333	56.669	0.9680719
Al3-07-J8-M3	38.2465	0.4755	38.722	0.98772016
Al3-07-J8-M4	53.939	2.547	56.486	0.95490918
Al3-07-J8-M6	52.477	5.03933333	57.5163333	0.91238431
Al3-07-J15-M2	52.9678	4.8122	57.78	0.91671513
Al3-07-J15-M7	32.783	27.6805	60.4635	0.54219488
Al3-07-J15-M8	52.96775	4.51625	57.484	0.92143466
Al3-07-J15-M11	54.9176667	1.659	56.5766667	0.97067696
			STD	0.13655208
			Average	0.8967634

Al3-07 - orthopyroxene

Mineral	Average Mg	Average Fe	Mg + Fe	Mg#
Al3-07-J8-M5	38.3006667	0.68066667	38.9813333	0.98253865
Al2-07-J15-M6	38.245	0.6085	38.8535	0.98433861
Al2-07-J15-M12	37.954	0.591	38.545	0.98466727
			Average	0.98384818
			STD	0.00093565

Al2-02 - olivine

Mineral	Average Mg	Average Fe	Mg + Fe	Mg#
Al2-02-J15-M2	24.3356667	36.005	60.3406667	0.40330457
Al2-02-J15-M4	34.378	16.592	50.97	0.67447518
Al2-02-J15-M5	48.9926667	9.03766667	58.0303333	0.84425961
			STD	0.18159834
			Average	0.64067979

Al2-02 - orthopyroxene

Mineral	Average Mg	Average Fe	Mg + Fe	Mg#
Al2-02-J15-M3	37.0153333	1.657	38.6723333	0.95715283
Al2-02-J15-M4	33.269	2.96066667	36.2296667	0.9182806
			Average	0.93771671
			STD	0.01943612

Al2-01- olivine

Mineral	Average Mg	Average Fe	Mg + Fe	Mg#
Al2-01-J15-M2	54.7546667	0.90166667	55.6563333	0.98379939
Al2-01-J15-M3	54.853	0.7305	55.5835	0.98685761
Al2-01-J15-M5	53.044	4.059	57.103	0.92891792
			STD	0.02662149
			Average	0.96652497

Table 7: Trace Element PPM for Olivine, Orthopyroxene and Clinopyroxene

No.	K	V	Na	Si	Co	Ca	Cr	Mg	Al	Ni	Ti	Fe	Mn	Total wt% (	Comment	Mineral
8	116.2273	258.3354	22.258905	197958.2	0	3809.6175	725.3262	346746.314	1360.54772	0	407.592	16246.824	232.35	1029770	Allende3_Chondrule7_olv1_Line 1	Olv
9	132.8312	251.5371	0	198135.85	0	3981.1575	821.124	344912.89	1312.90208	0	395.604	16246.824	232.35	1027360	Allende3_Chondrule7_olv1_Line 2	Olv
10	99.6234	190.3524	44.51781	196579.075	7.8658	3738.1425	1395.9108	342042.134	1122.31952	0	383.616	16246.824	232.35	1019330	Allende3_Chondrule7_olv1_Line 3	Olv
11	157.73705	81.5796	7.419635	195256.05	0	3244.965	1820.1582	333598.734	1085.2618	7.8585	449.55	16246.824	232.35	1002330	Allende3_Chondrule7_olv1_Line 4	Olv
12	157.73705	74.7813	89.03562	193091.525	39.329	2387.265	1580.6637	320728.58	989.97052	55.0095	503.496	16246.824	232.35	974930	Allende3_Chondrule7_olv1_Line 5	Olv
15	141.13315	81.5796	237.42832	191974.2	47.1948	2401.56	1840.6863	330981.28	1175.25912	55.0095	407.592	35058.936	387.25	1014730	Line 3 Allende3_Chondrule7_olv2	Olv
23	132.8312	115.5711	14.83927	276577.675	0	2594.5425	4625.6652	233297.173	4229.87404	39.2925	857.142	5286.048	309.8	1005850	Line 1 Allende3_Chondrule7_opx1	Opx
24	232.4546	81.5796	7.419635	277204.125	0	2644.575	4557.2382	233460.01	3954.58812	7.8585	845.154	5286.048	309.8	1006910	Line 2 Allende3_Chondrule7_opx1	Opx
25	190.94485	81.5796	0	278896.475	0	2751.7875	4632.5079	234189.761	3991.64584	23.5755	875.124	5286.048	309.8	1012080	Line 3 Allende3_Chondrule7_opx1	Opx
28	174.34095	142.7643	0	276213.025	0	3831.06	5706.8118	230456.572	6088.054	15.717	1024.974	4430.952	542.15	1006700	Line 1 Allende3_Chondrule7_opx2	Opx
29	182.6429	149.5626	0	275343.475	0	3659.52	6076.3176	229962.03	6871.56008	31.434	1150.848	4430.952	542.15	1006050	Line 2 Allende3_Chondrule7_opx2	Opx
30	232.4546	169.9575	0	276750.65	47.1948	3623.7825	5816.295	230613.378	6172.75736	7.8585	1102.896	4430.952	542.15	1008430	Line 3 Allende3_Chondrule7_opx2	Opx
31	307.17215	108.7728	0	275446.325	23.5974	3366.4725	5542.587	230510.851	5691.007	86.4435	1000.998	4430.952	542.15	1003700	Line 4 Allende3_Chondrule7_opx2	Opx
32	215.8507	101.9745	96.455255	275034.925	47.1948	3831.06	5426.2611	228894.543	5627.47948	47.151	1006.992	4430.952	542.15	1000500	Line 5 Allende3_Chondrule7_opx2	Opx
33	232.4546	88.3779	0	276853.5	39.329	3666.6675	3017.6307	234810.954	7512.12924	39.2925	1930.068	19589.472	1316.65	1035900	Line 1 Allende3_Chondrule3_opx2	Opx
34	116.2273	122.3694	81.615985	276563.65	7.8658	3652.3725	3065.5296	235456.271	6929.79364	0	1828.17	19589.472	1316.65	1035060	Line 2 Allende3_Chondrule3_opx2	Opx
35	124.52925	108.7728	0	275867.075	62.9264	3466.5375	3045.0015	235160.752	7173.3158	7.8585	1774.224	19589.472	1316.65	1033120	Line 3 Allende3_Chondrule3_opx2	Opx
36	232.4546	54.3864	155.812335	277531.375	0	3952.5675	2949.2037	235848.286	6103.93588	55.0095	1456.542	19589.472	1316.65	1036050	Line 4 Allende3_Chondrule3_opx2	Opx
37	1054.34765	115.5711	2871.39875	264539.55	0	3952.5675	2928.6756	223701.852	14113.6974	70.7265	1342.656	19589.472	1316.65	1007790	Line 5 Allende3_Chondrule3_opx2	Opx
40	273.96435	61.1847	163.23197	278728.175	0	3516.57	2860.2486	239153.274	4743.38816	47.151	1186.812	29073.264	1471.55	1052790	Line 1 Allende3_Chondrule3_opx1	Opx
45	315.4741	95.1762	118.71416	228219.475	251.7056	169853.19	116.3259	2943.128	608.8054	15.717	11.988	203901.528	5189.15	1002050	Line 1 Allende3_Chondrule3_cpx1	Cpx
46	356.98385	67.983	178.07124	232230.625	235.974	165000.038	102.6405	23532.962	614.09936	125.736	35.964	203901.528	5189.15	1038220	Line 2 Allende3_Chondrule3_cpx1	Cpx
49	307.17215	0	393.240655	250257.425	0	152942.205	5125.1823	121500.526	16601.8586	0	6899.094	3498.12	1858.8	1008910	Line 1 Allende3_Chondrule3_cpx2	Cpx
50	58.11365	13.5966	222.58905	245563.725	0	157495.163	7068.5091	112815.886	23012.8441	0	8907.084	3498.12	1858.8	1008630	Line 2 Allende3_Chondrule3_cpx2	Cpx
52	224.15265	101.9745	118.71416	198308.825	0	1486.68	424.2474	338272.759	31.76376	55.0095	287.712	19589.472	1394.1	1015970	Line 1 Allende3_Chondrule3_olv2	Olv
53	365.2858	693.4266	719.704595	190693.25	39.329	1207.9275	20199.6504	321192.967	2048.76252	86.4435	1342.656	19589.472	1394.1	1007380	Line 2 Allende3_Chondrule3_olv2	Olv
62	207.54875	237.9405	0	198963.325	0	1822.6125	978.5061	340184.586	439.39868	55.0095	563.436	9172.848	464.7	1008470	Line 1 Allende3_Chondrule6_olv1	Olv
63	207.54875	135.966	44.51781	196602.45	0	1808.3175	862.1802	339044.727	391.75304	172.887	563.436	9172.848	464.7	1001310	Line 2 Allende3_Chondrule6_olv1	Olv
68	116.2273	115.5711	0	195527.2	23.5974	1779.7275	650.0565	337428.419	259.40404	133.5945	497.502	11116.248	619.6	998100	Line 1 Allende3_Chondrule6_olv2	Olv
69	182.6429	156.3609	0	196191.05	0	1751.1375	697.9554	336330.777	275.28592	141.453	545.454	11116.248	619.6	997960	Line 2 Allende3_Chondrule6_olv2	Olv
74	282.2663	537.0657	155.812335	264721.875	0	20806.3725	4755.6765	211133.248	12604.9188	47.151	4417.578	3342.648	1316.65	990970	Line 1 Allende3_Chondrule6_opx1	Opx
75	257.36045	475.881	74.19635	266825.625	31.4632	20884.995	5022.5418	214178.903	11646.712	15.717	4333.662	3342.648	1316.65	998840	Line 2 Allende3_Chondrule6_opx1	Opx
80	107.92535	448.6878	133.55343	263197.825	0	34586.7525	6308.9694	203431.661	12483.1577	7.8585	6431.562	4120.008	1626.45	1000600	Line 1 Allende3_Chondrule6_opx2	Opx
86	257.36045	54.3864	1298.43613	133274.9	527.0086	2187.135	1676.4615	119136.374	58863.5412	212.1795	1738.26	279771.864	6196	973200	Line 1 Allende2_Chondrule2_olv1	Olv
89	240.75655	54.3864	704.865325	160834.025	542.7402	2330.085	6890.5989	148869.204	5214.5506	337.9155	1300.698	280082.808	6273.45	987060	Line 1 Allende2_Chondrule2_olv2	Olv
90	141.13315	88.3779	690.026055	169557.575	534.8744	743.34	5542.587	165442.392	1498.19068	212.1795	341.658	280082.808	6273.45	1020130	Line 2 Allende2_Chondrule2_olv2	Olv
92	174.34095	156.3609	37.098175	268812.5	7.8658	2430.15	6096.8457	223955.154	2879.91424	23.5755	503.496	11971.344	1394.1	982660	Line 1 Allende2_Chondrule2_opx1	Opx
93	174.34095	156.3609	51.937445	269621.275	7.8658	2394.4125	6042.1041	224160.208	3107.55452	0	509.49	11971.344	1394.1	985030	Line 2 Allende2_Chondrule2_opx1	Opx
99	74.71755	142.7643	66.776715	267213.65	23.5974	2465.8875	5761.5534	223231.434	2609.92228	0	455.544	13292.856	1688.41	978980	Line 2 Allende2_Chondrule2_opx2	Opx
104	182.6429	203.949	103.87489	194232.225	47.1948	3838.2075	1409.5962	330649.575	894.67924	47.151	1210.788	7004.0136	216.86	984930	Line 1 Allende2_Chondrule1_olv1	Olv
107	157.73705	74.7813	44.51781	192105.1	62.9264	1701.105	198.4383	318406.645	47.64564	70.7265	395.604	31483.08	456.955	983910	Line 1 Allende2_Chondrule1_olv2	Olv
108	0	101.9745	118.71416	192633.375	23.5974	2315.79	171.0675	317526.119	0	102.1605	341.658	31483.08	456.955	984160	Line 2 Allende2_Chondrule1_olv2	Olv
110	199.2468	251.5371	44.51781	237873.35	47.1948	159346.365	1218.0006	111084.989	26676.2644	31.434	10543.446	4975.104	425.975	993430	Line 1 Allende2_Chondrule1_cpx1	Cpx
111	132.8312	251.5371	126.133795	238144.5	0	154414.59	1300.113	113593.885	25209.8375	0	10333.656	4975.104	425.975	988200	Line 2 Allende2_Chondrule1_cpx1	Cpx
116	174.34095	61.1847	118.71416	244586.65	7.8658	142942.853	1758.5739	124606.491	21715.8239	0	10123.866	1321.512	240.095	992740	Line 1 Allende2_Chondrule1_cpx2	Cpx
117	83.0195	81.5796	267.10686	242510.95	0	137639.408	1758.5739	123659.624	19815.2923	31.434	9470.52	1321.512	240.095	974780	Line 2 Allende2_Chondrule1_cpx2	Cpx

Table 8: Trace element concentrations normalized to CI chondrite

Ordered by increasing Zr ratio

Allende3 Chondrule 7

	Olivine	Clinopyroxene	Othopyroxene
Ni ppm	0.00512871		0.032013047
Mn ppm	0.03261053		0.247659884
Ti ppm	0.62887869		1.544683279
Cr ppm	0.564374		2.227745113

Allende3 Chondrule 3

	Olivine	Clinopyroxene	Othopyroxene
Ni ppm	0.00744489	0.003722447	0.003860316
Mn ppm	0.14674737	0.370944737	0.780503876
Ti ppm	1.33636721	6.497594262	2.60067541
Cr ppm	4.48345604	1.349201935	1.294658674

Allende3 Chondrule 6

	Olivine	Clinopyroxene	Othopyroxene
Ni ppm	0.01323537		0.001861224
Mn ppm	0.05706842		0.855552326
Ti ppm	0.88927377		8.932042623
Cr ppm	0.34659763		2.542955576

Allende 2 Chondrule 2

	Olivine	Clinopyroxene	Othopyroxene
Ni ppm	0.02998638		0.002895237
Mn ppm	0.65628684		0.162237368
Ti ppm	2.12737869		0.776272131
Cr ppm	2.65526511		2.65154625

Allende 2 Chondrule 1

	Olivine	Clinopyroxene	Othopyroxene
Ni ppm	0.01075374	0.001654421	
Mn ppm	0.03546395	0.035056316	
Ti ppm	1.23073525	16.58667541	
Cr ppm	0.32651579	0.656006674	

CI Normalization Factors from Rollinson (1993)

K	Ti	V	Mn	Fe	Cr	Co	Ni
850	610	49	1720	265000	2300	470	9500

Table 9: Distribution Coefficients of trace elements in olivine, orthopyroxene and clinopyroxene in each chondrule

Allende 2 Chondrule 1

	Olivine	Clinopyroxene	Othopyroxene
Ni	0.09823125	0.0151125	
Mn	3.369075	3.33035	
Ti	0.008749983	0.117923916	
Cr	0.736261103	1.479230735	

Allende2 Chondrule 2

	Olivine	Clinopyroxene	Othopyroxene
Ni	0.14484947		0.013985466
Mn	3.400759091		0.840684545
Ti	2.994694615		1.092752308
Cr	1.420258081		1.418268924

Allende3 Chondrule 3

	Olivine	Clinopyroxene	Othopyroxene
Ni	0.050725386	0.025362693	0.026302052
Mn	1.025713193	2.592775015	0.987723815
Ti	0.466875042	2.270008248	0.90857545
Cr	3.057617136	0.920125661	0.882928372

Allende3 Chondrule 6

	Olivine	Clinopyroxene	Othopyroxene
Ni	0.088832492		0.012492069
Mn	0.450617055		1.223103436
Ti	0.086006532		0.863866718
Cr	0.209508017		1.537141439

Allende3 Chondrule 7

	Olivine	Clinopyroxene	Othopyroxene
Ni	0.009118661		0.056918093
Mn	0.174089366		0.239372878
Ti	0.371121191		0.911566425
Cr	0.220562391		0.870622658

Table10: Archean whole rock and mineral data

Archean- Whole rock	Ni ppm Average	Cr ppm Average	Ti ppm Average	Mn ppm Average	Age
[5400]- Kaapvaal	1540.2740	4789.7392	2169.915	1456.0921	3.4
[5319][6810]- western Australia	1796.4625	5069.6048	1753.315	1246.9725	2.7
[16702]-Kaapvaal	1821.6098	5366.1788	1407.447	1194.3053	3.4
[5590]- Kaapvaal	1982.0987	6242.4411	1871.535	1381.2221	3.4
[5611] - Superior	1218.0739	4873.2812	3196.928	1626.4859	2.7
[5996]- Zimbabwe	751.8004	2826.5031	3415.646	1423.9198	2.7
[8628]- Superior	465.1297	3087.4073	1941.052	1476.1830	2.7
[8498]- Zimbabwe	1142.6319	4984.6705	2062.018	1440.6018	2.7
[6819]- Superior	1590.5455	2645.7273	1903.444	1225.1452	2.7
[5415]- Zimbabwe	1212.2000	2528.4000	4152.8092	1353.8558	2.8

Archean- Olivine	NI ppm Average	CR ppm Average	Ti ppm Average	MN ppm Average	Age
[5400]	3497.0508	2552.6711		1239.2273	3.4
[5319][6810]	3536.3435	2227.7857	1258.7903		2.7
[16702]	3132.1899	2486.3679	28.2586	929.4205	3.3
[5590]	3156.5140	2088.5491	119.8848	1161.7756	3.4
[5611]	3300.5872	2575.8772	179.8272	1161.7756	2.7
[5996]	2898.9285	1750.4030		438.8930	2.7
[8628]	3426.3239	3326.2078			2.7
[6819]	3144.5391	2583.8336	20.55167849	902.8656162	2.7
[5415]	3005.8920	2478.4116	359.6543736	1128.58202	2.8

Archean- Clinopyroxene	NI ppm Average	CR ppm Average	Ti ppm Average	MN ppm Average	Age
[5400]					3.4
[5319][6810]					2.7
[16702]					3.4
[5590]	1178.78116	9885.798943	2737.369399	1084.323902	3.4
[5611]	392.9270533	5151.754379	3146.975769	1394.130731	2.7
[5996]					2.7
[8628]			4179.619765	910.0575604	2.7
[8498]		2300.430863	2032.829068	1481.6847	2.7
[6819]					
[5415]	235.756232	2831.144298	3876.274915	1936.292505	2.8

Table 11: CI-normalized trace element concentrations in olivine and clinopyroxene in Archean-aged mafic rocks

Komatiite- Olivine	Ni ppm Average	Mn ppm Average	Ti ppm Average	Cr ppm Average	Age
[5400]- Kaapvaal	3497.050774	1239.227316		2552.671089	3.4
[5319][6810]- western Australia	3536.34348		1258.790307	2227.785677	2.7
[16702]-Kaapvaal	3132.189939	929.4204872	28.25855792	2486.367943	3.3
[5590]- Kaapvaal	3156.513995	1161.775609	119.8847912	2088.549073	3.4
[5611] - Superior	3300.587248	1161.775609	179.8271868	2575.877189	2.7
[5996]- Zimbabwe	2898.928482	438.8930079		1750.403032	2.7
[8628]- Superior	3426.323905			3326.207782	2.7
[8498]- Zimbabwe					
[6819]- Superior	3144.539075	902.8656162	20.55167849	2583.833567	2.7
[5415]- Zimbabwe	3005.891958	1128.58202	359.6543736	2478.411566	2.8

Komatiite- Clinopyroxene	Ni ppm Average	Mn ppm Average	Ti ppm Average	Cr ppm Average	Age
[5400]- Kaapvaal					3.4
[5319][6810]- western Australia					2.7
[16702]-Kaapvaal					3.3
[5590]- Kaapvaal	1178.78116	1084.323902	2737.369399	9885.798943	3.4
[5611] - Superior	392.9270533	1394.130731	3146.975769	5151.754379	2.7
[5996]- Zimbabwe					2.7
[8628]- Superior		910.0575604	4179.619765		2.7
[8498]- Zimbabwe		1481.6847	2032.829068	2300.430863	2.7
[6819]- Superior					2.8
[5415]- Zimbabwe	235.756232	1936.292505	3876.274915	2831.144298	

Table 12: Distribution coefficients for trace elements in olivine and clinopyroxene with the Archean samples

KDS OLV

Sample	Ni	Mn	Ti	Cr
[5400]- Kaapvaal	2.270408163	0.85106383		0.532945736
[5319][6810]- western Australia	1.968503937		0.717948718	0.439439714
[16702]-Kaapvaal	1.719462591	0.778210117	0.020077878	0.4633405
[5590]- Kaapvaal	1.592511013	0.841121495	0.06405694	0.334572491
[5611] - Superior	2.709677419	0.714285714	0.05625	0.528571429
[5996]- Zimbabwe	1.509090909	0.308228731		0.294642857
[8628]- Superior	7.366384087			1.077346605
[8498]- Zimbabwe				
[6819]- Superior	1.977019309	0.736945813	0.010797104	0.976606166
[5415]- Zimbabwe	2.479699685	0.833605754	0.086605081	0.980229222

KDs Clinopyroxene

Sample	Ni	Mn	Ti	Cr
[5400]- Kaapvaal				
[5319][6810]- western Australia				
[16702]-Kaapvaal				
[5590]- Kaapvaal	0.373443983	0.785046729	1.462633452	4.733333333
[5611] - Superior	0.119047619	0.857142857	0.984375	2
[5996]- Zimbabwe				
[8628]- Superior		0.616493747	2.153275581	
[8498]- Zimbabwe		1.028517905	0.985844287	0.461501093
[6819]- Superior				
[5415]- Zimbabwe	0.19448625	1.430205819	0.933410316	1.119737501

Table 13: Orthopyroxene data used for two-pyroxene thermometer

Opx	Wt% O				Cation					Cation * 6				
Average	Al3-03	Al3-06	Al3-07	Al2-02	Average	Al3-03	Al3-06	Al3-07	Al2-02	Average	Al3-03	Al3-06	Al3-07	Al2-02
SiO2	58.6415185	56.2315	58.865	57.2548333	Si	0.33023704	0.322375	0.330590909	0.33064	Si	1.98142222	1.93425	1.98354545	1.98384
TiO2	0.18972414	1.0045	0.11545455	0.07016667	Ti	0.0008037	0.00435	0.000481818	0.00026	Ti	0.00482222	0.0261	0.00289091	0.00156
Al2O3	1.07580952	2.16025	0.79936364	0.84983333	Al	0.0069963	0.0146	0.005290909	0.00486	Al	0.04197778	0.0876	0.03174545	0.02916
FeO	0.47934483	0.5075	0.625	2.30883333	Fe	0.00219259	0.002425	0.002945455	0.00912	Fe	0.01315556	0.01455	0.01767273	0.05472
MnO	0.08603448	0.1845	0.05990909	0.29483333	Mn	0.00040741	0.0009	0.000290909	0.0014	Mn	0.00244444	0.0054	0.00174545	0.0084
MgO	37.8875517	32.9935	38.2072727	35.1421667	Mg	0.31865556	0.281875	0.319854545	0.30738	Mg	1.91193333	1.69125	1.91912727	1.84428
CaO	0.49617241	5.4795	4.62578571	1.52466667	Ca	0.00301111	0.033725	0.002336364	0.0062	Ca	0.01806667	0.20235	0.01401818	0.0372
Na2O	0.03282759	0.0125	0.00518182	0.05416667	Na	0.00031852	0.000125	6.36364E-05	0.00034	Na	0.00191111	0.00075	0.00038182	0.00204
K2O	0.04558621	0.02075	0.02218182	0.02466667	K	0.00032593	0.000125	0.000145455	0.00016	K	0.00195556	0.00075	0.00087273	0.00096
Cr2O3	0.41903448	0.81525	0.65490909	0.94733333	Cr	0.00186667	0.003675	0.002909091	0.00434	Cr	0.0112	0.02205	0.01745455	0.02604
xFeOPX	0.01249371	0.0151488	0.01609486	0.06164944						m1	0.03942222	0.07	0.03563636	0.0406
										m2	0.02242222	0.2085	0.01614545	0.04764
										1- m1	0.96057778	0.93	0.96436364	0.9594
										1-m2	0.97757778	0.7915	0.98385455	0.95236
										Mg #	0.98737636	0.98586273	0.98384818	0.93771671
										xMgm1	0.94845179	0.91685234	0.9487874	0.89964542
										xMgm2	0.96523719	0.78031035	0.9679635	0.89304389
										Al (4)	0.01857778	0.06575	0.01645455	0.01616
										Al (6)	0.0234	0.02185	0.01529091	0.013
										xFeOPX	0.01249371	0.0151488	0.01609486	0.06164944

Table 14: Clinopyroxene data used for two-pyroxene thermometer

CPX	cations				cations *6				
Average	Al3-03	Al3-06	Al3-07	Al2-02	Average	Al3-03	Al3-06	Al3-07	Al2-02
Si	0.3269	0.30652	0.3249	0.29645	Si	1.9614	1.83912	1.9494	1.7787
Ti	0.00413333	0.01682	0.00285	0.005025	Ti	0.0248	0.10092	0.0171	0.03015
Al	0.00826667	0.031	0.0107	0.056325	Al	0.0496	0.186	0.0642	0.33795
Fe	0.09976667	0.0033	0.08045	0.00615	Fe	0.5986	0.0198	0.4827	0.0369
Mn	0.003	0.00116	0.0019	0.00445	Mn	0.018	0.00696	0.0114	0.0267
Mg	0.07426667	0.16976	0.09785	0.155075	Mg	0.4456	1.01856	0.5871	0.93045
Ca	0.14586667	0.12396	0.1438	0.124775	Ca	0.8752	0.74376	0.8628	0.74865
Na	0.00053333	0.0031	0.0007	0.001525	Na	0.0032	0.0186	0.0042	0.00915
K	0.00043333	0.00022	0.00035	0.000275	K	0.0026	0.00132	0.0021	0.00165
Cr	0.00143333	0.00464	0.00245	0.014075	Cr	0.0086	0.02784	0.0147	0.08445
					m1	0.0444	0.15388	0.0454	0.23125
					m2	0.8964	0.76932	0.8784	0.7845
					1- m1	0.9556	0.84612	0.9546	0.76875
					1-m2	0.1036	0.23068	0.1216	0.2155
					Mg #	0.51380993	0.96869214	0.966826572	0.93366988
					xMgm1	0.49099677	0.8196298	0.922932645	0.71775872
					xMgm2	0.05323071	0.2234579	0.117566111	0.20120586
					Al (4)	0.0386	0.16088	0.0506	0.2213
					Al (6)	0.011	0.02512	0.0136	0.11665

Table 15: Orthopyroxene - Clinopyroxene Thermometer (Wells, 1977)

T(K) = 7341 / (3.355 + 2.44*Xfeopx - lnK) error +/- 70 degrees

K = aMgcpx / aMgopx aMgcpx = Xmgm2 + Xmgm1 Xmgm2 = Mg/(Ca+Mg+Fe2+Mn+Na)M2

aMgopx = Xmgm2 + Xmgm1 Xmgm1 = Mg / (Fe3+ + Fe2+ AlVI + Ti + Cr + Mg)M1

Assuming - Mg/(Mg+Fe2+)M2 = Mg/(Mg+Fe2+)M1 = Mg/(Mg+Fe2+)mineral

SUMCATM2 = SUMCATM1 = (SUMCATmineral - SUMCATtot)/2

Sample	**XMgm2-cpx**	**XMgm1-cpx**	**XMgm2 - opx**	**XMgm1-opx**	**Xfeopx**	**aMgcpx**	**aMgopx**	**K**	**lnK**	**T(K)**	**T(degC)**
Example	0.068	0.793	0.881	0.857	0.092	0.053924	0.755017	0.071420908	-2.63916462	1180.482316	907.48
Al3-03	0.053230709	0.490996773	0.965237189	0.948451791	0.012493709	0.026136106	0.915480941	0.028549045	-3.5561318	1057.534662	784.53
Al3-06	0.223457904	0.819629798	0.780310352	0.91685234	0.015148802	0.183152757	0.715429373	0.256003966	-1.36256234	1544.002682	1271.00
Al3-07	0.117566111	0.922932645	0.9679635	0.948787405	0.01609486	0.108505602	0.918391577	0.118147427	-2.13582205	1327.463991	1054.46
Al2-02	0.20120586	0.717758723	0.893043891	0.899645416	0.061649444	0.144417261	0.803422843	0.179752495	-1.7161744	1405.891172	1132.89

*excel table set up by Jillian Kendrick 2015

Table 16: Kd's Stabdard deviation

Al3-07	Olivine Average Kd	Olivine Kd standard deviation	Clinopyroxene Average Kd	Clinopyroxene Kd standard deviation	Orthopyroxene Average Kd	Orthopyroxene Kd standard deviation
Ni	0.009118661	0.088923015			0.056918093	0.123083266
Mn	0.174089366	0.045876576			0.239372878	0.068814864
Ti	0.371121191	0.117797337			0.911566425	0.128268039
Cr	0.220562391	0.093545098			0.870622658	0.110073221
Al3-03	Olivine Average Kd	Olivine Kd standard deviation	Clinopyroxene Average Kd	Clinopyroxene Kd standard deviation	Orthopyroxene Average Kd	Orthopyroxene Kd standard deviation
Ni	0.050725386	0.015941451	0.025362693	0.043536022	0.026302052	0.019739954
Mn	1.025713193	0	2.592775015	1.414689938	0.987723815	0.046527295
Ti	0.466875042	0.427227717	2.270008248	2.647294703	0.90857545	0.171393305
Cr	3.057617136	4.146223381	0.920125661	1.051634006	0.882928372	0.023290169
Al3-06	Olivine Average Kd	Olivine Kd standard deviation	Clinopyroxene Average Kd	Clinopyroxene Kd standard deviation	Orthopyroxene Average Kd	Orthopyroxene Kd standard deviation
Ni	0.088832492	0.035405534			0.012492069	0.014601595
Mn	0.450617055	0.074332537			1.223103436	0.148665073
Ti	0.086006532	0.004938155			0.863866718	0.196848337
Cr	0.209508017	0.039740461			1.537141439	0.311654553
Al2-02	Olivine Average Kd	Olivine Kd standard deviation	Clinopyroxene Average Kd	Clinopyroxene Kd standard deviation	Orthopyroxene Average Kd	Orthopyroxene Kd standard deviation
Ni	0.14484947	0.04345197			0.013985466	0.020763032
Mn	3.400759091	0.024390425			0.840684545	0.092683613
Ti	2.994694615	1.559905754			1.092752308	0.092445636
Cr	1.420258081	0.830956941			1.418268924	0.07014329
Al2-01	Olivine Average Kd	Olivine Kd standard deviation	Clinopyroxene Average Kd	Clinopyroxene Kd standard deviation	Orthopyroxene Average Kd	Orthopyroxene Kd standard deviation
Ni	0.09823125	0.059497972	0.0151125	0.017450412		
Mn	3.369075	1.386189129	3.33035	1.07317868		
Ti	0.008749983	0.152855616	0.117923916	0.159013369		
Cr	0.736261103	0.645353905	1.479230735	0.284645151		

Tbale 17: Chondrite-Normalized Concentrations and Stadard deviation

Al3-07	Olivine Average	Olivine standard deviation	Clinopyroxene Average	Clinopyroxene standard deviation	Orthopyroxene Average	Orthopyroxene standard deviation
Ni	0.005128705	0.050013915			0.032013047	0.069227028
Mn	0.032610526	0.047464807			0.247659884	0.071197211
Ti	0.628878689	0.199611978			1.544683279	0.217354973
Cr	0.564373996	0.239362751			2.227745113	0.281654834
Al3-03	Olivine Average	Olivine standard deviation	Clinopyroxene Average	Clinopyroxene standard deviation	Orthopyroxene Average	Orthopyroxene standard deviation
Ni	0.007444895	0.002339705	0.003722447	0.006389722	0.003860316	0.002897206
Mn	0.146747368	0	0.370944737	1.117894459	0.780503876	0.036766082
Ti	1.336367213	1.222882059	6.497594262	7.577526155	2.60067541	0.490590356
Cr	4.483456043	6.079705027	1.349201935	1.542035719	1.294658674	0.034150923
Al3-06	Olivine Average	Olivine standard deviation	Clinopyroxene Average	Clinopyroxene standard deviation	Orthopyroxene Average	Orthopyroxene standard deviation
Ni	0.013235368	0.005275156			0.001861224	0.002175527
Mn	0.057068421	0.051995091			0.855552326	0.103990182
Ti	0.88927377	0.051058586			8.932042623	2.035334507
Cr	0.34659763	0.065744261			2.542955576	0.515582798
Al2-02	Olivine Average	Olivine standard deviation	Clinopyroxene Average	Clinopyroxene standard deviation	Orthopyroxene Average	Orthopyroxene standard deviation
Ni	0.029986382	0.00899532			0.002895237	0.004298312
Mn	0.656286842	0.025997546			0.162237368	0.098790673
Ti	2.127378689	1.10812977			0.776272131	0.065671763
Cr	2.655265109	1.553528194			2.65154625	0.131137455
Al2-01	Olivine Average	Olivine standard deviation	Clinopyroxene Average	Clinopyroxene standard deviation	Orthopyroxene Average	Orthopyroxene standard deviation
Ni	0.010753737	0.006513462	0.001654421	0.001910361		
Mn	0.035463947	0.080592391	0.035056316	0.062394109		
Ti	1.230735246	0.731702292	16.58667541	0.761178749		
Cr	0.326515793	0.286200427	0.656006674	0.126233936		